A study of the development of the pore structure of some polymer carbons by reaction with carbon dioxide

Stanley Michael Rowan

THE   UNIVERSITY   OF   DURHAM

A STUDY OF THE DEVELOPMENT OF THE PORE STRUCTURE OF SOME POLYMER

CARBONS BY REACTION WITH CARBON DIOXIDE.

BEING A THESIS SUBMITTED FOR THE DEGREE OF

MASTER OF SCIENCE

BY

STANLEY MICHAEL ROWAN, B.Sc.

SEPTEMBER, 1966.

For Sandra and My Parents

Acknowledgements

The Author wishes to express most sincerely his gratitude to
Dr. B. McEnaney for his help and advice which were always available
throughout the course of this work.

Thanks are also due to:-

Dr. G. Kohnstam of Durham University for kindly acting as Supervisor
of the work;

The Principal, the Governors, and Dr. E.P. Hart Head of the Department
of Chemistry, at Sunderland Technical College for the facilities and a
grant to carry out the research;

Mr. A. Lewis and the laboratory staff for their continual help;

Dr. C. Allen of the Chemistry Department for the production of the
micrographs;

Dr. C. Jackson of the Pharmacy Department for carrying out E.S.R.
Analyses;

Dr. D. Ganderton of the Pharmacy Department for his help and advice
in the production of pellets of the polymers;

Mr. Reay and Staff of the Mechanical Engineering Department for their
help in constructing modifications to the furnace;

Messrs. J. Hindmarch and P. Melvin of the Chemistry Department Workshops
for help in construction of apparatus;

Mr. C.J. Weedon and other members of the staff of the Chemistry
Department for valuable discussion throughout the course of the work;

and finally Mrs. R. Speck for typing this manuscript.

CONTENTS

CHAPTER 3

The Rates of Activation of the Carbons by Carbon dioxide

<u>CHAPTER 4</u>

<u>The Development of Porosity in the Carbons.</u>

<u>CHAPTER 5</u>

<u>Correlations between the rates of activation and</u>

<u>the Development of Porosity of the Carbons</u>

CHAPTER 6

Summary and Conclusions

APPENDIX

CHAPTER 1

1.1

General Introduction

A good deal of work has been done on the detailed kinetics of the reactions of carbons with oxidising gases, and also on the detailed pore structure of the activated carbons produced by such reactions. However, relatively little has been done to attempt to relate the development of pore structure in activated carbons to the rate of the activation process.

Part of the reason for this is that traditional starting materials such as coconutshell and coal do not yield homogeneous or reproducible carbons. In addition to the variability in the nature of the starting materials, the resulting carbons contain varying amounts of inorganic matter which can markedly affect both the rate of activation and the development of pore structure.

In recent years, a range of carbons have been produced by pyrolysis of certain polymers. These carbons are more homogeneous and reproducible than traditional carbons; they can be prepared free from inorganic matter, and have a wider range of graphitic character.

The work reported in this thesis is an investigation of the relation between the development of pore structure in three

polymer carbons by reaction with carbon dioxide, and the rates of the activation processes.

Before discussing the aims and outline of the thesis, a brief summary of the physical structure of carbons follows.

1.2 The Physical Structure of Carbons

X-ray analyses have shown that all carbons have a varying degree of order in their structure (1), the ordered regions being graphite-like microcrystals linked by a network of non-graphitic carbon. The graphitic layer-planes consist of hexagonal units in which the C-C distance is 1.415 $\overset{o}{A}$. The layer-planes may be parallel to each other but have no particular stacking sequence as in natural graphite. This type of structure is termed turbostratic, and carbons having this structure have been called mesomorphous i.e. neither truly crystalline nor truly amorphous.

Franklin (2) classified carbons into three groups.

(i) Graphitic carbons, which show a large degree of three-dimensional graphitic structure.

(ii) Graphitisable carbons, which develop this structure on heating. Graphitisable carbons contain packets of microcrystalline graphite in nearly parallel orientation; further orientation readily occurs on heating.

(iii) Non-graphitising carbons, which do not develop this structure on heating.

More recently this classification has been shown to be oversimplified. A number of carbons have been prepared with graphitic characters intermediate between the Franklin classes.

Ubbelohde and Lewis (3) have considered non-graphitic structures of carbon in terms of structural defects. Carbon is considered to be a thermo-set high polymer containing macro-molecules. In partly graphitised or grosaly defected carbon only small regions of the carbon polymer approximate to the graphite structure, they are joined together by various kinds of carbon structures which are amorphous with respect to the graphite lattice.

1.3 The Pore Structure of Carbons

The development of pore structure by removal of part of the carbon surface by certain reagents is a process known as activation. Two methods of activation are recognised:-
(i) chemical activation, in which dehydrating and/or oxidising agents are added to the starting materials before carbonisation, and (ii) gaseous activation in which the carbon reacts with a gas at high temperatures, as in the present work.

In the unactivated state, carbons have open pore volumes which range from 0.05 cm^3 to 0.5 cm^3 per gram of carbon.

On activation these pore volumes can be increased by as much as 1 cm^3/g. in the case of the highly porous carbons, and

by a smaller amount in the case of the carbons of low porosity.

The pores in carbons have been classified into three types(4), micro-, macro-, and transitional pores. Macro- and transitional pore widths lie in the ranges 1200 to 160,000 Å and 100 to 1200 Å respectively, whilst micro-pore widths are less than 100 Å.

Macro-pores are formed either by major defects in the carbon structure, which can result from the evolution of bubbles during the decomposition of the parent substance, or by extensive activation of the carbon structure.

Transitional pores are produced by carefully controlled activation. Macro- and transitional pores usually contribute little to the total surface area of the carbon. For example macro- and transitional pores have been shown to contribute only $3 \text{ m}^2\text{g}^{-1}$ to a total surface area of $1500 \text{ m}^2\text{g}^{-1}$ in the case of an activated wood charcoal (5).

Micro-pores arise from the nature of the micro-structure of carbons. Spaces and channels occur between the microcrystals and it is these small cavities that constitute micro-pores. As the microcrystals are very small, a large proportion of the carbon atoms form the walls of micro-pores. The high adsorption potential of the walls of the micro-pores is further enhanced by overlap with the adsorption potential of neighbouring walls of the pores, and is responsible for the powerful adsorbent properties of porous carbons.

1.4. The Aims of the Present Work

The development of the porosity of a carbon by reaction with carbon dioxide probably depends on a number of factors which in turn may influence the kinetics of the activation process.

In this project three polymer carbons were selected principally to investigate the influence of two factors.   These factors are degree of graphitic character of the carbons and the nature of the carbonisation process.   Carbonisation processes fall into two broad classes: charring processes, in which the material remains solid throughout the carbonisation and coking processes in which the material fuses at some stage in the decomposition.   Table 1.1. lists the carbons selected and their characteristics.

Table 1.1.

The Characteristics of the Polymer Carbons

Polymer	Carbonisation Process	Nature of Carbon	Porosity of Un-activated carbon $(cm.^3 g.^{-1})$
Cellulose	Charring	non-graphitic	0.40
Cellulose triacetate	Coking	non-graphitic	0.44
Polyacenaphthylene	Coking	graphitic	0.04

Cellulose and cellulose triacetate, although differing in the nature of their carbonisation processes, both form non-graphitic carbons of high porosity.

The high porosity of these carbons is due to the presence of spaces which occur between the crystallites of the disordered regions

of their structures (Section 1.3). In the more highly ordered structure of polyacenaphthylene carbon such spaces are fewer, consequently the porosity is much lower.

Some work on carbons that has been reported has proved of limited value, due to a failure to specify carefully experimental conditions. On the one hand some work reported on the kinetics of gas-carbon reactions contains little detail about the nature of the carbon, its surface or the influence of these factors on reactivity. On the other hand some work reported on the porosity of activated carbons contains little detail of conditions of activation. A number of anomalies that have arisen in the interpretation of results in both fields of study may well be due to these omissions.

In work reported in this thesis, an attempt has been made to carefully control as many experimental aspects of the work as possible in order to facilitate meaningful correlations between the two parts of the work.

The main aims of the work reported in this thesis may be summarised under four headings. These aims are:

(i) To prepare under carefully controlled conditions three polymer carbons having widely different properties and to assess the reproducibility of these carbons.

(ii) To conduct an integrated study of the rates of reaction of the three polymer carbons with carbon dioxide and the consequent

development of pore structure.

(iii)To attempt to relate the development of pore structure to the kinetics of the activation process.

(iv) To compare the behaviour of the three carbons in order to investigate the influence of carbonisation process and degree of graphitic character on the rates of reaction and on the development of pore structure.

The practical programme therefore involved four main stages.

(i) The three polymers were carbonised using carefully controlled conditions. Information, concerning the carbonisation of the polymers, was obtained from carbon yields, non-isothermal kinetic analyses of the resultant thermograms, electron spin resonance measurements and optical microscopy.

(ii) The kinetics of activation of the three carbons, by reaction with carbon dioxide, were investigated in the temperature range 830 - 950°C and Arrhenius parameters were obtained in order to identify the general reaction mechanisms.

(iii)Activated series of the three carbons were prepared at 935°C, a few activated samples of each carbon were also obtained at other temperatures in order to investigate the effect of temperature of activation on porosity.

(iv) The porosities of the prepared samples of each carbon were obtained from measurements of adsorption of carbon dioxide at 195°K and measurements of mercury densities.

The outline of the Thesis

A general discussion of the carbonisation of polymers, the results and discussion of the present work on carbonisation are presented in Chapter 2. A review of the carbon-carbon dioxide reaction, the results and discussion of the rates of activation obtained in the present work are to be found in Chapter 3. Chapter 4 contains a critical review of the methods available for the characterisation of porous solids, together with the results and discussion of the present investigations of porosity. Correlations between rates of activation and the development of porosity of the three carbons are discussed in Chapter 5, together with the influence of graphitic character and the nature of the carbonisation on these two processes. Chapter 6 contains a summary of the results presented in this thesis and a summary of conclusions drawn from them. This chapter is concluded with suggestions for further work in this field.

Experimental details have been omitted from the main body of the thesis and are included in the Appendix. The Appendix is in five parts; in addition to containing details of apparatus and experimental procedure, it contains primary experimental data and the list of references quoted in the thesis.

CHAPTER 2

The Carbonisation of the Polymers

2.1 Introduction (37)

Carbonisation has been defined as the gradual progress of organic compounds towards carbon under the influence of heat (6). For the carbonisation of coal this 'gradual process' has been conveniently separated into three, major, temperature-determined stages: (i) less than $300^{\circ}C$, (ii) $300 - 550^{\circ}C$, (iii) above $550^{\circ}C$. The carbonisation of many organic polymers is analogous to the carbonisation of coal, particularly in the second and third stages of carbonisation.

Stage (i) involves loss of water and carbon dioxide by decarboxylation reactions for coal and other cellulosic materials. For most carbonising vinyl polymers loss of substituents from the side chain occurs in Stage (i). For example, in the case of polyvinyl chloride the first stage of decomposition involves the quantitative loss of hydrogen chloride. Hence generally in Stage (i), peripheral matter is lost from the substance undergoing carbonisation.

Stage (ii) is usually termed 'The Primary Carbonisation' and involves the major breakdown of the carbonising material. It results in the expulsion of volatile products as liquids and gases,

with simultaneous condensation reactions to yield a carbon residue.

The chemical changes in the primary carbonisation stage are accompanied by physical changes which are of great importance in determining the structure of the resultant carbon. Carbonisation can be subdivided into two classes: coking and charring processes. The coking process as exemplified by the carbonisation of polyvinyl chloride or cane sugar, consists of four stages: (a) fusion, (b) intumescence, (c) solidification, and (d) after contraction. In the charring process as exemplified by the carbonisation of cellulose, true fusion does not occur; the substance may swell and contract during the carbonisation but retains some vestige of its original shape.

The factors which determine whether polymers undergo coking or charring processes will be discussed later in this chapter (Section 2.1.2.)

Stage (iii) is usually called 'The Secondary Carbonisation' and occurs at temperatures above $500^{\circ}C$. In the region of $500 - 550^{\circ}C$ the carbonisation of substances undergoes a fundamental change. Evolution of liquids ceases and evolution of gases (mainly hydrogen and methane) increases sharply (6).

For the carbonisation of many materials, paramagnetic susceptibility becomes a maximum in the region $550 - 650^{\circ}C$ (7) and corresponding maxima in electron spin resonance absorption have also been reported (8, 9). The maxima in both cases are followed by a

sharp decrease in the region $650^{\circ}C - 750^{\circ}C$. It has also been shown (10, 11) that above $500^{\circ}C$, the electrical conductivity increases continuously until a temperature of ca.$1100^{\circ}C$ is reached. The increases in paramagnetic susceptibility and E.S.R. absorption indicate the production of a large number of unpaired electrons. These are produced during the formation of the layer planes of the graphitic microcrystals, (Chapter 1. Section 1.2). The latter are formed from polynuclear aromatic compounds in lamellar orientation by homolytic elimination of aliphatic side chains. Such reactions would produce the two effects observed in this temperature region: (a) the sharp increase in the evolution of gases and (b) the trapping of odd electrons in the condensed ring structure where C-C bonds are not formed to replace ruptured linkages. Resonance-stabilised free radicals such as the following have been suggested. (12):-
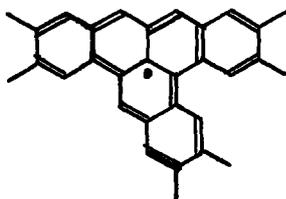
The elimination of side chains from the polynuclear compounds and the evolution of gases can be explained by reactions of the following type (6):-

$$R_2 \cdot CH_3 + R_1 \cdot H = R_1 \cdot R_2 + CH_4 \qquad - \qquad (i)$$

$$R_1 \cdot H + R_2 \cdot H = R_1 \cdot R_2 + H_2 \qquad - \qquad (ii)$$
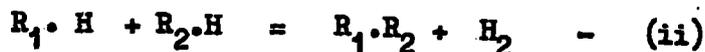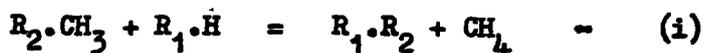
The proportions of gases recovered indicated that at first (550°C) reaction (i) is dominant, whilst at higher temperatures reaction (ii) becomes the more important as the transition to graphitic carbon proceeds.

X-ray evidence from the carbonisation of coals (13) shows that in the region 550°C - 650°C, the crystallite thickness and the mean aromatic layer diameter increase rapidly. This effect points to the formation and growth of graphitic microcrystals in this region. Thus it is clear that the fall in odd electron concentration and increase in electrical conductivity above 650°C are due to the increasingly graphitic nature of the carbon.

Before discussing the factors which influence the graphitisation of polymer carbons it will be necessary to discuss the factors which influence the carbonisation process of polymers, since these in turn influence the degree of graphitic character of the carbons.

2.1.1. <u>Factors influencing the Nature of the Carbonisation Process</u>

Polymer carbons can be produced by coking or charring processes, depending apparently on one or both of the following factors:-

(a) The degree of cross-linking, either in the parent material or produced by the nature of the decomposition. A fully cross-linked substance such as phenol-formaldehyde resin produces a char (14); similarly, substances such as polyacrylonitrile and polyvinylidene chloride, whose initial decompositions are known (14), to involve extensive cross-linking, yield chars on carbonisation.

(b) The presence of oxygen in the first stage of the carbonisation profoundly affects the subsequent carbonisation in certain cases. In the case of polyvinyl chloride, the effect appears to be a great increase in the degree of cross-linking, and may result in the conversion of the carbonisation from a coking process to a charring one. This effect has been explained (15) on the assumption that oxygen is readily adsorbed by the active (probably free-radical) sites resulting from dehydrochlorination, and produces cross-linking during the first stage of decomposition, thus limiting the quantity of material which can volatilise during the second stage. It has been shown (16) that the presence of chlorine during the first stage of decomposition of polyvinyl chloride also produces cross-linking and eliminates fusion during the second stage, whilst the presence of hydrogen has the opposite effect to oxygen and chlorine. The rate of heating affects the carbonisation of some polymers, for example when the rate of heating was $6^{o}C$ min^{-1}. McEnaney and Kipling (16) found that the temperature range over which the main decomposition of cellulose occurred was ca.320° - $330^{o}C$ whereas for a rate of heating of $2^{o}C$ $min.^{-1}$ this temperature range was ca. 250° - $270^{o}C$.

Since the structure and properties of the resultant carbons depend critically on the rate of heating, the atmosphere and the rate of degasification during the carbonisation, it is clear that to obtain reproducible carbons it is essential to have carefully controlled conditions for carbonisation. In the present work, an

attempt has therefore been made to carefully control these factors.

2.1.2. Factors influencing the graphitisation of polymer carbons

J.J. Kipling and his collaborators (17) have extensively investigated the factors which influence the graphitisation of polymer carbons.

They found that the occurrence of graphitisation is determined by the behaviour of the carbon in the carbonisation stage, and in some cases in the earliest stages of decomposition. A graphitising carbon is not obtained unless fusion occurs during carbonisation; substantial cross-linking therefore prevents graphitisation by preventing fusion. For graphitisation to be possible, it is probable that a fused state must be maintained over a range of temperature during carbonisation. Examination of a wide range of carbons by Kipling and co-workers (17) showed that fusion sometimes occurred prior to the formation of a non-graphitic carbon, but a graphitic carbon was not prepared without the occurrence of a fusion stage. More recently Kipling and Shooter (18) have shown that fusion is a necessary but not sufficient step in the formation of a graphitising carbon. They assert that the formation of a graphitising carbon requires the formation of polycyclic aromatic structures at a relatively low temperature, and fusion at a higher temperature to permit appropriate orientation of these structures.

The occurrence of graphitisation is best assessed by X-ray methods, but it is useful to make an initial assessment in terms of a

property of the carbon which is easily measured. Both helium and mercury densities of carbons have been used by Kipling and co-workers (17) to distinguish between graphitic and non-graphitic carbons. Generally graphitic carbons prepared with heat treatment to $2,700^{\circ}C$ have helium densities of over 2 $g.cm.^{-3}$, and mercury densities of over 1.8 $g.cm.^{-3}$, whilst non-graphitic carbons similarly prepared have values of about 1.6 $g.cm.^{-3}$ and less than 1.5 $g.cm.^{-3}$ for helium and mercury densities respectively.

In addition to these properties which distinguish clearly between graphitising and non-graphitising carbons, other physical properties which can be used include E.S.R. and magnetic susceptibility (19), densities in various fluids and polarised light microscopy. Blayden and Westcott (19) examined a number of carbons using polarised light microscopy. Their results show that non-graphitising carbons, whether prepared at high or low temperatures are optically isotropic when viewed through "crossed Nicols". Graphitising carbons however show distinct optical anisotropy which is associated with striations in the carbon which appear to be the result of flow of the material during carbonisation.

2.1.3. The carbonisation of (a) Cellulose, (b) Cellulose Triacetate and (c) Polyacenaphthylene

(a) Examination of the carbon, produced by the thermal decomposition of cellulose in nitrogen, has clearly indicated (20) that the carbonisation is a charring process. Urbanski and co-workers (21)

and more recently Tang and Bacon (22) have followed the decomposition
of cellulose, using infra-red absorption spectra to characterise the
nature of the residue at various stages of the carbonisation.
Cobb (23) has analysed the gaseous products of the decomposition over
the temperature range $300^{\circ}C$ - $1000^{\circ}C$. Their results may be
summarised as follows. Below $300^{\circ}C$, small amounts of water and
carbon dioxide are liberated. The main decomposition commences at
about $300^{\circ}C$ and 90% of the weight loss (mainly aromatic tars)
occurs over the temperature range $300^{\circ}C$ to $400^{\circ}C$. The main
decomposition can be formally represented as a dehydration process,
but the spectral evidence shows the process to be an aromatisation
of the aliphatic structure. Between $330^{\circ}C$ and $575^{\circ}C$, the aromatic
ring systems condense to form larger systems with evolution of
carbon monoxide, methane and other hydrocarbons. At temperatures
above $500^{\circ}C$, hydrogen is evolved in increasing quantities up to
$800^{\circ}C$, whence the decomposition is complete.

(b) The chemical differences between the thermal decomposition
of cellulose and cellulose triacetate are much less marked than the
physical changes which accompany them. The products of the
decomposition of both polymers are similar. The main decomposition
of cellulose triacetate also starts at about $300^{\circ}C$, but in contrast
to the decomposition of cellulose, is accompanied by fusion and
bubble formation (18).

(c) Brazier (24) has investigated the thermal decomposition of

polyacenaphthylene. The thermogravimetric curve for the decomposition of polyacenaphthylene shows it to involve two stages which overlap each other slightly. The carbon produced at $700^{\circ}C$ is a coke, hence the carbonisation process involves fusion. The main decomposition commences at about $370^{\circ}C$ and in the early stages the decomposing polymer remains solidified. As the decomposition proceeds, fusion occurs and a darkening red liquid is formed. This stage results mainly in the liberation of acenaphthylene due to chain sission reactions, other hydrocarbons liberated include fluorocyclene and decacyclene, by cyclodehydrogenation reactions. At $450^{\circ}C$ the second stage begins and results in further loss of hydrocarbons such as acenaphthene. During the second stage bubble formation occurs and the state of the decomposing polymer changes from a black liquid to a solid. Liberation of hydrogen and methane also occurs in the second stage of the decomposition, hydrogen continues to be evolved until a temperature of ca. $900^{\circ}C$ is reached.

2.2 <u>Results obtained in the present Investigations for the Carbonisation of the three Polymers</u>

The experimental details of the preparation and characterisation of the polymers is given in Appendix I. The polymers were carbonised in a modified Stanton Thermobalance, full experimental details of the procedure for carbonisation are given in Appendix II.

2.2.1. Thermogravimetric Data

Thermograms for the carbonisation of the three polymers (Figs.2.1 to 2.3) resemble those reported in earlier studies (14,18,24), except that for small starting weights of polymers (ca.0.1g) the carbon yields were much lower than previously reported (Table 2.1). It was found that for larger starting weights of polymers (ca.2g.) carbon yields increased to about the values quoted in the earlier work. Table 2.1 illustrates the variation of carbon yield at $900^{\circ}C$ with starting weight of the three polymers. The carbon yields were in all cases reproducible within experimental error.

2.2.2. Electron Spin Resonance Data

Electron spin resonance measurements of free spin concentrations in carbons affords an alternative and possibly more sensitive means of testing the reproducibility of carbons than measurements of carbon yields. It has already been mentioned (Section 2.1.1.) that maximum concentrations of unpaired electrons during carbonisation occur in the temperature range $550 - 700^{\circ}C$. Hence the technique is of little value in testing the carbons prepared with heat treatment to ca.$900^{\circ}C$, since the concentration of unpaired electrons is too low to be measured in such cases. However, if the carbonisations are stopped in the temperature range $550^{\circ}C - 700^{\circ}C$ when free-spin concentration is a maximum, a measure of the reproducibility of the carbons is possible.

The following procedure was used to obtain E.S.R. spectra of samples. The polymers were carbonised in the normal manner (Appendix II) but the decompositions were stopped at 650°C and the samples were left in the furnace to cool in an atmosphere of nitrogen. At room temperature they were withdrawn and outgassed at 200°C and 10^{-5} cm.Hg, they were then examined in an E.S.R. spectrometer.

Within the limits of experimental error, three samples of cellulose carbon were found to have the same concentration of unpaired electrons. Similar results were obtained for samples of cellulose triacetate and polyacenaphthylene carbons.

2.3. Discussion of the Results obtained from Carbonisation Studies

2.3.1. Carbon Yields and E.S.R. Data

The reproducibility of carbon yields obtained from a given weight of polymer (Table 2.1.) for all three polymers is strong evidence for the reproducibility of the carbonisation process. This conclusion is supported by the E.S.R. data. (Section 2.2.2.)

The differences in carbon yields previously reported by different workers may be due in part to differences in starting weight of polymer. The higher yields obtained for large weights of polymer must be due to relatively involatile products of carbonisation being trapped in the carbon matrix due to the increased bulk of carbon. Evidence in support of this conclusion is given by Brazier (24), who found that the yield of polyacenaphthylene carbon decreased considerably when the decomposition was carried out

in vacuum. He found that under these conditions, carbonisation
products such as decacyclene and fluorocyclene could escape easily,
whilst at atmospheric pressure they tended to condense in the
structure of the carbon thus increasing the carbon yield.

The maxima found in the E.S.R. spectra of the three polymer
carbons at 650°C agree with Ingram's findings (25). Jackson (26)
has found E.S.R. measurements of carbons to vary sensitively with
their structure; he asserts (27) that such measurements give an
extremely sensitive means of comparing the reproducibility of the
carbonisation procedure used to prepare each carbon.

2.3.2. Non-Isothermal Kinetic Analysis of the Carbonisation of the Polymers

Recent developments in non-isothermal kinetic analysis of
thermogravimetric data provide a further means of characterising
carbonisation processes since the significance of the thermogravimetri
curve can be assessed in terms of experimental kinetic parameters.
A number of workers have devised different methods of analysing
thermogravimetric data of pyrolitic reactions, in order to obtain
the kinetic parameters of the pyrolyses. (28, 29, 30, 31.)

In some cases pyrolysis occurs through a multi-stage mechanism,
where the temperature ranges overlap, resulting in irregular
thermograms that are difficult to analyse. In many cases, however,
including the decomposition of many polymers, the trace follows an
approximately sigmoidal pattern, i.e. the sample weight drops slowly
at first, then drops precipitously over a narrow temperature range

and finally drops slowly until the reaction is complete.

Some of the methods devised to obtain kinetic parameters of pyrolyses have required graphical differentiation of the thermograms (eg.28). This procedure is cumbersome and subject to large errors when the curves are highly precipitous as they usually are. Integral methods, (29, 30), require a curve fitting procedure to obtain the integrals and are not easy to apply. More recently, approximate methods of integrating the rate expressions of the pyrolyses have been employed by Horowitz and Metzger (31) and Coats and Redfern (32). The two methods are similar, differing only in choice of approximation to the integral. It is proposed to discuss in detail the method of Horowitz and Metzger and subsequently to apply the method to the decomposition of the three polymers investigated in the present work.

2.3.3. Horowitz and Metzgers' Method of Non-isothermal Kinetic Analysis

If α is the fraction of reactant which has decomposed after a time t, then the equation connecting the fraction of reactant remaining $(1 - \alpha)$ after a time t with the rate of the reaction at a given temperature is given by:-

$$- \frac{d(1 - \alpha)}{dt} = k(1 - \alpha)^n - \text{Equation 2.1.}$$

where n is the order of reaction for the pyrolysis, and k is the rate constant for the reaction.

The variation of k with temperature T may be expressed as a

function of the activation energy of the reaction by the Arrhenius Equation: $k = A\ e^{-E_a/RT}$ - Equation 2.2. where A is the pre-exponential factor and E_a is the activation energy. If the rate of rise of temperature q is defined as dT/dt then substituting in Equations 2.1. and 2.2. for k and dt, gives:

$$\frac{d(1-\alpha)}{(1-\alpha)^n} = A/q.\ e^{-E_a/RT}.\ dT \quad - \quad \text{Equation 2.3.}$$

In order to integrate Equation 2.3. Horowitz and Metzger have used the fact that near the temperature, T_m, at which the rate of decomposition is a maximum, the following equality is reasonably valid

$$e^{-E_a/RT} = e^{-E_a(1-\theta/T_m)/RT_m} \quad \text{where } \theta = T - T_m \quad - \text{Equation 2.4.}$$

Integration of Equation 2.3. when $n \neq 1$ gives:-

$$\ln\ \frac{1-(1-\alpha)^{1-n}}{1-n} = \frac{E_a\ T}{RT_m^2} - \frac{E_a}{RT_m} + \ln B \quad - \quad \text{Equation 2.5.}$$

where $B = A/q.\ e^{-E_a/RT_m}.\ RT_m^2/E_a$ - Equation 2.6.

By considering the condition for the reaction rate to be a maximum (i.e. $d^2(1-\alpha)/dt^2 = 0$) it can be shown that:-

$$nB = (1-\alpha)_m^{1-n} \quad - \quad \text{Equation 2.7.}$$

where $(1-\alpha)_m$ is the value of $(1-\alpha)$ at T_m. If $T = T_m$ then substituting for B from Equation 2.7., in Equation 2.5. shows that when $n \neq 1$, $B = 1$.

Integration of Equation 2.3. when $n = 1$ yields:-

$$\ln \ln \frac{1}{(1-\alpha)} = \frac{E_a T}{RT_m^2} - \frac{E_a}{RT_m} + \ln B \quad - \text{ Equation } 2.8.$$

From Equation 2.7. when $n = 1$, $B = 1$, hence $\ln B$ in Equations 2.5. and 2.8. disappears. When $n = 1$, a plot of $\ln \ln \frac{1}{(1-\alpha)}$

against T should give a straight line whose slope is related to E_a, the energy of activation of the reaction. The reaction order n, when $n \neq 1$, can be estimated from the value of $(1-\alpha)_m$ using Equation 2.7. Horowitz and Metzger have tabulated values of $(1-\alpha)_m$ for common reaction orders (33).

Values of $\ln \ln {}^{1/}(1-\alpha)$ were plotted against corresponding values of temperature, $T^\circ K$, for the decomposition of the three polymers used in the present investigations (Figs. 2.4. to 2.6.). For polyacenaphthylene (Fig. 2.6.) the analysis was applied to the first stage of the decomposition only. The termination of this stage was estimated by a method suggested by Smith (34). The results have been obtained using a value of $n = 1$, and the plots (Figs.2.4. to 2.6.) are linear for values of α from 0. to 0.9.

The thermograms obtained for the decomposition of the polymers (Figs. 2.1. to 2.3.) involved precipitous weight losses and made the estimation of the value of $(1-\alpha)$ at the maximum rate of decomposition of a polymer, $(1-\alpha)_m$, difficult. In each case, however, $(1-\alpha)_m$ was estimated to be ca. 0.35 and hence using Equation 2.8. $n = 1$. Since plots of $\ln \ln {}^{1/}(1-\alpha)$ against $T^\circ K$ (Figs. 2.4. to 2.6.) were straight lines the choice of $n = 1$ appears

to be justified. From the slopes of Figs. 2.4. to 2.6. the activation energy E_a for each decomposition was calculated and corresponding T_m values were obtained from the intercepts on the temperature axis. These values are tabulated in Table 2.2.

The extremely rapid first stage of the decomposition of polyacenaphthylene is reflected in the unrealistically high value of 225 k.cal.mole.$^{-1}$ obtained for the activation energy of the decomposition. The values of 57 and 36 k.cal.mole,$^{-1}$ obtained for the activation energies of the relatively slow decompositions of cellulose and cellulose triacetate are of the same order of magnitude as those obtained for various polymers by Madorsky (35) and are in marked contrast to the value obtained for polyacenaphthylene.

The unrealistically high value obtained for the activation energy of the decomposition of polyacenaphthylene is almost certainly due to a mass transport effect. In support of this explanation, Van Krevelen and co-workers have shown (36) that in the degasification of coals, some of the metaplast escapes from the reaction system because it is carried along as a tar mist by the escaping gases. The effect is to give spuriously high activation energies. Van Krevelen has also asserted (37) that as the rate of heating is increased then mass transport becomes more important. It seems likely therefore that using the present rate of heating, (ca 4°C min^{-1}) tars produced in the decomposition of polyacenaphthylene are removed along with the escaping gases. In the Horowitz and Metzger method of non-isothermal kinetic analysis the activation energy Ea is assumed to be independent of the rate of heating q. In view of the results obtained in the present work for polyacenaphthylene, it would appear that if mass transport contributes to the weight loss accompanying the decomposition

of a polymer the value of E_a so obtained may depend on q. In such

cases care must be taken in employing the Horowitz and Metzger method

2.3.4. Micrographical Evidence

The optical micrographs of the three unactivated carbons

(Figs.2.7. to 2.9.) clearly illustrate the differences between them.

These show that a pellet of unactivated cellulose carbon has an outer

surface pitted with holes about a micron across, which presumably are

large macro-pores. Cellulose triacetate carbon on the other hand

has an extremely clean surface, one or two large blow holes being

the only notable feature.

Unactivated polyacenaphthylene carbon in contrast to the

non-graphitic cellulose and cellulose triacetate carbons has a surface

typical of a graphitic carbon with flow patterns and striations

characteristic of an optically anisotropic material.

As might be expected from Blayden's and Westcott's findings

(Section 2.1.2.), polyacenaphthylene carbon being graphitic displayed

birefringence on examination with polarised light.

Brookes and Taylor (38) have recently studied the formation of

graphitising carbons from the liquid phase with the aid of electron

and optical microscopy. They assert that the formation of

graphitising low-temperature carbons by solidification from a liquid

phase proceeds via the separation of a mesophase having properties

similar to those of liquid crystals. Initially the mesophase,

consisting of planar aromatic compounds of high molecular weight,

separates from the isotropic liquid as spherical droplets having a considerable degree of molecular order, with the aromatic sheets stacked in parallel array. As the temperature rises, the spheres coalesce and extended regions of uniform orientation are formed until on solidification a semi-coke is formed. It is the lamellar arrangement of the molecules in these regions of uniform orientation that favours the formation of a graphitic carbon at high temperatures. Hence when isolated spheres are heated to graphitising temperatures, Brooks and Taylor have observed (38) that contraction of the spheres occurs in the direction perpendicular to the preferred orientation. The bodies become elliptical in section and each is converted to a mass of small graphite crystals. They have concluded from these studies that the spheres consist of polynuclear aromatic molecules of the order of tens of aromatic rings in average size. The molecules appear to have local stacking symmetry only and no general three-dimensional order. The orientation of the structure so formed varies regularly through the sphere from lamellar at the centre to radial at the surface. This structure is therefore due to two major factors:- (i) the overall spherical shape is a result of surface tension forces, and (ii) the presence of large planar molecules and their tendency to pack together changes their orientation from radial at the surface of the spheres to lamellar in the interior.

It is clear that the three polymers give rise to very different carbons on thermal degradation. Cellulose does not fuse and forms a

non-graphitic carbon; cellulose triacetate fuses but does not form a graphitic carbon; polyacenaphthylene fuses and forms a graphitic carbon. The reason that cellulose triacetate fuses but does not form a graphitic carbon is due to the fact that the fusion occurs at too low a temperature for the necessary orientation to take place (18). Hence the nature of the carbonisation process is also characteristic and reproducible for each polymer. In Chapter 5 it will be shown how the different natures of each carbon affect the development of porosity when the carbons are activated with carbon dioxide.
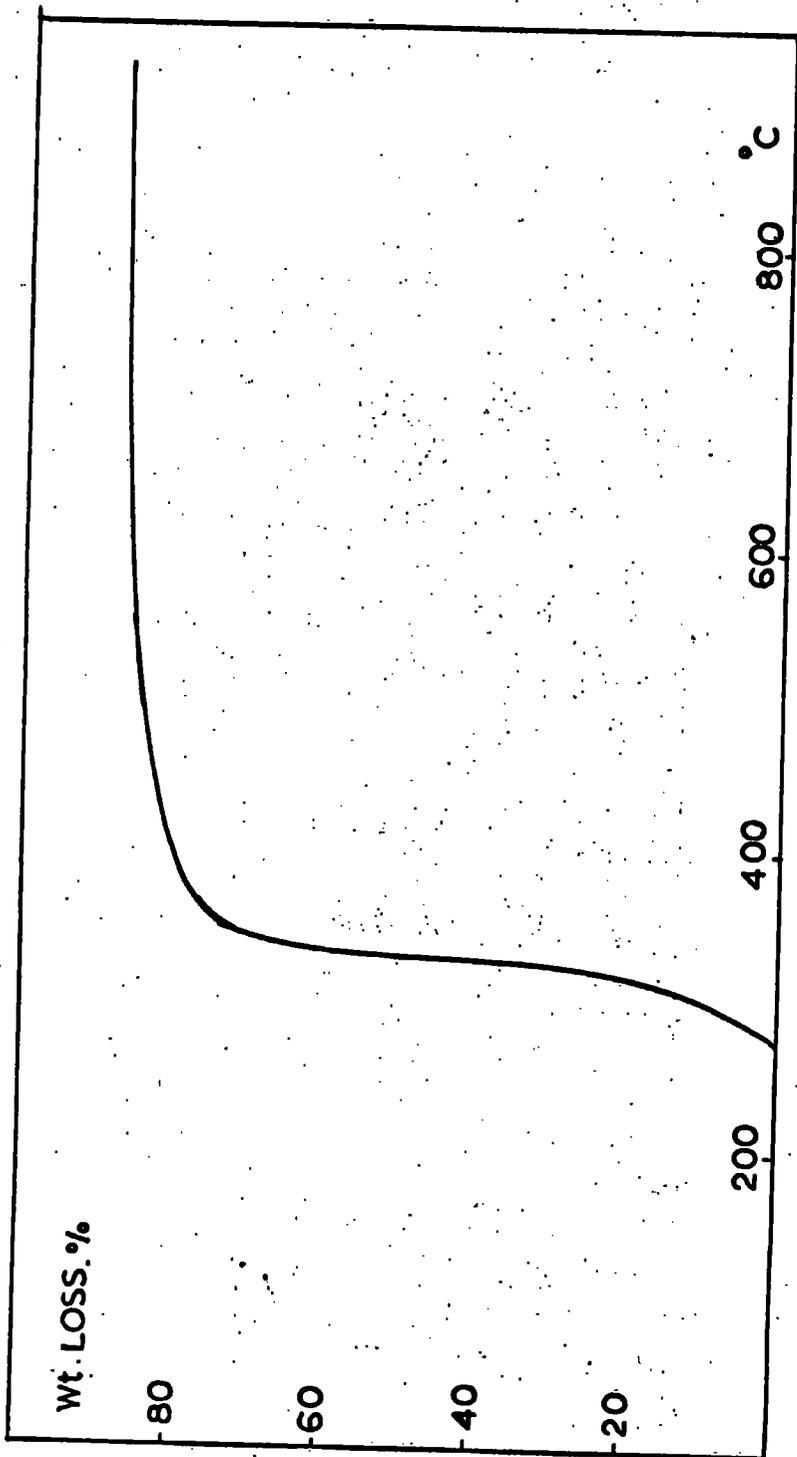
FIG. 2.1.   DECOMPOSITION OF CELLULOSE
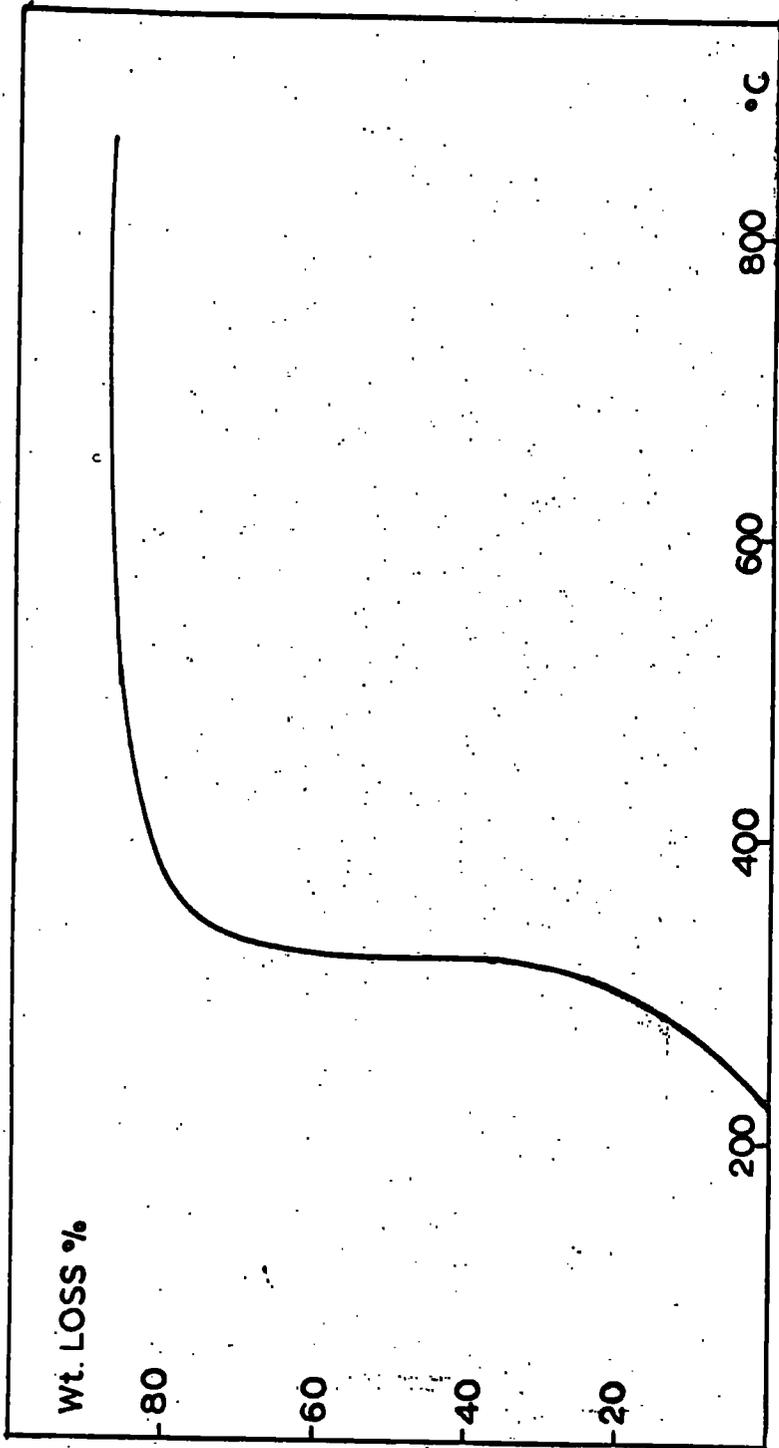
FIG. 2.2. DECOMPOSITION OF CELLULOSE TRIACETATE
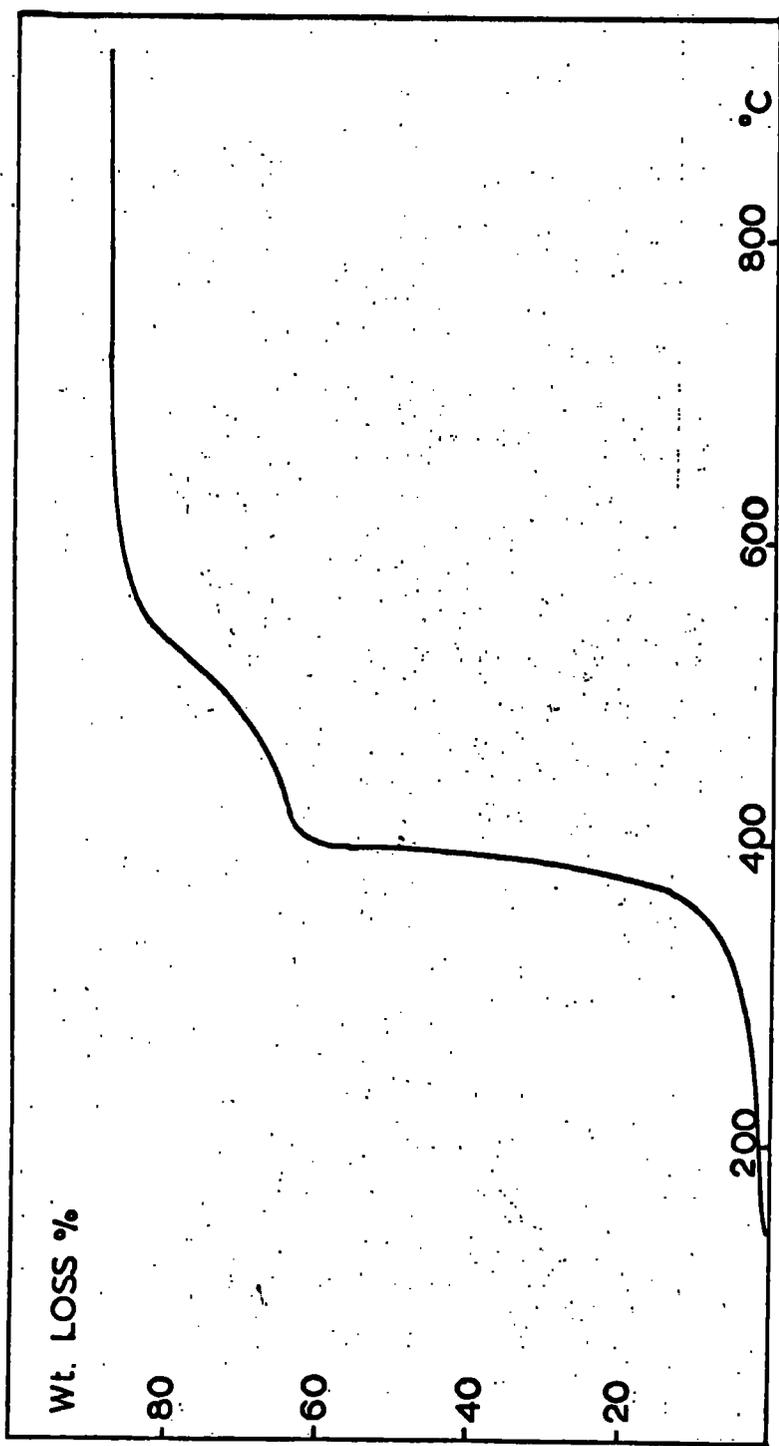
FIG. 2.3. DECOMPOSITION OF POLYACENAPHTHYLENE
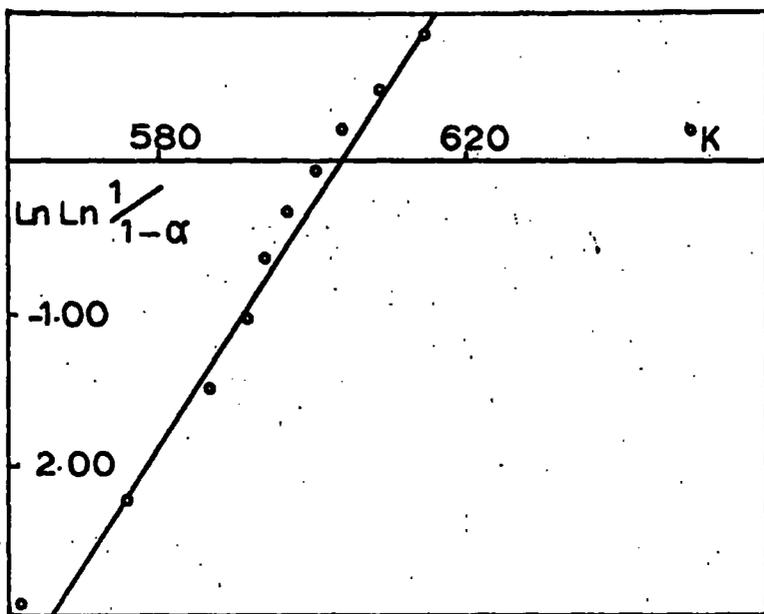
FIG. 2.4. NON – ISOTHERMAL KINETIC
ANALYSIS OF CELLULOSE
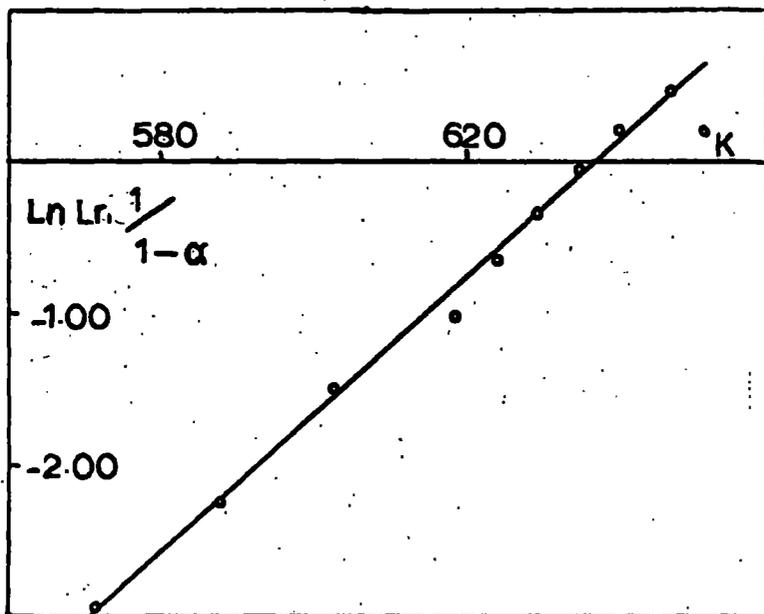
FIG. 2.5. NON ISOTHERMAL KINETIC
ANALYSIS OF CELLULOSE TRIACETATE
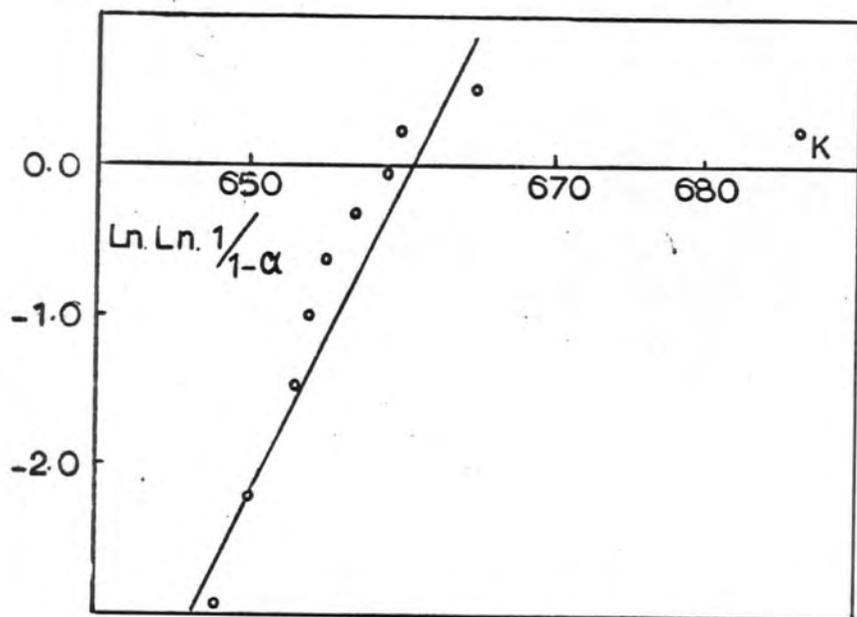
FIG. 2.6. NON–ISOTHERMAL KINETIC
ANALYSIS OF POLYACENAPHTHYLENE.
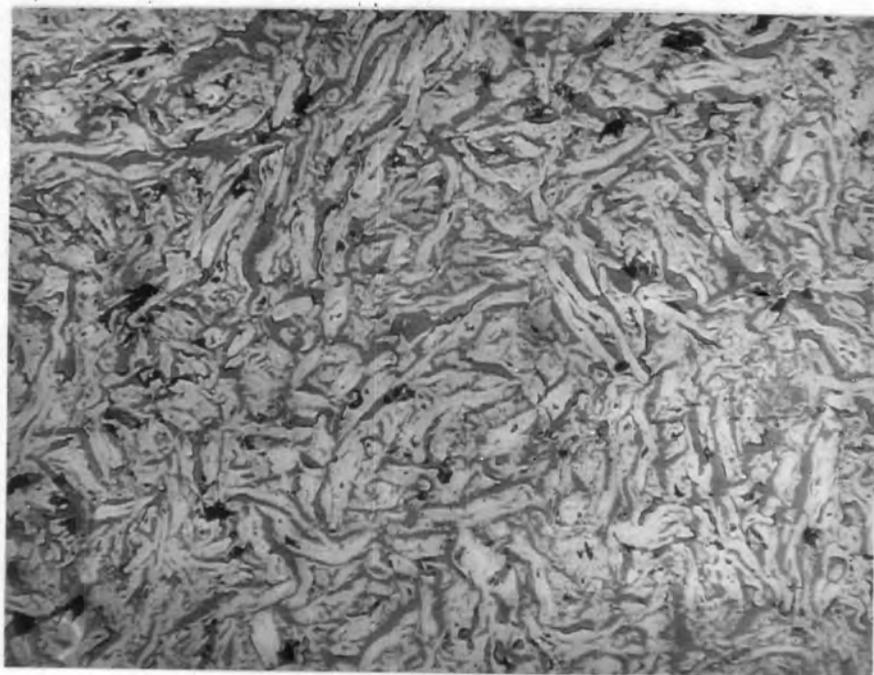
FIG. 2.7. UNACTIVATED CELLULOSE CARBON
(×300)

FIG. 2.8. UNACTIVATED CELLULOSE TRIACETATE
          CARBON (×100)
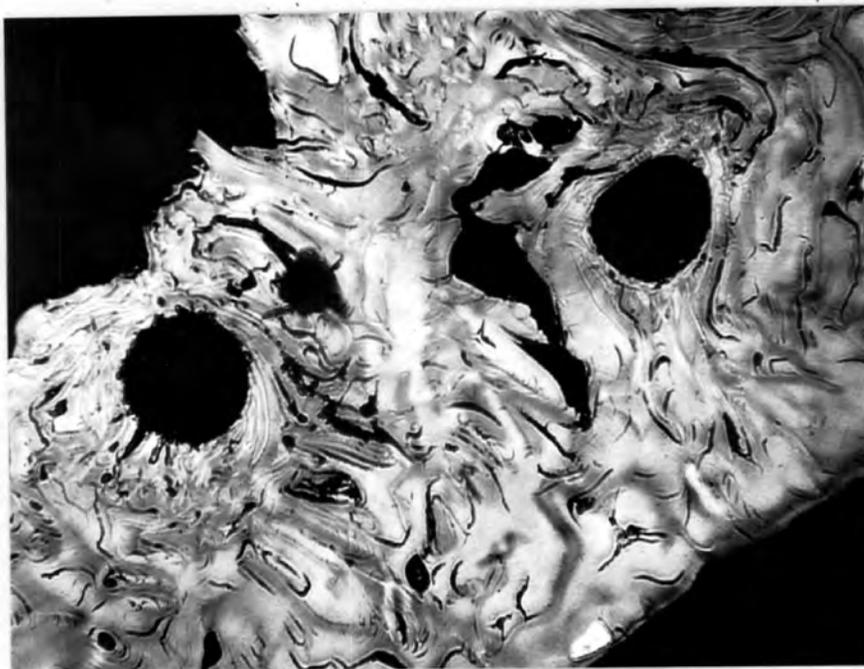
FIG. 2.9. UNACTIVATED POLYACENAPHTHYLENE
          CARBON (×150)

Table 2.1.

Variation of Carbon Yield with Starting Weight of Polymer

Polymer	Approximate Starting Weight (g)	Carbon Yield at 950°C. (%)	Reference
Cellulose	0.15	14.9 ± 1.2	*
	0.7	17.4 ± 0.5	*
	1.0	23.5	(14)
	2.0	20.5 ± 0.5	*
Cellulose	0.08	11.8 ± 1.2	*
Triacetate	2	14.8 ± 0.5	*
	1	16	(14)
Polyacenaphthylene	0.08	13.4 ± 1.2	*
	2	36.0 ± 0.5	*
	1	32.5	(24)

* denotes present work.

Table   2.2.

Non-Isothermal Kinetic Parameters

Polymer	T_m ($^\circ$K)	E_a(k.cal.mole^{-1})
Cellulose	603	57 ± 5
Cellulose Triacetate	639	36 ± 5
Polyacenaphthylene	659	225 ± 20

Rate of heating = 4°C.min^{-1}.

Chapter 3

The Rates of Activation of the Carbons by Carbon Dioxide

3.1 Introduction

In this chapter previous work on the reaction of carbon
with carbon dioxide is reviewed and the results obtained in the
present work are presented and discussed.

Although it is not the principal purpose of the present work
to contribute to the elucidation of the mechanism of the carbon-
carbon dioxide reaction, a clear understanding of the factors which
govern the rate of this reaction is necessary, if a correlation
between the rates of activation and the development of porosity of
the carbons is to be attempted.   It will be useful, therefore, to
discuss at length, the thermodynamic, chemical, and physical factors
which affect the rate of the carbon-carbon dioxide reaction;   these
have been comprehensively reviewed by Walker and his co-workers.(39)

3.1.1. Thermodynamics of the Carbon-Carbon Dioxide Reaction

The reaction between carbon and carbon dioxide, $C + CO_2 = 2\ CO$,
is endothermic and the heat of reaction, ΔH is $+ 40.79$ k.cal. at
$18^{\circ}C$ and 1 atmosphere, the carbon being β graphite. $Log_{10}Kp$ for the
reaction has values of 1.08 and 1.76 respectively at temperatures of
$1100^{\circ}K$ and $1200^{\circ}K$ and at 1 atmosphere pressure.   Hence at these
temperatures the forward reaction is regarded as unrestricted

by equilibrium considerations.

3.1.3. The Mechanism of the Carbon-Carbon Dioxide Reaction

In this section the factors influencing the rate of reaction when it is controlled by the chemical reaction of the surface of the carbon, are considered. The role of mass transport will be considered in Section 3.2.

A large amount of evidence has been accumulated which shows that one of the steps involved in any gas-carbon reaction is the chemisorption (in whole or in part) of the gas on the surface of the carbon. It is also known that some of the products of the reactions are chemisorbed under certain conditions. Hence the first step in the reaction between carbon and carbon dioxide is postulated to be the chemisorption of a molecule of carbon dioxide on the carbon surface,

(i) $2C_f + CO_2 \longrightarrow C_f + C(CO_2)$

where C_f represents a free carbon site, and $C(CO_2)$ represents a chemisorbed molecule of carbon dioxide. It is generally agreed that chemisorption takes place on a relatively small fraction of the total surface of the carbon.

As early as 1915 Langmuir (40) pointed out that the stoichiometric representation of the carbon-carbon dioxide reaction: $C + CO_2 \rightleftharpoons 2CO$; was not true mechanistically, and at $950^{\circ}C$, what happened was more accurately represented by the following equation:- $C + CO_2 \rightleftharpoons CO + C(O),$

where $C(0)$ represents a chemisorbed oxygen atom.

Gadsby and co-workers (41) in 1948 and subsequently other workers, (42, 43,) have agreed that the experimental data of the carbon-carbon dioxide reaction fit an equation of the following form:-

$$\text{Rate} = \frac{k_1 \, P_{CO_2}}{1 + k_2 P_{CO} + k_3 \, P_{CO_2}} \qquad - \text{ Equation 3.1.}$$

where P_{CO_2} and P_{CO} are the partial pressures of carbon dioxide and carbon monoxide, and the constants k_1, k_2 and k_3 are functions of one or more rate constants. The following steps have been postulated for the reaction:-

(i) $C_f + CO_2(g) \rightleftharpoons C(CO_2)$

(ii) $C_f + C(CO_2) \rightleftharpoons C(0) + C(CO)_A$

(iii) $C_f + C(0) \rightleftharpoons C(CO)_B$

(iv) $C(CO)_A \rightleftharpoons CO(g) + C_f$

(v) $C(CO)_B \rightleftharpoons CO(g) + C_f$

(vi) $CO(g) + C_f \rightleftharpoons C(CO)_c$
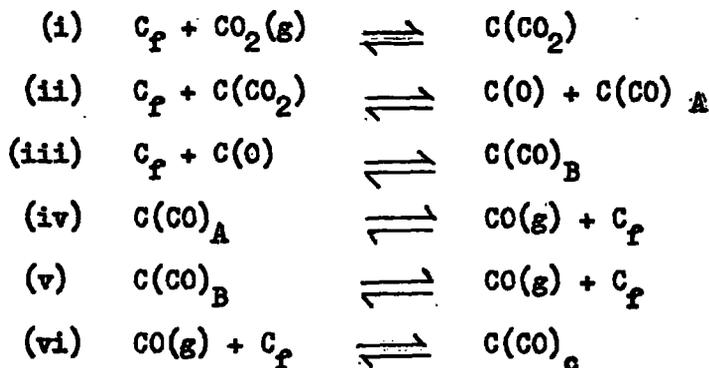
where C_f, $C(0)$, and $C(CO_2)$ are as previously described and $C(CO)$ represents a chemisorbed molecule of carbon monoxide.

To obtain Equation 3.1. from this mechanism it is necessary that some of the steps (i) to (vi) occur at a negligible or extremely fast rate. It has been observed (42) that carbon monoxide gas is an immediate product of the chemisorption of carbon dioxide on carbon and that step (i) is not immediately reversible, i.e. adsorbed carbon

dioxide does not immediately desorb. It may be assumed consequently that the lives of the species $C(CO_2)$ and $C(CO)_A$ are short, and the number of steps reduces to four.

(vii) $C_f + CO_2(g)$ $\rightleftharpoons$ $C(O) + CO(g)$

(iii) $C_f + C(O)$ $\rightleftharpoons$ $C(CO)_B$

(v) $C(CO)_B$ $\rightleftharpoons$ $CO(g) + C_f$

(vi) $CO(g) + C_f$ $\rightleftharpoons$ $C(CO)_c.$
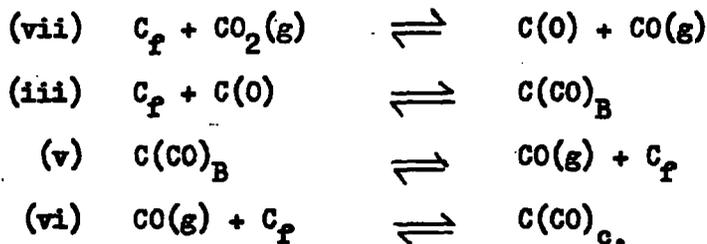
There is a further possibility that reaction (iii) may be slow (Case 1 or fast, (Case 2.) in comparison with reaction (v). The rate expression to be derived will be the same in each case, however, the interpretation of the rate constant J_3 in Equation 3.2. will be different. In Case 1. J_3 represents the rate constant for the surface rearrangement, of reaction (iii); in Case 2. J_3 represents the rate constant for the desorption of $(CO)_B$, reaction (v). The experimental evidence at the moment is insufficient to decide whether Case 1.or 2. holds, in fact it may be that both hold, but in different temperature ranges. Assuming that Case 1. holds, the number of steps can now be reduced to three:-

(vii) $C_f + CO_2(g)$ $\rightleftharpoons$ $C(O) + CO(g)$

(viii) $C(O)$ $\rightleftharpoons$ $CO(g)$

(vi) $CO(g) + C_f$ $\rightleftharpoons$ $C(CO)_c$
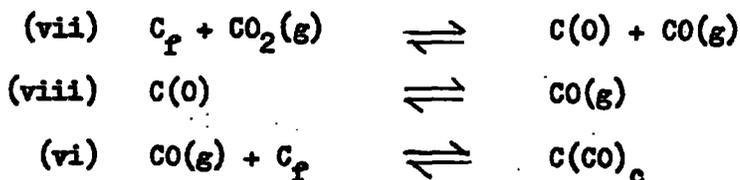
Equation 3.1. can now be shown to be consistent with at least two mechanisms where carbon monoxide retards the gasification reaction. Mechanism A applies when the rates of back reactions (vii) and (viii)

are negligible.

Mechanism A

(vii) $\quad C_f + CO_2(g) \quad \xrightarrow{\quad i_1 \quad} \quad C(O) + CO(g)$

(viii) $\quad C(O) \quad \xrightarrow{\quad J_3 \quad} \quad CO(g)$

(vi) $\quad CO(g) + C_f \quad \underset{J_2}{\overset{i_2}{\rightleftharpoons}} \quad C(CO)_c$
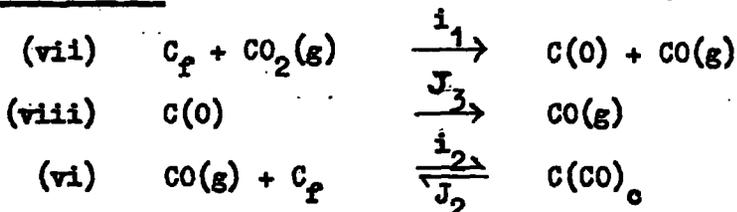
where i_1, J_3, i_2, and J_2 are the rate constants for these reactions. In the steady state the rates of formation and removal of surface complexes are assumed equal. If θ_1 and θ_2 are the fractions of the active surface area covered by oxygen atoms and carbon monoxide molecules, respectively, then the relative number of active free carbon sites (C_f) can be expressed as $(1 - \theta_1 - \theta_2)$. Hence by equating the rates of formation and removal of $C(O)$ and $C(CO)_c$, and eliminating θ_2, the following expression for the rate is obtained:-

$$\text{Rate} = J_3 \theta_1 = \frac{i_1 P_{CO_2}}{1 + i_2/J_2 P_{CO} + i_1/J_3 P_{CO_2}} \quad - \text{Equation 3.2.}$$

which is identical to Equation 3.1. if $i_1 = k_1$ and $i_2/J_2 = k_2$ and $i_1/J_3 = k_3$.

Mechanism B applies when the rate of back reaction (viii) is negligible and (vi) does not take place to any extent.

Mechanism B

(vii) $\quad C_f + CO_2(g) \quad \underset{J_1}{\overset{i_1}{\rightleftharpoons}} \quad C(O) + CO(g)$

(viii) $\quad C(O) \quad \xrightarrow{\quad J_3 \quad} \quad CO(g)$
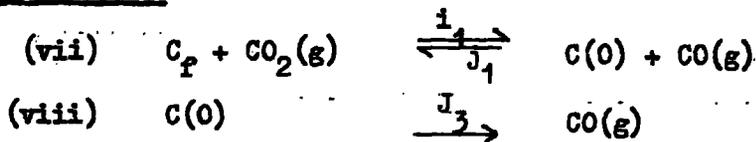
Equating the rates of formation and removal of C(O), and letting θ, b
the fraction of the surface covered with oxygen atoms,

$$\text{Rate} = J_3\,\theta_1 = \frac{i_1\,P_{CO_2}}{1 + J_1/j_3\,P_{CO} + i_1/j_3\,P_{CO_2}} \quad \ldots \ldots \ldots \quad - \text{Equation 3.3.}$$

which is again identical to Equation 3.1. if $i_1 = k_1$, $J_1/j_3 = k_2$,
and $i_1/j_3 = k_3$.

Mechanisms A and B both state that carbon monoxide retards the
gasification of carbon by carbon dioxide, by decreasing the number
of surface oxygen atoms in the steady state. In mechanism A, θ_1
is reduced by chemisorption of carbon monoxide molecules by a fraction
of the active sites. In mechanism B, θ_1 is decreased by the
reaction of gaseous carbon monoxide with chemisorbed oxygen atoms.

Gadsby and co-workers (41) support mechanism A with evidence
from chemisorption experiments and measurements of activation energy,
whilst Reif (42) disputes the interpretation by Gadsby and co-workers
of their results for the chemisorption experiments and supports
mechanism B. Reif however does admit the possibility that both
retardation mechanisms hold but under different conditions of
temperature and pressure.

Ergun's results (43) support mechanism B. Using three types
of carbon of different graphitic character, having varying mineral
content, (and, although not reported, were most probably of varying

surface area) he found that the equilibrium constant K for the reaction $C_f + CO_2(g) \rightleftharpoons C(0) + CO(g)$ was independent of the carbon used and that the reaction had an average value for ΔH over the temperature range of 800 - 1400°C, of + 23 k.cal.mole^{-1}. Ergun thus thinks that the equilibrium has an effect on the rate of gasification. Strickland-Constable (44) supports mechanism B; he found (45) that the rate of adsorption of carbon monoxide on carbon was too low to account for the retardation.

A number of workers have used radioactive carbon, C^{14}, as a tracer to study oxygen and carbon exchange reactions occurring during the gasification of carbon with carbon dioxide. Bonner and Turkevich (46) have found that the forward reaction (vii) is rapid on charcoal at temperatures of about 800°C and a pressure of a quarter of an atmosphere. They also found that reaction (viii) was slow and unidirectional, since there was no detectable transfer of activity to a charcoal surface left in contact with radioactive carbon monoxide for some time. However, they did find evidence that a small amount of carbon from radioactive carbon dioxide was transferred to the charcoal surface. Brown (47) has suggested that in the case of sugar carbon, the exchange with carbon from radioactive carbon dioxide, occurs immediately the radioactive carbon dioxide molecule hits the carbon surface, and the oxygen atoms depart with two new carbon atoms.

Greenhalgh and co-workers (48) have recently claimed to have shown that the general mechanism of the carbon-carbon dioxide reaction

as previously discussed in this chapter is oversimplified. If retardation of the rate of reaction by carbon monoxide gas does not occur then Equation 3.1. reduces to:-

$$Rate = \frac{k_1 \, P_{CO_2}}{1 + k_3 \, P_{CO_2}} \quad\quad - Equation \; 3.4.$$

which has the form of the Langmuir Isotherm Equation. Hence at high pressures of carbon dioxide, the rate should be independent of the pressure. Greenhalgh and co-workers, studying the activation of polyvinyl chloride and polyvinylidene chloride carbons by carbon dioxide, have found a different pressure dependence to that predicted by Equation 3.4. They studied the reactions in the pressure range 1 - 12 cm.Hg, and in the temperature range 750 - 850°C. The amount o burn-out of the carbons was very small in order to prevent the formation of a significantly large amount of carbon monoxide gas which would thus retard the reaction.

In order to interpret the pressure dependence of their results, Greenhalgh and co-workers have devised a mechanism for the reaction which involves two types of reactive site, A and B. At type A sites the following reactions are postulated to occur:-

$$CO_2 + C_{nf} \quad \underset{k_1}{\overset{k_1}{\rightleftharpoons}} \quad C_n(CO_2)$$

$$C_n(CO_2) + CO_2 \quad \overset{k_2}{\longrightarrow} \quad C_{n-1}(CO_2) + 2\,CO\,(g)$$

where C_{nf} represents n free carbon sites capable of reaction, and

from which the rate is given by:-

$$\text{Rate} = X_A \frac{k_1 \; k_2 \; P_{CO_2}^2}{k_1 \; P_{CO_2} + k_1'} \qquad - \text{Equation 3.5.}$$

where X_A is the concentration of type A sites.

At type B sites, the following reactions are postulated to occur:

$$CO_2 + C_{nf} \xrightarrow{k_1} C_n(CO_2)$$

$$C_n(CO_2) \xrightarrow{k_3} C_n(O) + CO(g)$$

$$C_n(O) \xrightarrow{k_4} CO(g) + C_{n-1}$$
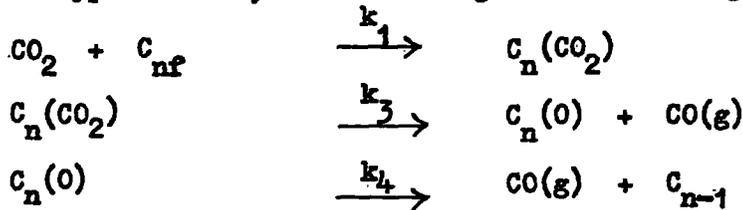
and the rate is given by:-

$$\text{Rate} = X_B \frac{k_1 \; k_3 \; k_4 \; P_{CO_2}}{k_1 \; (k_3 + k_4) \; P_{CO_2} + k_3 \; k_4} \qquad - \text{Equation 3.6.}$$

where X_B is the concentration of type B sites. Greenhalgh and co-workers have concluded that the reactive sites in the non-graphitising polyvinylidene carbon are predominantly of type A and hence the rate of activation of this carbon has the simple pressure dependence given by Equation 3.5. For the graphitising polyvinyl chloride carbon they have concluded that the concentrations of type A and type B sites are approximately equal and the reaction rate has the more complicated pressure dependence of the rate equation obtained by the addition of Equations 3.5. and 3.6.

This reaction mechanism postulates that chemisorption of carbon dioxide is a relatively slow step in the reaction, in contrast to the

mechanisms derived by Gadsby and earlier workers, in which the
life time of surface carbon dioxide complexes were assumed to be
extremely short. Greenhalgh and co-workers assert that the
evidence against the existence of chemisorption of carbon dioxide
at temperatures above $600^{\circ}C$ is weak, and claim to have shown in
unpublished work that desorption of carbon dioxide from carbon
surfaces is possible at temperatures in excess of $1000^{\circ}C$. In
conclusion, Greenhalgh and co-workers claim that the results of other
workers, including Gadsbycan be explained in terms of their mechanism.

3.2. The Role of Mass Transport in Gas-Carbon Reactions

3.2.1. Introduction

Heterogeneous reaction rates involving a porous solid and a gas
may be controlled by one or more of three main steps:

Step (i)   Mass transport of the reacting gas and products across a
relatively stagnant layer of gas between the exterior surface of the
solid and the main gas stream.

Step (ii)   Mass transport of the reacting gas from the exterior
surface to an active site beneath the surface and mass transport of
the products in the opposite direction.

Step (iii) Chemisorption of the reactant, wholly or in part; a
rearrangement of the chemisorped species on the surface to a
desorbable product(s); and desorption of the product or products from
the surface. Ideally the variation of reaction rate with temperature
can be divided into three main zones, as shown in Fig.3.1. as
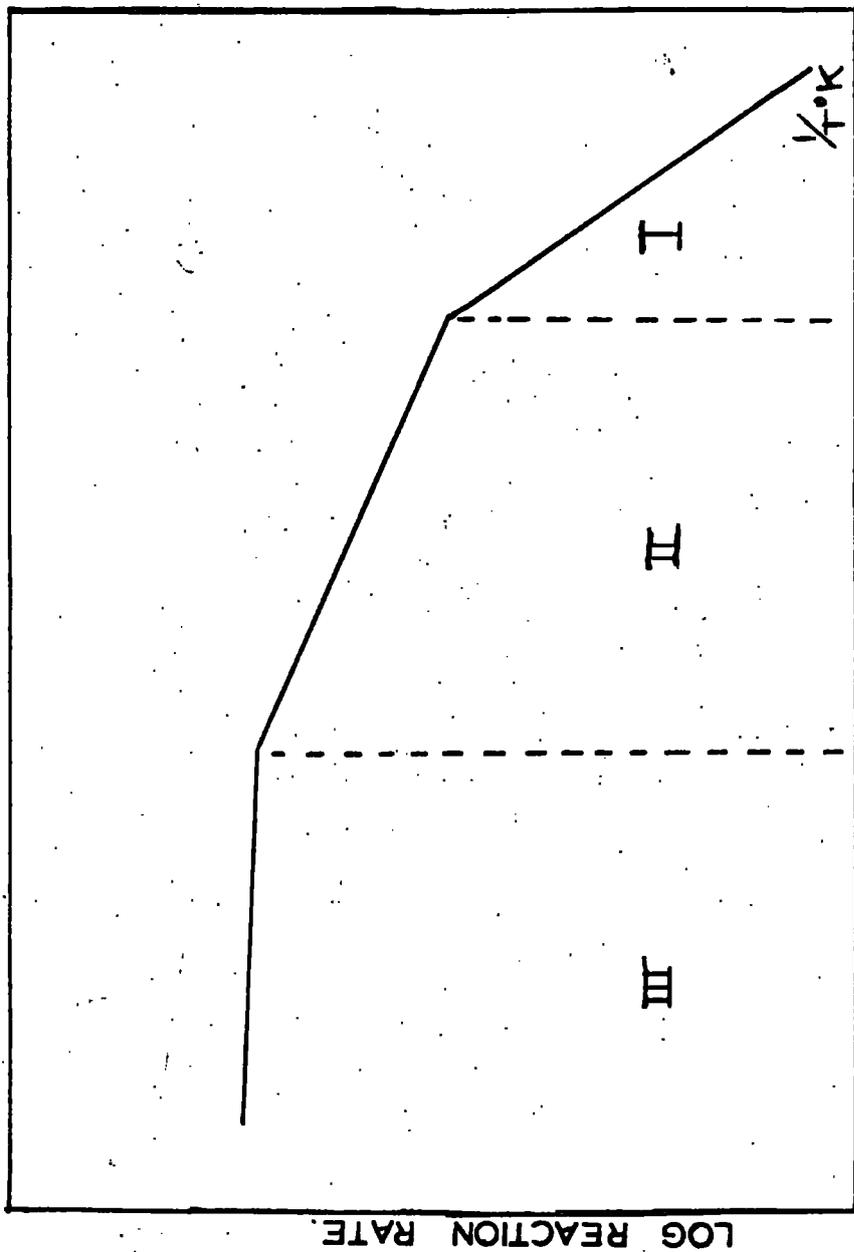
FIG. 3.1. WICKE'S CLASSIFICATION OF REACTION ZONES.

discussed by Wicke and co-workers (49, 50, 51.).

In the low-temperature zone, i.e. Zone I, the reaction rate is controlled solely by the chemical reactivity of the solid (step iii). The measured activation energy Ea has been called the "true" activation energy E_t of the reaction by Wicke and his co-workers. The utilisation efficiency factor η of the reaction is defined as the ratio of the experimental reaction rate to the rate which would be found if the gas concentration was uniform throughout the solid; this is almost unity in Zone I.

In the intermediate temperature zone, i.e. Zone II, the concentration of the reactant gas falls to zero within the solid, at some distance from the centre of the solid. The reaction rate is controlled jointly by steps (ii) and (iii). It has been shown (52) that in this zone the activation energy is one-half of the "true" activation energy, as defined by Wicke and η is less then one-half.

In the high temperature zone, i.e. Zone III, the concentration of reactant gas goes to a small value at the exterior surface of the solid. (This does not mean that reaction penetration into the porous carbon is necessarily zero.) The reaction rate is controlled by step (i). Increase in temperature affects the reaction rate by determining how much additional reactant can reach the exterior surface per unit time. Since bulk transport processes have low activation energies, the apparent activation energies in Zone III are low, usually less than 10 k.cal.mole.$^{-1}$; η is very much less than one.

In practice the ideal conditions of steps (i) and (iii) may not hold and the simplified picture of Fig. 3.1. may not be correct, as the following examples show:

(i) The reactant concentration gradient across the relatively stagnant gas film between the exterior surface of the solid and the main gas stream, can vary considerably from zero before the reactant concentration goes to zero in the solid. This has the effect of removing Zone II and results in a longer transition from Zone I to III. This situation is most likely to occur at low flow rates and with small particle sized samples, where the external surface area-to volume ratio becomes large and the possibility of the reactant concentration going to zero in the particle becomes less.

(ii) The rate controlling part of step (iii) (the chemical step) can change with increasing temperature, hence in Zone II the contribution to the measured activation energy by the chemical step in the reaction may also have changed. In such a case the measured activation energy will correspond to one-half the activation energy of the chemical step in this Zone, and not one-half the activation energy of the chemical step in Zone I.

(iii) In Zone I, the concentration of products within the porous solid is negligible and reaction retardation is likewise negligible. In Zone II the concentration of products within the solid becomes comparable with that of the reactant and reaction retardation may occur to a significant degree. (Chapter 3. Section 3.6.2.) If

retardation of the reaction occurs then the activation energy of the chemical step in the reaction becomes a complex mixture of activation energies for different rate constants which refer to the different processes in the chemical step of the reaction.

3.2.2. Rates of Reaction in Zones II and III

It has been shown (53) that the rate of reaction in Zone II i.e. the diffusion and chemically controlled zone is given by:-

$$dw/dt = C_R^{(m + 1)/2} \sqrt{K_v \, Deff} \qquad - \text{Equation 3.7.}$$

where dw/dt is the rate of the reaction per unit area of exterior surface, C_R is the reactant gas concentration at the exterior surface of the sample, K_v is the specific rate constant per unit volume, m is the order of reaction, and Deff is the effective diffusion coefficient of the reactant gas through the sample. The derivation of Equation 3.7. requires certain assumptions. It assumes that all the pore surface area at a given penetration corresponding to a gas concentration C_R is available for reaction at concentration C_R. Statistically it is assumed that the gas concentration at any depth of penetration into the sample is constant over the sample, that is the profile of gas concentration is the same in each series of pores reaching the centre of the sample. This will be true if the pores are interconnected at short distances. It is also assumed that the coefficient of diffusion remains constant throughout all pores, and finally that the surface area available for reaction and the over-all reaction rate remain constant over a considerable range of burn-out.

Both Wicke and Walker (49, 54.) have produced evidence which support this last assumption.

Due to the absence of data concerning the gas concentration for a given penetration of the sample, Equation 3.7. has not been used in the present work.

It has been shown (39) that the rate of reaction in Zone III is given by:-

$$\frac{dw}{dt} = \frac{C_g \, D_{FREE}}{S} \qquad - \text{Equation 3.8.}$$

where C_g is the concentration of the gas stream flowing over the sample and D_{FREE} is the diffusion coefficient of the gas through the stagnant film of gas, which covers the external surface of the carbon, the stagnant film having a thickness S. It can be seen that the reaction rate is first order with respect to the concentration of the gas stream. Day (55) has confirmed this conclusion for the carbon-oxygen reaction. He also confirms that the temperature dependence of the reaction rate is very small in Zone III. The activation energy reported by Day for the carbon-oxygen reaction in Zone III is about 8 k.cal.mole.$^{-1}$

3.3. **Factors other than Mass Transport which affect the Rate of Gas-Carbon Reactions**

3.3.1. **Introduction**

At present there is no clear understanding of why a given carbon

reacts at a particular rate with a given gas under a fixed set of operating conditions. In this section the possible effects of crystallite orientation and size, surface area and preheat treatment are briefly discussed.

3.3.2. Crystallite orientation and size

Carbon is a polycrystalline material, which can present varying degrees of surface heterogeneity depending upon the size and orientation of the crystallites. The two main orientation of crystallites in the carbon surface to be considered are:

(i) crystallites with their basal planes parallel to the surface;

(ii) crystallites with their basal planes perpendicular to the surface.

Grisdale (56) has found that the rate of oxidation of carbon crystallites is about 17 times faster in the direction parallel to the basal planes (along their edges) than perpendicular to them. Hence for a graphitic carbon in which the majority of the crystallites have their basal planes parallel to the surface of the carbon, the reactivity would be expected to be less than that of a non-graphitic carbon where a large number of the basal planes are perpendicular to the surface. Smith and Polley (57) have indeed found that the specific reactivity of a carbon is at a minimum when its surface contains a maximum number of crystallites with their basal planes parallel to the surface.

Walker et Al (58) have confirmed Smith's and Polley's findings

from their investigations of the reactivity of graphitised carbon plates to carbon dioxide. Armington (59) has concluded from experiments using non-porous carbon blacks, that the specific reactivity of carbons increases as the crystallite size increases. These findings will be further considered in relation to the present work (Section 3.2.1. and Chapter 5. Section 5.2.), when the reactivity of the graphitic polyacenaphthylene carbon is compared to that of the non-graphitic cellulose and cellulose triacetate carbons.

3.3.3. The Effect of Heat Treatment of Carbons on their subsequent Reactivity to Gases

If heat treatment of a carbon produces an increase in graphitisation of the carbon then generally the reactivity of the carbon decreases due to the effects described in Section 3.3.2. However, if heat treatment in addition to graphitising the carbon, increases the crystallite size, then it is possible that the reactivity will increase rather than decrease as Walker and Nichols (60) have found.

Gregg and Tyson (61) have studied the oxidation of carbons, prepared from petroleum coke and pitch and with heat treatment to various temperatures in the range $1000^{\circ}C$ to $3000^{\circ}C$. Using a partial pressure of oxygen of 0.1, they measured the rates of oxidation of these carbons in the temperature range $500^{\circ}C - 560^{\circ}C$, and obtained activation energies for each carbon. They found that as the temperature of

preparation of the carbons increased from 1000°C to 3000°C, the activation energy increased from 44 k.cal.mole.$^{-1}$ to a maximum of ca. 65 k.cal.mole.$^{-1}$ for the carbon prepared at 1500°C, and then decreased again to ca.44 k.cal.mole.$^{-1}$ for the carbon prepared at 3000°C.

They have concluded that as the temperature of preparation of the carbons increases, the increasing graphitic character of the carbons tends to reduce the measured activation energy. They have also concluded that in competition with this effect, is the decrease of porosity of the carbons which occurs on increasing the temperature of preparation, and which would tend to increase the activation energy. However, they have suggested that an alternative explanation for these findings is that for the carbons prepared to 1500°C, oxidation in the temperature range 500°C to 560°C is in Zone II of the Wicke classification, whilst for the carbons prepared above 1500°C, oxidation in the same temperature range is in Zone I of the Wicke classification.

3.4. A Summary of the Experimental Kinetic Parameters obtained for the Carbon–Carbon Dioxide Reaction in Previous Studies

3.4.1. Reaction Orders (39)

When the rate of a gas–carbon reaction is entirely chemically controlled, i.e. Zone I, then a relatively simple discussion of order is possible. The rate of the carbon–carbon dioxide reaction (expressed as loss of wt. of carbon) can be assumed to be determined by

---

* Case 1 on page 33, neglecting retardation by carbon monoxide.

the rate of surface rearrangement of the C(0) complex to a rapidly
desorbable product.   If the fraction of surface area covered by the
complex is Θ, the reaction rate is proportional to the product of
Θ and a rate constant.   At a given temperature the reaction order
depends upon the relationship between the change in Θ with the
change in pressure of the reacting gas.   If Θ tends to one
throughout a range of pressure change then the reaction will be zero
order with respect to carbon dioxide pressure.   On the other hand
if Θ is small, the change in Θ will be directly proportional to
the change in pressure, and the reaction will be first order.   At
intermediate values of Θ, the reaction order will vary from zero to
one.   The value of Θ is a function of the magnitude of the individual
rate constants for the formation of the surface complex and its
conversion to a desorbable product and the pressure of carbon dioxide

Reaction temperature, and product retardation in mass transfer
processes also affect the reaction order.   Workers have reported
orders between zero and one depending on the experimental conditions.
In general the carbon-carbon dioxide reaction shows zero order
kinetics with respect to P_{CO_2} when $k_2\ P_{CO} \ll 1$ and $k_3\ P_{CO_2} \gg 1$,
(Equation 3.1.).   These conditions are satisfied at high pressures
of carbon dioxide and low temperatures when the production of
carbon monoxide is small.   The reaction becomes first order at
low pressures of carbon dioxide and low temperatures ,
i.e. when $k_2\ P_{CO}$ and $k_3\ P_{CO_2}$ are both $\ll 1$.   In   the

present work, the activation of the carbons was carried out at about atmospheric pressure of carbon dioxide, in the temperature range $850^{\circ}C - 950^{\circ}C$ and in a flow system. The pressure dependence of the reaction rate has not been studied in the present investigations but in the light of previous work (41.) it would appear that the reaction is occurring under conditions in which the rate is independent of the partial pressure of carbon dioxide.

3.4.2. Activation Energies reported for the Carbon-Carbon Dioxide Reaction

The experimentally observed activation energy for the $C-CO_2$ reaction need not refer necessarily to the same rate controlling step in every case. This applies not only when mass transport is the rate controlling step rather than chemical reaction but also when the reaction is entirely chemically controlled. Under different conditions of temperature and pressure, the rate controlling step of the reaction may change from the formation of the $C(O)$ complex to the removal of $C(O)$. Hence if conditions are such that the rate of the reaction is controlled by both steps, then it becomes difficult to assign a physical significance to the overall activation energy.

Rossberg (62) has postulated that an activation energy of 86 k. cal.mole.$^{-1}$ should be obtained for all carbons undergoing gasification with carbon dioxide in the region of chemical control. He bases this postulate on the experimental findings of Wicke (49) that a high purity electrode carbon and a medium purity activated charcoal have the same activation energy. (Section 3.6.1.) Since Wicke's

experiments were conducted in a flow system close to atmospheric pressure, the rate determining step was presumably the desorption of the C(O) complex.   It seems likely, therefore, that Wicke's activation energy refers to the value of the activation energy belonging to the rate constant J_3 in Equation 3.4.   Ergun (43) has found that the activation energy for three different carbons (Ceylon graphite, activated charcoal and activated graphite) to be the same in each case, (59 k.cal.mole.$^{-1}$) and also concludes that this value belongs to the rate constant J_3 in Equation 3.4.   Other workers have reported various values between these figures;   it has been concluded that in some cases diffusion has contributed to the overall reaction rate thus resulting in a reduced activation energy. Greenhalgh and co-workers (48) have recently suggested, however, that there is an alternative explanation for some of the low activation energies reported.   They found that the activation energies for the reaction of carbon dioxide with well outgassed samples of polyvinyl chloride and polyvinylidene chloride carbons were identical and equal to 85 k.cal.mole.$^{-1}$.   For poorly outgassed samples or samples which had been highly oxidised the activation energy was again identical for both carbons but had fallen to ca. 70 k.cal.mole^{-1}.

Activation energies reported (39) for Zone II conditions of the carbon-carbon dioxide reaction vary from 30 to 45 k.cal.mole.$^{-1}$ and in general follow the pattern predicted from Wicke's findings.

3.5. Results of the Present Work

3.5.1. Introduction

The polymer carbons were activated by carbon dioxide at atmospheric pressure in a flow system, the rate of reaction being followed gravimetrically. Full details of the apparatus and procedure are given in Appendix II.

The rates of activation of the three polymer carbons were investigated over the temperature range $830^{\circ}C$ to $950^{\circ}C$ in order to attempt to locate the reaction within the Wicke classification of reaction zones. (Section 3.2.1.)

Initially small samples of unactivated carbons were used; these results for cellulose, cellulose triacetate and polyacenaphth-ylene carbons are shown in Figs.3.2. to 3.4. respectively. The preparation of the activated carbons for measurements of pore volume require larger amounts of carbon. At least 0.2g. of carbon is required for adsorption and mercury density measurements, thus, for example, 0.4g. of unactivated carbon is required to produce a carbon activated to a burn-out of 50%. Since the results of Wicke (Section 3.2.1.) indicate that diffusion may play an important role, the influence of the starting weight of carbon on the rate of reaction was, therefore, investigated for cellulose and cellulose triacetate carbons at $935^{\circ}C$, over the weight range 0.02 to 1g; these results are shown in Fig.3.5. Since these results indicate a marked difference in the rates of activation between small(ca.0.02g.)

and large (0.1g.) samples of carbon, the rates of activation of the three carbons were also investigated for large samples over the temperature range 890°C to 975°C. The results for cellulose, cellulose triacetate and polyacenaphthylene carbons are shown in Figs.3.6. and 3.8. respectively. The linear rates obtained from these results are summarised in Tables 3.1. and 3.3.

3.5.2. Reaction Rates

For small starting weights of cellulose carbon the rates of reaction* (Fig.3.2.) remain linear over the entire range of burn-out, throughout the temperature range covered. For larger starting weights of cellulose carbon (greater than 0.1g.) the rates of reaction are also linear up to a burn-out of ca.60%, but decrease slightly thereafter. The rates of reaction on the small scale are generally a factor of ten greater than on the large scale at the same temperature. The variation of the rate of reaction with the starting weight of cellulose and cellulose triacetate carbons at 935°C (Fig.3.5.) shows that as the starting weight of carbon is increased from 0.02g. to 0.1g. the rate of reaction decreases sharply. As the starting weight of carbon is increased from 0.1g. to 1g., the rate of reaction decreases slightly before becoming nearly constant.

The results for cellulose triacetate carbon (Figs.3.3. and 3.7.) follow the same trend as those for cellulose carbon except that

---

* Rates of reaction are expressed in units of g.sec.$^{-1}$ per gram of unactivated carbon. i.e.g.sec.$^{-1}$.g^{-1} and are initial rates.

initial rates of reaction for small starting weights of cellulose triacetate carbon (ca. 0.01g.) are not linear. The initial rates decrease slowly until they become linear at a burn-out of about 25%. For large starting weights of cellulose triacetate carbon, the reaction rates remained linear to a burn-out of almost 100%. This is in contrast to the slight decrease in rate observed for cellulose carbon above a burn-out of 60% when large starting weights were used.

The rates of reaction of polyacenaphthylene carbon with carbon dioxide differ considerably from those for cellulose and cellulose triacetate carbons. For small starting weights of polyacenaphthylene carbon, the rates of reaction were not linear and, as Fig.3.4. shows, were inconsistent. For example the reaction at 915°C. appeared to be faster than at 923°C. The reactions were extremely slow; for example, it took 13 hours to completely burn out a sample of 0.01g. of polyacenaphthylene carbon at 930°C, in contrast to a time of about an hour for similar amounts of cellulose and cellulose triacetate carbons. As further evidence of the inconsistent and slow reaction rates obtained for polyacenaphthylene carbon, Table 3.4. shows the times taken to reach a burn-out of 50% at various temperatures. However, for larger starting weights of polyacenaphthylene carbon (ca.0.4g.) the reaction rates were consistent and linear, although slower than the rates of activation of cellulose and cellulose triacetate carbons by factors of approximately 5 and

8.5. respectively at 935°C. (Tables 3.1. to 3.3.).

3.5.3. Activation Energies

Before considering the significance of the rates of reaction it is necessary to determine the experimental activation energy Ea, in order to define the region of the Wicke Classification in which the reaction lies.

Using the linear rates of reaction of the three carbons at different temperatures as overall rate constants, k, (Tables 3.1. to 3.3.), the results were plotted (Figs. 3.9. to 3.11.) according to the Arrhenius Equation: $k = Ae^{-Ea/RT}$ - Equation 3.9. to yield experimental activation energies, Ea, and pre-exponential factors, A. These are summarized in Table 3.5. for the three carbons.

The Arrhenius plots for both cellulose and cellulose triacetate carbons were linear throughout the temperature range investigated when small starting weights of carbon were used, and the activation energies were high (greater than 50 k.cal.mole.$^{-1}$).

For large starting weights of carbon, the Arrhenius plots were smooth curves for cellulose and cellulose triacetate carbons. In these cases the Arrhenius parameters were calculated over two temperature ranges by approximating each curve to a pair of straight lines over these temperature ranges.

Due to the inconsistent rates of reaction it was not possible to obtain Arrhenius parameters for the activation of small samples of

polyacenaphthylene carbon. However, for large samples of this
carbon (ca.0.4g.) the Arrhenius plot was linear throughout the
temperature range $890^\circ C$ to $975^\circ C$.

3.6. Discussion of the Kinetic Results

3.6.1. Activation Energies and Pre-Exponential Factors

It is clear from what was said in Section 3.4.2. that care
must be taken in the interpretation of Arrhenius Parameters obtained
experimentally for the carbon-carbon dioxide reaction. In particular
it is not usually possible to equate the overall rate constant to
the rate constant for a particular step in the reaction mechanism.
However, the experimental Arrhenius parameters can be used to locate
the reaction within the zonal classification of Wicke and so obtain
an indication of the relative importance of mass transport and
chemical reaction on the overall rate.

For the purposes of the present work this can be useful since
it is important to define the role of mass transport in the
development of pore structure.

The high activation energy obtained for small starting weights
of cellulose carbons (71 k.cal.mole.$^{-1}$) corresponds to the values
obtained by Greenhalgh and co-workers (Section 3.4.2.) for the
activation by carbon dioxide of poorly outgassed samples of polyvinyl
chloride and polyvinylidene chloride carbons (70 k.cal.mole.$^{-1}$).

This value for the activation energy, indicates that the
reaction is exclusively chemically controlled, and the difference from

the theoretical value of 86 k.cal.mole.$^{-1}$ predicted by Rossberg (61) for all carbons can be attributed to incomplete outgassing of the carbons prior to activation. However, an alternative explanation of this difference may be that diffusion is playing a small role in the reaction thus reducing the activation energy from the value predicted by Rossberg. The high value of 10^{10}g.sec.$^{-1}$g.$^{-1}$ obtained for the pre-exponential factor is further evidence that the reaction is predominantly chemically controlled.

The activation energy found when large starting weights of cellulose carbon were activated over the temperature range 930° to 960°, was 31 k.cal.mole.$^{-1}$ and is less than half the value of 67 k.cal.mole.$^{-1}$ found when large samples of cellulose carbon were activated over the temperature range 890° to 930°C. Hence it would appear that in the upper temperature range the reaction is controlled principally by diffusion and therefore lies in Zone II of the Wicke classification, whilst in the lower temperature range the reaction is predominantly chemically controlled and therefore within Zone I of the Wicke Classification.

It is interesting to note that in the upper temperature range, i.e. 930°C. to 960°C. the pre-exponential factor was low, (16g. sec.$^{-1}$ g.$^{-1}$) which is further evidence that in this temperature range the reaction is diffusion controlled for large samples of cellulose carbon. As further evidence that the activation of large samples of cellulose carbon in the lower temperature range studied,

is chemically controlled, the pre-exponential factor was found to be much higher (by a factor Ca. 10^7) than in the higher temperature range. However, the value of 1.5×10^8 for the pre-exponential factor of the reaction in the lower range of temperature ($890°$ to $930°C$) is slightly lower than the value (10^{10}) found for the activation of small samples of cellulose carbon in the same temperature range.

It thus appears that a change in the weight of sample can markedly influence the nature of the rate-controlling step in the reaction using the experimental system employed in the present work. An increase in the weight of sample appears to increase the contribution due to diffusion.

The values of the activation energies found for the activation of cellulose triacetate carbons are lower than those found for the activation of cellulose carbon, although the trend of them is precisely the same for both small and large samples of each carbon. It is tempting to ascribe these lower values to an increased diffusion effect in cellulose triacetate carbons compared with cellulose carbons.

Wicke (49) has found that the value of 86 k.cal.mole.$^{-1}$ for the activation energy applies to widely differing carbons undergoing activation in Zone I.

Although Ergun (43) also finds a universal activation energy for widely differing carbons he finds this value to be 59 k.cal.mole.$^{-1}$

The lack of agreement between Wicke and Ergun for the value of the 'Universal' activation energy throws some doubt on this concept. In this work distinctly different values of activation energy have been found for different carbons, activated in the same temperature range. It is, therefore, difficult to decide whether the differences in the activation energy for the activation of cellulose and cellulose triacetate carbons, reported in this work are due to different rate controlling steps of the chemical reaction operating for each carbon, or whether diffusion plays a more dominant role in the activation of cellulose triacetate carbon compared with cellulose cellulose carbon in this temperature range.

At the temperature $(935^{\circ}C)$ chosen to prepare the activated series of carbons for studies of porosity, there is little doubt that for large samples of cellulose and cellulose triacetate carbons, the reaction rate is predominantly diffusion controlled, i.e. the reaction occurs in Zone II of the Wicke classification.

The high activation energy (60 k.cal.mole.$^{-1}$) found for the activation of large samples of polyacenaphthylene carbon indicates that the reaction is predominantly chemically controlled throughout the temperature range studied. There are two possible reasons for this. Firstly, the reactivity of polyacenaphthylene carbon is inherently low due to its graphitisability, (Section 3.3.2.). Hence higher temperatures than those used in the present work are probably required, in order that diffusion to, and into the carbon becomes the

rate controlling step in the reaction. Secondly, diffusion into the pores of polyacenaphthylene carbon is not likely to be an important factor in determining the rate of reaction since as the adsorption results (Chapter 4) show polyacenaphthylene carbon has an extremely small porosity. It would appear, therefore, that the reaction between polyacenaphthylene carbon and carbon dioxide occurs predominantly on the external surface. This point will be further discussed in Chapter 5.

3.6.2. Reaction Rates

The almost universal linear rates of reaction reported in this work for the activation of the three carbons are almost certainly due to the experimental conditions. The high flow rates of gas employed ensure a rapid removal of carbon monoxide, which if it were allowed to build up in concentration, would inhibit the reaction according to Equation 3.1. In view of the fact that zero order kinetics have been observed, an explanation consistent with this evidence is that where the reactions are chemically controlled $k_2 P_{CO}$ is very much less than $k_3 P_{CO_2}$ and $k_3 P_{CO_2}$ is much greater than one; therefore Equation 3.1. reduces to:- Rate $= k_1/k_3$, thus under these conditions the rate may be expected to be linear and independent of the pressure of carbon dioxide. Where the reaction is diffusion controlled, the prompt removal of carbon monoxide prevents any retardation of diffusion.

The initial (non-linear) rates for small samples of cellulose triacetate carbon may be due to a small amount of relatively reactive matter present in the pores at the start of activation.   In support of this explanation pore size distribution measurements have shown that the principal process in the early stages of activation of carbons is the opening up of blocked pores(6 However, if this is the case, then it might be anticipated that the effect would also be noticeable for small samples of cellulose carbon.

The anomalous rates of reaction found for small samples of polyacenaphthylene carbon may arise from the fact that the reaction is surface area dependent.   Hence for small samples, which may differ considerably in surface area from run to run comparison of reaction rates is difficult unless the surface areas are known.   In Chapter 4 (Section 4.2.) it is shown that less than 10^{-3} cm^3. of carbon dioxide are adsorbed by 1g. of unactivated polyacenaphthylene carbon at $195^{\circ}K$.   If this amount of carbon dioxide was adsorbed as a monolayer it would cover an area of 2.3 $m^2 g^{-1}$ of carbon (Section 4.3.2.).   Therefore, the maximum surface area available for reaction of a 0.01g. sample of polyacenaphthylene carbon is likely to be less than 0.02 m^2.

(cm^3).

The non-linearity of the reaction rates for small samples of polyacenaphthylene carbon over a large range of burn-out, probably indicates that a reduction in surface area of the sample is occurring

on extensive activation. This effect will not be noticeable for the activation of large samples until almost total burn-out is reached, and the surface area of the carbon as a result becomes very small.

3.6.3. The Influence of Starting Weights of Carbons on the Rates of Activation and the Arrhenius Parameters

It is certain that the rapid reduction in reaction rates of cellulose and cellulose triacetate carbons (Fig. 3.5.) on increasing the starting weight of carbon from 0.02g. to 0.1g. is due to the increasing importance of diffusion with increasing mass of carbon. At a given temperature (935°C), the reaction rates become almost constant when the starting weight of the carbons is increased to a value greater than Ca.0.3g. The minimum starting weight of carbon, at which the reaction rate becomes independent of starting weight, is probably a function of the geometry of the furnace and crucible.

The effect of increasing the starting weight of carbon on the Arrhenius Parameters is two-fold. (Table 3.5.) Firstly the reactions above 930°C. become diffusion controlled, i.e. the effect of increasing the weight of the sample is to shift the Zone II boundary down the temperature scale. Secondly the pre-exponential factors are reduced, slightly when the reaction remains chemically controlled i.e. below 930°C., and are reduced considerably when the reaction is diffusion controlled above 930°C.
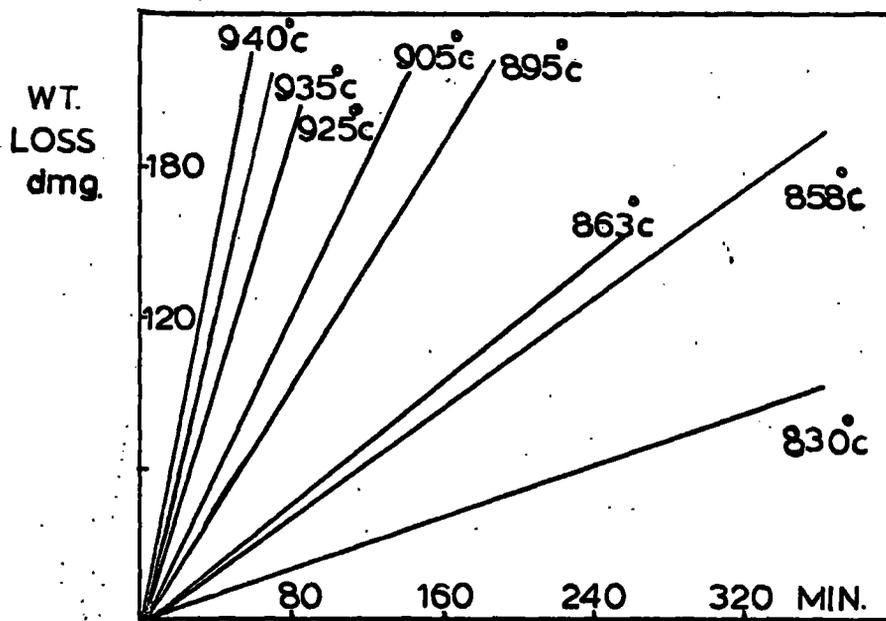
FIG 3.2 ACTIVATION OF CELLULOSE
CARBONS (SMALL SCALE)
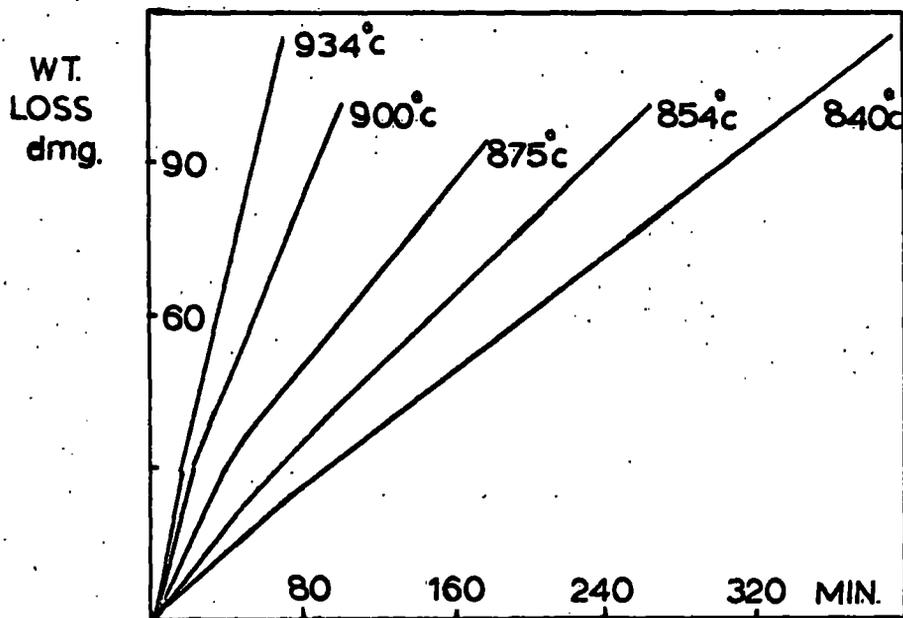
FIG. 3.3 ACTIVATION OF CELLULOSE
TRIACETATE CARBONS (SMALL SCALE)
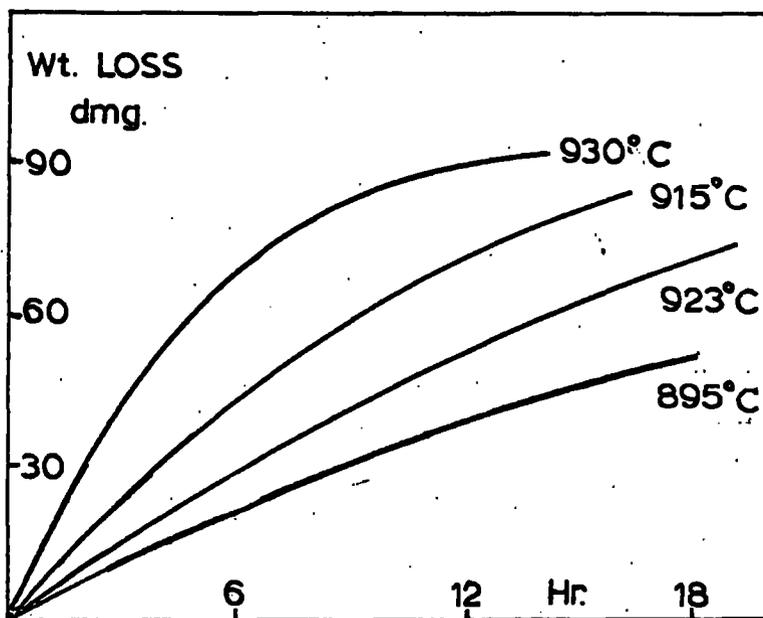
FIG. 3.4. ACTIVATION OF POLYACENAPHTHYLENE
CARBONS (SMALL SCALE)
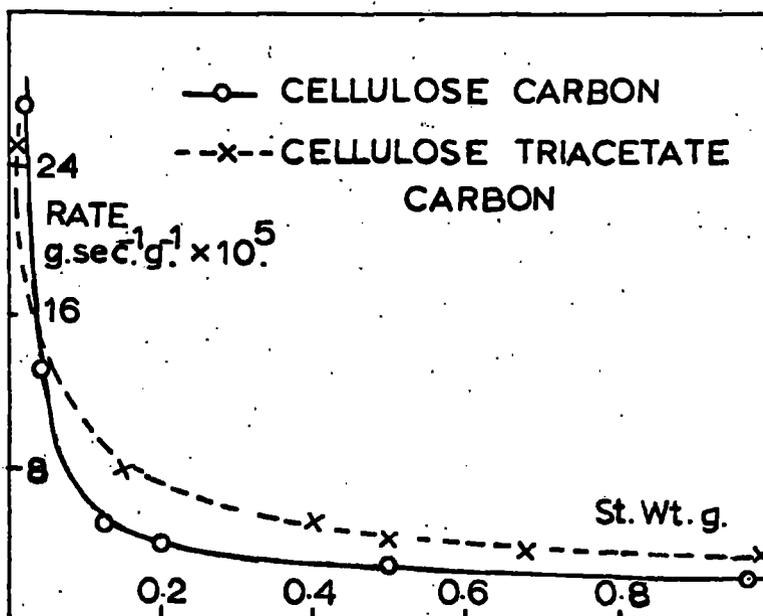
FIG. 3.5. ACTIVATION OF DIFFERENT
STARTING WEIGHTS OF CARBONS AT 935°C.
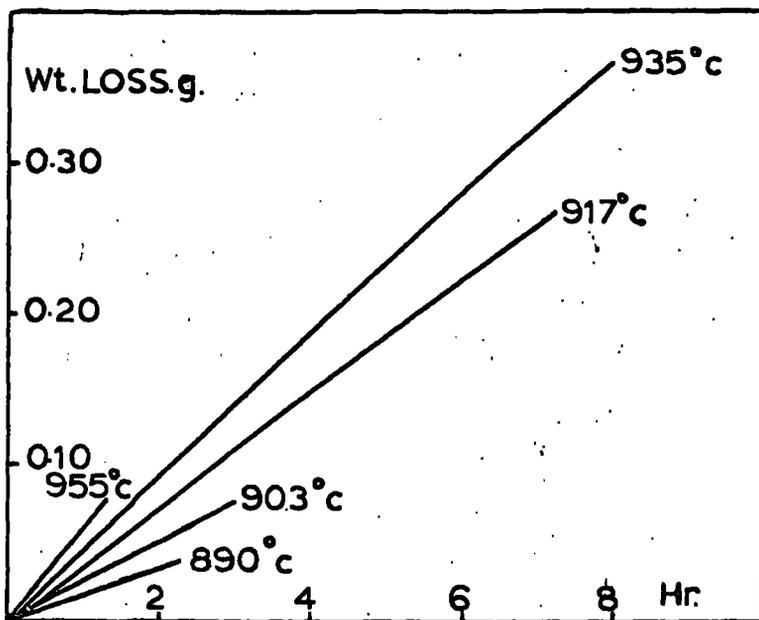
FIG. 3.6. ACTIVATION OF CELLULOSE
CARBONS (LARGE SCALE)
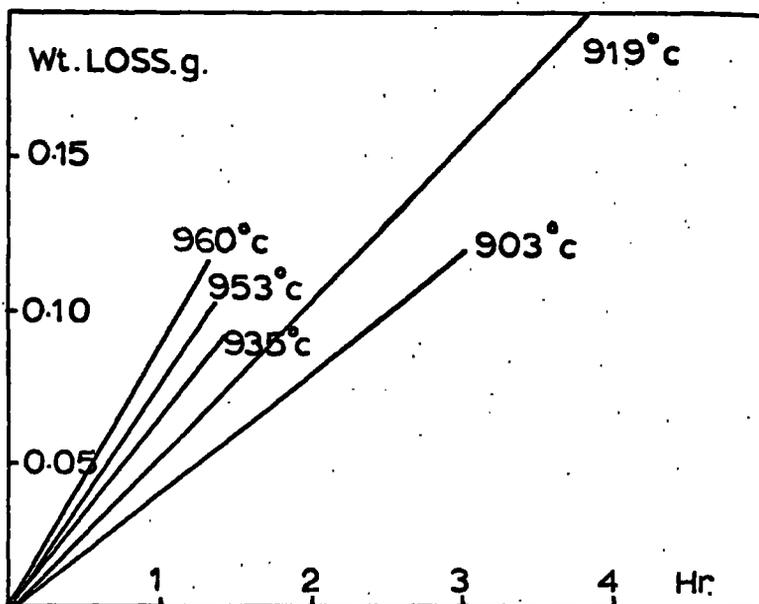
FIG. 3.7. ACTIVATION OF CELLULOSE
TRIACETATE CARBONS (LARGE SCALE)
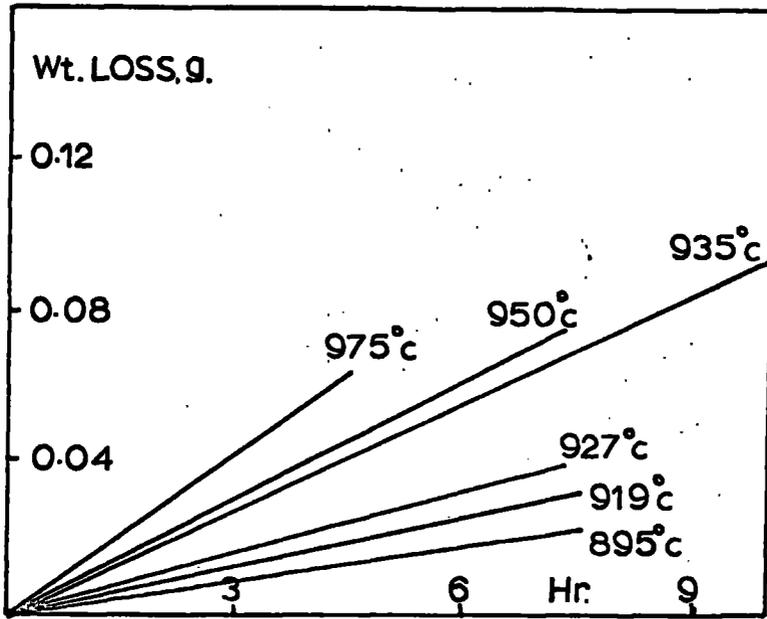
FIG. 3.8. ACTIVATION OF POLYACENAPHTHYLENE CARBONS. (LARGE SCALE).
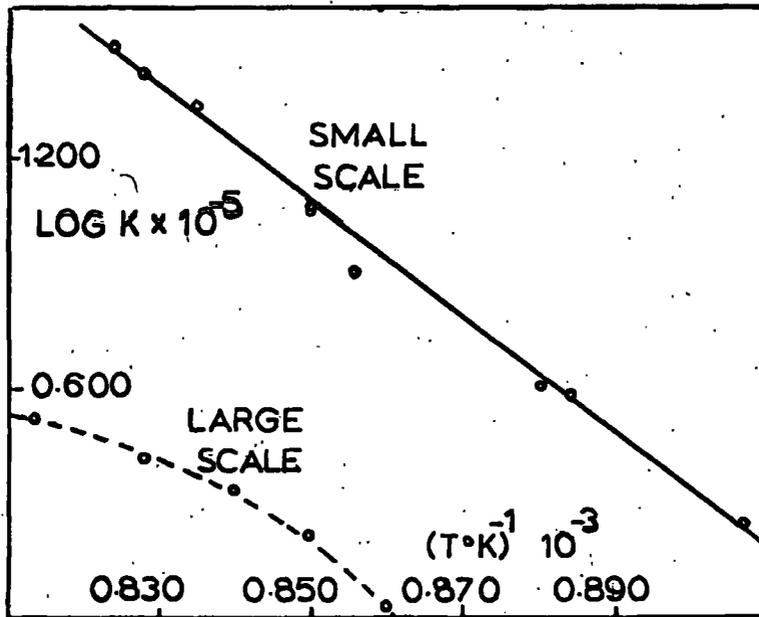
FIG. 3.9 ARRHENIUS PLOT CELLULOSE CARBONS.
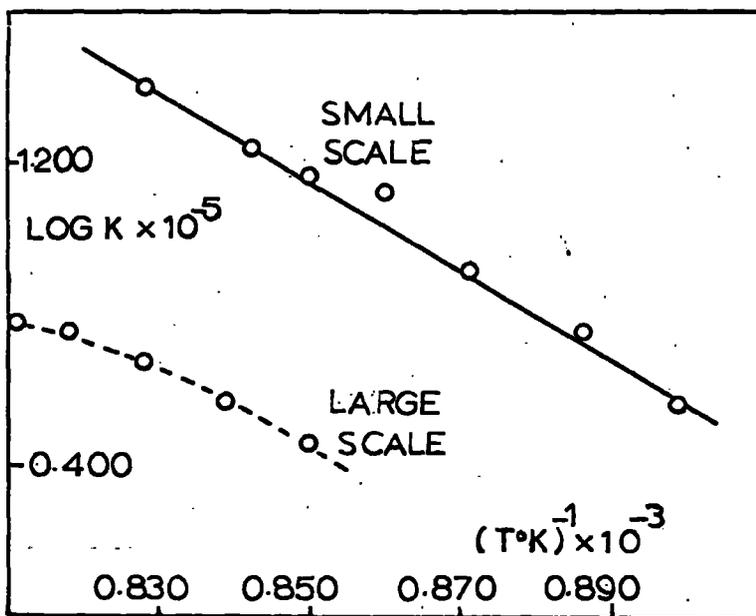
FIG. 3.10. ARRHENIUS PLOT CELLULOSE
TRIACETATE CARBONS.
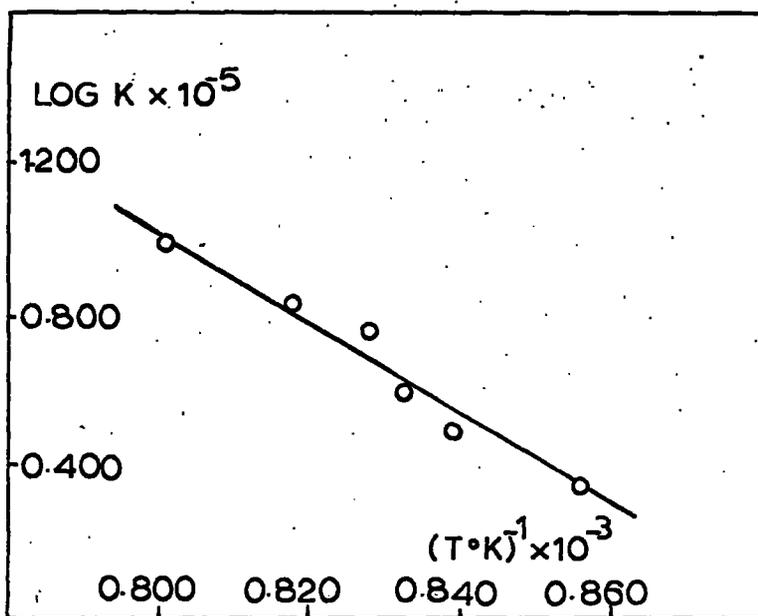
FIG. 3.11. ARRHENIUS PLOT FOR
POLYACENAPHTHYLENE CARBONS
(LARGE SCALE)

Table   3.1.

The Linear Rates of Activation of Cellulose Carbons

Starting Weight of carbon (g.)	Temperature (^{o}C.)	Reaction Rate (g.sec.$^{-1}$g.$^{-1}$) x 10^5
0.0210	935	27.10
0.0272	863	4.11
0.0244	895	8.06
0.0250	830	1.80
0.0195	940	31.00
0.0189	925	22.50
0.0216	905	12.00
0.0215	858	3.87
0.2000	935	3.37
0.5000	935	2.67
0.9600	935	2.08
0.5000	917	2.20
0.5000	903	1.66
0.5000	890	1.09
0.5000	955	3.32
0.1200	935	4.95
0.0450	935	13.00

Table 3.2.

The Linear Rates of Activation of Cellulose Triacetate Carbons

Starting Weight of carbon (g.)	Temperature (°C.)	Reaction Rate $(g.sec.^{-1} g.^{-1}) \times 10^5$
0.0097	900	14.80
0.0089	875	8.24
0.0099	934	25.10
0.0121	840	3.58
0.0103	854	5.66
0.0102	889	13.90
0.0085	916	17.40
0.4000	960	6.11
0.4000	935	4.68
0.5000	935	4.08
0.6750	935	3.54
1.0500	935	2.97
0.4000	953	5.75
0.4000	919	3.75
0.4000	903	2.92
0.1500	935	7.80

Table 3.3.

The Linear Rates of Activation of Polyacenaphthylene Carbons

Starting Weight of carbon (g.)	Temperature (^{o}C.)	Reaction Rate (g.sec.$^{-1}$ g.$^{-1}$) x 10^5
0.4000	895	0.22
0.4000	919	0.31
0.4000	927	0.38
0.4000	935	0.56
0.4000	950	0.67
0.4000	975	0.97

Table 3.4.

The Times Taken to Reach a Burn-out of 50% for the Activation of

Small Samples of Polyacenaphthylene Carbon

Starting Weight of carbon (g.)	Temperature (^{o}C.)	Time to Reach a Burn-Out of 50% (hr.)
0.0100	895	16.50
0.0097	915	5.50
0.0107	923	9.50
0.0088	933	6.25
0.0100	930	3.25
0.0081	933	10.40
0.0086	945	11.00

Table 3.5.

Arrhenius Parameters for the Activation of the Polymer Carbons

with Carbon Dioxide

Polymer carbon	Approximate Starting Weight (g.)	Temperature Range ($^{\circ}$C)	Activation Energy E_A (k.cal.mole.$^{-1}$)	Pre-Exponential Factor A (g.sec.$^{-1}$ g.$^{-1}$)
Cellulose	0.02	830 - 940	71 ± 5	10^{10}
	0.4	925 - 950	31 ± 3	1.6×10
	0.4	890 - 925	67 ± 5	1.5×10^{8}
Cellulose	0.01	830 - 950	50 ± 5	7.1×10^{5}
Triacetate	0.4	930 - 960	28 ± 3	1.1×10
	0.4	890 - 930	45 ± 4	5×10^{3}
Polyacenaphthylene	0.4	900 - 970	60 ± 5	2×10^{5}

Chapter 4

The Development of Porosity in the Carbons

4.1.1. Introduction

The internal surface of a carbon may be characterised from pore volume, surface area and measurements of pore size distribution. Before outlining the detailed theory of the methods used in the present work for porosity measurements, a brief critical review of the general methods for obtaining measurements of the internal surface of carbons is presented.

4.1.2. Methods for the Determination of Pore Volumes

The methods are divided into three main types:

(a) Adsorptive methods, (b) Molecular probes and density measurements, and (c) Optical and electron microscopy.

4.1.2.a. Adsorptive Methods

The total pore volume of a carbon may in some cases be calculated from an adsorption isotherm by application of the Gurvitsch Rule, provided that the isotherm intersects the line $P/Po = 1$ at a finite angle. The amount adsorbed at saturation, X_S^o, is then definite and assuming that the adsorbate fills all the pores with liquid having its normal density, ρ, at the temperature of the experiment, the pore-volume V is calculated from

$$V = X_S^o/\rho \qquad - \qquad \text{Equation 4.1.}$$

Although the Gurvitsch Rule gives a remarkably constant value
of pore volume, when the adsorption isotherms of different gases
on a given adsorbent are compared, it only applies to Type I, and
some of Type IV isotherms of the well-known Brunauer classification,
(64). This is because the line $P/P_o = .1$ is approached asymptotically
for the other types of isotherm in the classification and X_S^o is
therefore difficult to define. In addition the pores of the
adsorbent may not all be filled with adsorbate at $P/P_o = 1$. This
has been shown (14) to be the case for the adsorption of carbon
tetrachloride on cellulose and coconutshell carbons.

4.1.2.b. Molecular Probes and Density Measurements

Since mercury has a negative angle of contact with carbon, a
positive pressure is required for it to enter the pores of carbon.
It can be shown by application of the Kelvin Equation (Section 4.1.4.
that when a sample of carbon is immersed in mercury at atmospheric
pressure, the mercury cannot enter pores of less than 100,000 Å in
diameter, i.e. very large macro-pores. Hence by determination of
the density of a carbon in mercury, the volume occupied by the pores
and the carbon is obtained. By measuring the density of the carbon
in a liquid or gas whose molecular dimensions are such that all pores
are penetrated, the volume of the carbon alone may be obtained. The
density so determined has been termed the "true" density of the
carbon, whilst the density in mercury is called the apparent density.
The difference between the reciprocals of the apparent and "true"

densities gives a measure of the total open pore volume of a carbon. The density of a carbon determined in helium has often been used as a measure of the "true" density of the carbon, but is subject to several limitations. If the density of the carbon is determined in helium at room temperature, physical adsorption of helium may occur (64) to a significant degree, resulting in an incorrectly high value for the density.

In addition, if the carbon has a volume of closed pores, which are therefore inaccessible to the helium, the density as measured will be lower than the true density of the carbon. Errors in the measurements of helium densities of carbons, due to physical adsorption of helium have been eliminated by obtaining the densities at 300°C. (65)

A further practical limitation to obtaining helium densities of carbons is the relatively large amount of carbon required to perform a determination. Helium densities of carbons are conventionally determined volumetrically, and at least 5g. of carbon are required for accurate results. In the present work, the practical limit of production of activated carbons has been less than 1g. and helium densities of the carbons were therefore unobtainable.

Attempts have also been made (65) to estimate the "true" density of a carbon using X-ray data. The method is difficult to apply generally, since in order to evaluate a density for the carbon, it is necessary to have a crystallographic model for the carbon. This is a

difficult task for most types of carbon, whose structures have little order.   This is the case for the carbons investigated in the present work.   Cellulose and cellulose triacetate carbons are non-graphitic (Chapter 1. Section 1.4.) and therefore lack any regular three dimensional order.   Although polyacenaphthylene carbon is graphitisable, at the temperature of preparation in the present work (950°C) it only has a small degree of order.

The molecular probe technique of gaining quantitative information of the pore structure of carbons is not restricted to helium density determinations.   In the measurements of densities in liquids of larger molecular size than helium, the penetrating molecules will be excluded from pores, whose entrances are narrower than the molecular diameter.   Such densities should be lower than the corresponding helium densities.   In practice this has generally been found to be the case.   However, if the dilatometric fluid has a significantly increased density in the adsorbed phase compared with in the bulk liquid phase, then the density of the carbon in the fluid will be incorrectly high.   For example the density of some carbons in methyl alcohol are greater than in helium (67).   Another cause of error in the molecular probe technique in some cases is the slow or incomplete penetration of the pores by the dilatometric fluid, resulting in either a slow increase in apparent density with time or an anomalously low apparent density.

4.1.2.c.<u>Optical and Electron Microscopy</u>

It is now possible in favourable cases (68) using ultra thin specimens of carbons to examine with the aid of an electron microscope all but the smallest micro-pores. Replication techniques can be used in electron microscopy to examine pores greater than 200 Å in size, i.e. transitional pores; the loss of resolution which accompanies replication prevents an accurate assessment of smaller pores.

Optical microscopy can be used to examine the larger sized Macro-pores and etch pits of carbons. Hughes and Thomas (69) have measured the rates of expansion of etch pits during the oxidation of graphite using this technique.

It is possible using statistical counting methods in conjunction with electron microscopy to calculate the average number of pores of any given dimensions, hence the pore volume of a solid may be obtained.

4.1.3.<u>Methods for the Determination of Surface Areas of Solids</u>

The methods are of three main types:

(a) Adsorptive methods, (b) Heats of wetting measurements, (c) Low-angle scattering of X-rays.

4.1.3.a.<u>Adsorptive Methods</u>

The surface areas of solids are frequently determined from the application of the B.E.T. and Langmuir Isotherm Equations to the adsorption of a gas (usually nitrogen) on the solid. Both of these

theories have as a basic assumption the formation of a monolayer of the adsorbed phase. From these equations it is possible to obtain the monolayer capacity, X_m, defined as the weight of adsorbate which is adsorbed by one gram of the adsorbent in a full monolayer. if the cross-sectional area of the adsorbate molecule on the surface of the adsorbent, A_m, is defined, then the specific surface, S, of the adsorbent is given by:-

$$S = \frac{X_m}{M} \times N \times A_m \qquad - \text{Equation 4.2.}$$

where M is the molecular weight of the adsorbate and N is the Avogadro Number. The value of the surface area obtained clearly depends on the choice of cross-sectional area, Am, of the adsorbed molecules. Emmett and Brunauer (70) proposed that Am be calculated from the density, ρ, of the adsorbate in the ordinary liquid or solid form, assuming the molecule to have a co-ordination number of twelve in the adsorbed phase.

$$\text{Hence} \qquad A_m = 1.091 \left(\frac{M}{\rho N}\right)^{2/3} \qquad - \text{Equation 4.3.}$$

where 1.091 is a packing factor appropriate to twelve co-ordination. Emmett and Brunauer (70) consider that nitrogen at - 195°C. is the adsorbate which gives the most reliable values for specific surface areas. By comparison of the monolayer capacities obtained by using nitrogen, with those obtained using other adsorbates on the same solid Livingstone has compiled a list of values of Am for various

adsorbates (71) Livingstone has chosen a value of 15.4 $\overset{o}{A}^2$ for the cross-sectional area of the Nitrogen molecule as giving closest agreement with the specific surface area of an adsorbent estimated by an independent method. Cross-sectional areas of adsorbate molecules have been obtained from a comparison of the surface areas of carbon blacks determined by electron microscopy with those obtained by adsorption methods (72) and heats of wetting (73).

The Langmuir Theory (74) proposes that adsorption takes place on localised and energetically uniform sites on the surface of the solid and is limited to a monolayer.

In its linear form the Langmuir Equation may be written as:-

$$P/X = 1/BX_m + P/X_m \qquad - \qquad \text{Equation 4.4.}$$

where X is the amount adsorbed at pressure P, and B is a constant.

In the original kinetic derivation of Equation 4.4. the adsorbed layer is regarded as in dynamic equilibrium with the gas phase, so that the rate of condensation of adsorbed molecules on free sites of adsorbent is equal to the rate of re-evaporation from occupied sites. Fowler (75) has pointed out that the kinetic derivation is liable to obscure the essentially thermodynamic character of Equation 4.4. and he has derived the equation from statistical thermodynamics. The statistical derivation of Equation 4.4. gives an explicit definition of the constant B. Thus:-

$$B = \frac{h^3 \cdots\cdots\cdots f_a(T) e^{q/kT}}{(2 \pi m)^{3/2} (kT)^{5/2} f_g(T)} \qquad \text{Equation 4.5.}$$

where h is Planck's constant, k is the Boltzmann constant, m is the mass of an adsorbed molecule, $f_a(T)$ and $f_g(T)$ are the internal partition functions for a molecule in the adsorbed phase and gas phase respectively and q is the energy required to transfer a molecule from the lowest adsorbed to the lowest gaseous state.

On application of Equation 4.4. to an adsorption isotherm, a plot of P/X against P should give a straight line whose slope is $1/X_m$.

The limitations of the Langmuir Isotherm Equation when applied to real adsorbents stem from the inadequacies of the model proposed for adsorption.

Hill (76) has shown that fully localised adsorption is unlikely to occur except at very low temperatures. Even with highly homogeneous adsorbents such as graphitised carbon black, the presence of defects and edge atoms results in an appreciable degree of energetic heterogeneity of the adsorbent surface. The theory also fails to account for adsorbate-adsorbate interactions which play an appreciable part in adsorption particularly with polar adsorbents. It is also found that multilayer adsorption frequently occurs.

In order to account for multilayer adsorption, Brunauer, Emmett and Teller (77) introduced an equation known as the B.E.T. Isotherm Equation. The theory retains the idea of localised adsorption on energetically uniform sites but allows for the formation of an

infinite number of adsorbed molecular layers. As is the case with
the Langmuir Equation, the B.E.T. Equation has been derived
kinetically and statistically. In linear form the equation is:-

$$\frac{P}{X(Po - P)} = \frac{1}{XmC} + \frac{C-1}{XmC} \cdot \frac{P}{Po} \qquad \text{- Equation 4.6.}$$

where $C = e^{(E_1 - L_v)/RT}$, E_1 is the heat of adsorption of the first
layer, L_v is the heat of adsorption of the second and subsequent
layers and is equal to the latent heat of condensation of the
adsorbate. Thus experimental plots of $P/X(Po - P)$ against P/Po
should give straight lines from whose slope and intercept Xm can be
calculated. Equation 4.6. is capable of describing some Type II
or Type III isotherms, depending on the value of the constant C.
Equation 4.6. requires modification to describe isotherms of Types I,
IV and V of the Brunauer classification. Instead of regarding the
number of adsorbed layers as infinite, adsorption is restricted to
'n' layers. This form of the B.E.T. Equation may be written (78):-

$$\frac{\psi(n,y,)}{X} = \frac{1}{XmC} + \frac{\theta(n,y,)}{X_m} \qquad \text{- Equation 4.7.}$$

where $\psi(n,y,) = \dfrac{y - (n+1)\, y^{n+1} + n\, y^{n+2}}{(1 - y)^2} \qquad \text{- Equation 4.8.}$

and $\theta(n,y,) = \dfrac{y - y^{n+1}}{1 - y} \qquad \text{- Equation 4.9.}$

and $y = P/Po$

For suitable values of n and c, Equation 4.7. describes Type IV
and Type V isotherms; when n = 1, Equation 4.7. reduces to the
Langmuir Equation and hence describes a Type I isotherm.

Critisisms of the B.E.T. Theory

The B.E.T. theory has been critisised when applied to porous
carbons for a number of reasons.

The theory proposes that adsorption takes place on localised
sites of the adsorbent, which are assumed to be energetically
homogeneous. The surface of a porous carbon is likely to be extrem-
ely heterogeneous in character and except at very low temperatures
is likely to take place in a non-localised manner. In addition it
is assumed in the B.E.T. theory that during the formation of the
monolayer, adsorption forces of opposite walls of pores do not
interact with each other and that the value of 'n' is determined by
pore width only. The first of these assumptions is unlikely, since
in micro-porous carbons in particular, the pore walls are in close
proximity to each other. The second assumption is also unlikely
since 'n' has been found to decrease on increasing activation of
carbons, (14), whereas all other evidence points to the fact that
pore widths increase on activation. Finally anomalously high
surface areas of highly activated carbons have been reported when
the B.E.T. Equation has been used. This has been attributed to
micro-pore filling concurrent with the formation of the monolayer
at relative pressures of less than 0.05.

The failure of the B.E.T. theory when applied to porous carbons has led in recent years to a re-appraisal of the Potential theory of adsorption by Dubinin and his collaborators (4,83,84,85.). This work will be discussed in Section 4.1.6.

4.1.3.b. <u>Surface Areas from Heats of Immersion (Heats of Wetting)</u>

The heat evolved, Q cal.g.$^{-1}$ of solid, when a solid is immersed in a liquid provides a direct measure of the specific surface area S of the solid since $Q = hS$ - Equation 4.10. where h is the heat evolved when 1 square unit of surface is immersed in the liquid. In practice, however, the method is difficult to apply since h has to be obtained from the heat of immersion of a sample of a solid whose surface area has been independently determined. In the case of porous carbons, the value of h is usually obtained from the heat of immersion of a carbon black whose surface area has been obtained from electron microscopy. Since most carbon blacks are non-porous and have a more homogeneous surface than porous carbons, the use of the value of h so obtained is open to question.

Also for some carbons with fine pores, accessibility of the immersing liquid to the pores is often slow or limited resulting in a very slow or a reduced liberation of the heat of immersion. This makes measurement of the heat liberated a difficult task.

4.1.3.c. <u>Surface Areas from the Low-Angle Scattering of X-Rays</u>

In this method monochromatic X-radiation is passed through a

thin layer of the sample under examination, and the scattered

radiation is collected on a photographic plate. From the

intensity distribution of the scattered radiation the average

particle size and surface area of the solid may be obtained. To

obtain the surface area of a carbon using this method however, it

is necessary to postulate a model for the pore structure of the

carbon. Usually relatively simple models are postulated so that

the results are of limited value.

4.1.4. Methods for the Determination of Pore Sizes and Pore Size

Distributions

a. Volume to Surface Ratio

The numerical value of the ratio of pore volume to internal

surface area V/S of a solid can give a guide to the pore size.

Making the assumption that the pores are all cylindrical and of

the same radius r, then:

$$V/S = r/2 \qquad \text{Equation 4.11.}$$

For pores of the same shape but of different size, r represents a

value of the mean pore radius. The method tends to be of

qualitative value only when applied to porous carbons. Quite

apart from the difficulties in obtaining accurate data for V and

S, it is unrealistic to assume the pores to be all cylindrical and

of equal size.

b. Application of the Kelvin Equation

If a porous adsorbent exhibits hysteresis when subjected to an

adsorption-desorption cycle, this is usually attributed to capillary condensation into the pores, and a pore size distribution curve may be obtained by application of the Kelvin Equation to the desorption branch of the isotherm. Assuming that the pores consist of non-intersecting cylindrical capillaries the appropriate form of the Kelvin Equation is: $r = \dfrac{-2 M \gamma \cos\theta}{\rho RT \ln P/P_o}$ - Equation 4.12.

where M/ρ is the molecular volume, γ the surface tension and θ is the angle of contact of the adsorbate in the pores; the pore radius is r and P/P_o is the relative pressure. The pore size distribution is obtained by plotting dV_r/dr against r for various points on the isotherm. At each point chosen, V_r^{**} is calculated from X/ρ, where X is the weight adsorbed at each point and ρ is the density of the adsorbate. Since the Kelvin Equation is derived from classical thermodynamics it is only strictly applicable to macroscopic systems and therefore the limiting pore size to which it is normally applied is 25Å. In micro-pores (less than 25Å in width) concepts such as surface tension and angle of contact break down, and other techniques are required to examine them.

A form of the Kelvin Equation is also used in the application of mercury porosimetry. It has already been noted (Section 4.1.2.b. that a positive pressure is required for mercury to enter the pores of a carbon. In mercury porosimetry, mercury is forced into smaller and smaller pores by increasing the pressure. Pressures of

---

* V_r is the pore volume containing pores of radius r or less than r.

60,000 atmospheres are required to penetrate micro-pores. The method has been used by Wiggs and co-workers (79) with success in the determination of pore sizes of carbons.

4.1.5. <u>The Potential Theory of Adsorption</u>

It has already been said that the failures of the B.E.T. theory have led to a re-appraisal of the Potential theory. (Section 4.1.3.c. As this theory is exclusively used in the present work it will be considered in some detail in this section.

In 1914 Polanyi introduced the theory of adsorption potential (8(It proposed that the forces which attract a molecule to an adsorbent surface decrease with increasing distance from the surface. The force of attraction at any given point in an adsorbed film is measured by the potential E, defined as the work done by the adsorption forces in bringing a molecule from the gas phase to that point.

Polanyi considered that above an adsorbent surface the adsorption space may be represented as a series of layers, each with an adsorption potential E_i, each layer enclosing a volume W_i. W_i increases from zero to W_o the entire adsorption space, as E_i decreases from its maximum value at the adsorbent surface to zero at the outermost adsorbed layer. The process of building up an adsorbed film may therefore be represented in general by the equation:-

$$E = f(W) \qquad - \quad \text{Equation 4.13.}$$

Polanyi further postulated that the adsorption potential is

independent of temperature, so that the curve $E = f(W)$ should be the same for a given gas at all temperatures. For this reason it is known as the Characteristic Curve or Universal Isotherm.

For adsorbates well below their critical temperature, Polanyi equated the adsorption potential E_W for a volume filling, W, of the adsorption space, with the amount of work necessary to compress the adsorbate from its equilibrium pressure P to its saturation vapour pressure Po.

i.e. $E_W = nRT \ln (P/Po)_W$ - Equation 4.14.

where n = no. of molecules adsorbed at pressure P and temperature T^oK. The value of W corresponding to E_W is X/ρ_T, where X is the weight of the adsorbed film and ρ_T is the density of the adsorbate at temperature T.

The success of the Potential Theory in predicting the temperature dependence of physical adsorption was shown by Berenyi (81). Using the results of Titoff for the adsorption of carbon dioxide on charcoal (82), he derived a characteristic curve from the isotherm at 273^oK, and successfully predicted isotherms at other temperatures.

4.1.6. The Dubinin Modification of the Potential Theory

In 1951 Dubinin and Radushkevich (83, 84.) extended the Potential Theory by attempting to predict adsorption isotherms for any gas, given a single isotherm for one gas on the same solid.

Dubinin introduced into the Potential Equation the term β, the

affinity coefficient for the adsorbate in question on a given

adsorbent. Hence $E = \beta f(W)$ is the Equation for the Characteristic

Curve of all gases on the given adsorbent. The value of β was

determined relative to a standard adsorbate. Dubinin (83) also

found empirically that the molar volume of an adsorbate in its liquid

state is a physical property closely related to β. More recently

Dubinin (85) has found that the parachor of an adsorbate is also

closely related to β.

A particular feature of the Potential Theory is that no

explicit adsorption model is required to derive an adsorption

isotherm equation. This is particularly useful when considering

adsorption on porous carbons. The structure of porous carbons is

so complex that it is very difficult to postulate an adequate model

for adsorption. It has also already been noted (Section 4.1.3.a.)

that conventional isotherm equations such as the Langmuir and B.E.T.

Equations are based on simple adsorption models and in consequence

have serious limitations when applied to porous carbons.

In considering the application of the Potential Theory to

adsorption on porous adsorbents, Radushkevich (83) classified porous

adsorbents into two extreme structural types. For adsorbents with

small pores of molecular dimensions, overlap of the adsorption

potentials of the pore walls occurs, and the variation of adsorption

potential in the pores is represented by the equation:

$$W = W_0 \, e^{-KE^2/\beta^2} \qquad - \qquad \text{Equation 4.15.}$$

where K is a constant dependent on pore dimensions. Wo is the total volume of the adsorption space and can be equated to the micro-pore volume of the adsorbent. For adsorbents with extremely large pores where no overlap of adsorption potential occurs, and for non-porous adsorbents the equation becomes: $W = W_0' \; a^{-mE/\beta}$ - Equation 4.16 where m is a constant which depends on the energetic non-uniformity of the surface of the adsorbent and is independent of pore dimensions. W_0' is the total volume of the adsorption space and has no particular physical significance.

Dubinin (83) considered the application of Equations 4.15. and 4.16. to a number of carbons activated by reaction within the temperature range 850° - $950^\circ C$. For carbons activated up to 50% burn-out, pores exist with similar dimensions to the adsorbate molecule and Equation 4.15. applies. Carbons activated to a burn-out greater than 75% have large pores, so that Equation 4.16. is obeyed. Carbons activated to 50 - 75% burn-out exhibit intermediate behaviour.

Since $E_W = 2.303 \; nRT \log (P_0/P)$ W Equation 4.15. becomes:-

$\log W = \log W_0 - D \log^2 (P_0/P)_W$ - Equation 4.17.

where $D = \dfrac{2.303 \; (n \; RT)^2 k}{\beta}$

Equation 4.16. becomes:-

$\log W = \log W_0' - D' \log (P_0/P)_W$ - Equation 4.18.

where $D' = \dfrac{nRT}{\beta} \; m$

Equations 4.17.and 4.18. represent adsorption isotherms for appropriate adsorbents and a plot of log W against $\log^2(Po/P)$ or $\log(Po/P)$ as the case may be, will be a straight line, whose intercept gives a value of Wo. For adsorbents of the first structural type for which Equation 4.17 applies, Wo represents the micro-pore volume of the adsorbent. For Equation 4.17. the slope of the line gives D, which since it is related to k, can be used as a semi-quantitative measure of the micro-pore size distribution.

In the present work adsorption isotherms were obtained using the McBain - Bakr method, full details of which are given in Appendix III In this method values of X, the weight of the adsorbed film are measured. X is related to W by the equation $W = X/\rho$, where ρ is the density of the adsorbate. In the present investigations carbon dioxide has been chosen as the adsorbate. Carbon dioxide was chosen in preference to nitrogen since it has been shown (86,91.) that for unactivated and slightly activated carbons the adsorption of nitrogen is limited by activated diffusion. Also in a recent paper (87) Walker and Kini have selected carbon dioxide as the most suitable adsorbate for the measurement of the surface area of coals. At the temperature of $195^\circ K$ at which the isotherms have been determined, carbon dioxide is considered to be a supercooled liquid of density 1.23 g.cc.$^{-1}$ and to have a saturation vapour pressure of 141.36 cm.Hg. These values have been taken from the data of Dubinin et Al (89) and Bridgeman (90) respectively. Walker and Kini

have recently suggested (87) that the true state of carbon dioxide

in the adsorbed phase at 195°K is intermediate between a perfect

bulk liquid and a perfect bulk solid, however, they do not make any

suggestion of an alternative value of density to be used in micro-

pore volume calculations.

4.2. Results of the Present Investigations of Porosity

4.2.1. Adsorption Isotherms and Micro-Pore Volumes

Full details of the apparatus and experimental procedure for

obtaining the adsorption isotherms are given in Appendix III.

The detailed adsorption data are given in Appendix IV.

The adsorption isotherms for cellulose and cellulose triacetate

activated series of carbons are shown in Figs. 4.1. and 4.2., Some

samples of the isotherms for the two activated series, plotted

according to Equation 4.17. are shown in Figs. 4.3. and 4.4.

Tables 4.1. and 4.2. contain the micro-pore volumes and values of D

obtained from application of Equation 4.17. to the adsorption

isotherms.

It was found experimentally (Chapter 3. Section 3.) that the

rate of activation of cellulose and cellulose triacetate carbons

varies with starting weight of carbon. Therefore, the list of

carbons in Tables 4.1. and 4.2. has been subdivided into three

series. Series (i) refers to carbons activated from different

starting weights to varying degrees of burn-out at 935°C. Series(ii)

refers to carbons activated from a constant starting weight

(ca. 0.5g.) at the same temperature (935°C). Series (iii) refers

to carbons activated to varying degrees of burn-out, from a constant starting weight (ca.0.5g.) at different temperatures in the range $890^{\circ}C$. to $960^{\circ}C$.

No adsorption of carbon dioxide was detectable for both an unactivated sample of polyacenaphthylene carbon and a sample activated to a burn-out of 50% at $935^{\circ}C$. Thus it was concluded that the micro-pore volumes of the samples examined were less than $10^{-3}cc.g.^{-1}$ the minimum volume detectable by the apparatus.

4.2.2. Mercury Density Results

The apparatus and experimental procedure for the determination of mercury densities of the carbons are described in Appendix A iii. It was found that the mercury densities of both an unactivated sample of polyacenaphthylene carbon and a sample activated to a burn-out of 50% at $935^{\circ}C$ were equal to 1.72 g.cm.$^{-3}$.

Values of mercury densities obtained for cellulose carbons of Series (i) and (ii) and cellulose triacetate carbons of Series (i) are listed in Tables 4.5. and 4.6.

4.3. Discussion of the present Results

4.3.1. Adsorption Isotherms

For the purpose of applying Equation 4.17. to the adsorption isotherms, it was only necessary to explore the relative pressure range 10^{-5} to 0.3, since at a relative pressure of 0.3, the value of $\log^2 Po/p$ is close to zero. Since the full relative pressure range was not explored it is not possible to identify the isotherms

according to the classification of Brunauer, (64).

The extent of the adsorption occurring at relative pressures less than 0.05 is greater than over the remainder of the relative pressure range for all but the most highly activated carbons. (Figs. 4.1. and 4.2.) This indicates that the major part of the carbon surface is contained in very fine pores. In general the isotherms for the adsorption of carbon dioxide on activated cellulose and cellulose triacetate carbons (Figs. 4.1. and 4.2.) follow the pattern found by Lamond and Marsh (88) for adsorption of the same gas on an activated series of polyvinylidene chloride carbons. At low relative pressures of carbon dioxide (ca.10^{-3}) adsorption takes place to a greater extent for the unactivated and slightly activated carbons compared with the highly activated carbons. This can be attributed to the fact that the pores in the slightly activated carbons are finer than in the highly activated carbons. Thus at low relative pressures, the higher adsorption potential of the fine pores compared with the adsorption potential of the large pores results in greater adsorption in the fine pores. In contrast, at higher relative pressures (ca.0.3) adsorption takes place to the greatest extent for the highly activated carbons. This can be attributed to pore filling occurring at higher relative pressures. Hence the adsorption isotherms for the activated series of the two carbons provide evidence that the sizes of the pores in the carbons increase on increasing activation. Further examination of Figs.4.1.

and 4.2. reveals that either new pores are formed or closed pores
are opened in the initial stages of activation. This is
evidenced by the fact that for both unactivated cellulose and
cellulose triacetate carbons (0% burn-out) the extent of adsorption
at low relative pressures is less than the adsorption at similar
relative pressures for samples of both carbons activated to a
burn-out of ca. 25%. McEnaney has concluded (14) that in the
initial stages of activation of cellulose and coconut-shell carbons
the predominant process is the opening of blocked pores accompanied
to a lesser degree by the creation of new pores. McEnaney has
also confirmed the evidence of the present work that shows that the
predominant process occurring in the later stages of the activation of
carbons is the widening of existing pores rather than the creation
of new pores. If this were not the case then even for highly
activated carbons, considerable adsorption at low relative pressures
might be anticipated if new pores are found in the later stages of
activation.

4.3.2. Data obtained from the Application of the Dubinin Equation

At first sight the plots (Figs. 4.3. and 4.4.) of the isotherms
according to the Dubinin Equation (Equation 4.17.) appear to follow
the pattern found by Dubinin. For carbons activated to a burn-out
of 40%, the plots are linear almost, over the entire pressure range
(10^{-3} - 40 cm.Hg.); above a burn-out of 40% the carbons give plots
which have two linear sections, and at a burn-out of 75% the isotherm

plotted according to Equation 4.18. is almost linear. (Fig.4.5.)
Closer examination of the isotherms plotted according to Equation
4.17. reveals, however, that the plots vary from a very shallow
curve for slightly activated carbons to very pronounced curves for
highly activated carbons. These curves can in nearly all cases be
approximated to a pair of intersecting straight lines. The point
of intersection of these lines moves from low relative pressures
for slightly activated carbons, (P/Po = Ca.10^{-4}) to higher relative
pressures (P/Po = ca.10^{-1}) for the highly activated carbons.

These results are in accordance with the qualitative
interpretation of the isotherms themselves and show that for carbons
activated to a burn-out of 40%, the pores remain comparable in size
with the adsorbate molecule and the assumptions of Equation 4.17.
are justified. On increasing the degree of activation above a burn-
out of 40%, the pores increase in size relative to the adsorbate
molecule and Equation 4.17. applies separately to two pressure ranges.
The two linear sections of the plots of log X against log $^2Po/p$
(Equation 4.17.) can be interpreted in terms of a two stage adsorption
process. In a recent paper (85), Dubinin has interpreted the
adsorption of benzene on activated charcoal, in terms of the filling
of two types of micro-pore, represented by the equation:-

$$W = Wo1 \ e^{-k_1 E^2/\beta^2} + Wo2 \ e^{-k_2 E^2/\beta^2} \quad - \text{ Equation 4.19.}$$

where W_{o1} and W_{o2} are the micro-pore volumes of the two types of pore. An alternative explanation for the two-stage process has been advanced by Marsh and Lamond (92). They have attributed the first stage at low relative pressures to monolayer formation and the second stage at high relative pressures to micro-pore filling. This point is discussed later in this Chapter.

In the present work the two possibilities for extrapolation of the Dubinin plots are illustrated in Fig. 4.6. The values of X_o obtained from the extrapolation of the linear section the Dubinin plot at higher relative pressures yield reasonable values for the micro-pore volumes of the carbons. (Tables 4.1. and 4.2.)

It can be seen from Fig. 4.7. that for cellulose carbons of Series (i) the relationship between development of micro-pore volume and degree of burn-out is a smooth curve. This implies that the pore sizes increase on activation and agrees with the qualitative evidence of the isotherms for the activated series of cellulose carbons. The development of micro-pore volume in cellulose triacetate carbons of Series (i) (Fig. 4.8.) is a linear function of the degree of burn-out. The extent of micro-pore development in cellulose and cellulose triacetate carbons virtually coincide until a burn-out of ca. 30% is reached. After a burn-out of 30%, the micro-pore development in cellulose carbons exceeds to an increasing degree, the corresponding development in cellulose triacetate carbons. For example at a burn-out of 75% the micro-pore

volumes of the cellulose and cellulose triacetate carbons are 1.01 and 0.72 cm.^{3}g.$^{-1}$ respectively.   The micro-pore volumes for the cellulose carbons of Series (ii) and (iii) and the micro-pore volumes of cellulose triacetate carbons of Series (iii) are plotted as a function of burn-out in Figs. 4.9. and 4.10.   For comparison the corresponding curves of micro-pore volume as a function of burn-out from Figs. 4.7. and 4.8. have been superimposed on Figs.4.9 and 4.10. respectively.   It can be seen from Fig. 4.9. that the variation of micro-pore volume with degree of burn-out for cellulose carbons of Series (ii) and (iii) is identical to that found for Series (i).   This shows that variations in the starting weight of unactivated cellulose carbon over the weight range 0.4g. to 1.0g. for Series (i) have no detectable effect on the development of micro-pore volume.   It also shows that variation of the temperature of activation in the range 890°C - 960°C has no detectable effect on the development of micro-pore volume.   It should/be noted, however, that although Series (ii) was investigated to a burn-out of 76%, Series (iii) was only investigated to a burn-out of 25% and variation of micro-pore development in cellulose carbons with temperature may, therefore, occur at higher burn-out.

For cellulose triacetate carbons of Series (iii) (Fig. 4.10.) a slight variation of micro-pore volume occurs for variations in temperature of activation for a given burn-out, when the burn-out exceeds 25%.   For example at 30% burn-out, samples of cellulose

triacetate carbons had the following micro-pore volumes at various temperatures of activation:- 0.38 cc.g.$^{-1}$ at 960°C, 0.41 cc.g.$^{-1}$ at 935°C, 0.45 cc.g.$^{-1}$ at 903°C. Hence it would appear that an increase in the temperature of activation, (which results in an increase in the rate of activation of cellulose triacetate carbons, Chapter 3. Section 3.2.) produces a slight reduction in micro-pore volume. It should be noted, however, that the slight variation found is of the order of the experimental error for the determination of micro-pore volume, and therefore the significance of the variation remains doubtful.

Values of the slopes, Du, were obtained from the linear sections at high relative pressures of the Dubinin plots, and are listed in Tables 4.1. and 4.2.; these values are also plotted as functions of burn-out for cellulose (Series (i) and (ii)) and cellulose triacetate (Series (i)) carbons in Figs.4.11. and 4.12. respectively. Values of Du for these three series of activated carbons increase with increasing activation, and the increase becomes asymptotic as a burn-out of 100% is approached. Since Du can be regarded as a semi-quantitative measure of pore size distribution this indicates that the micro-pore size increases with increasing activation. This conclusion is in accordance with the evidence from the isotherms and the values of micro-pore volume previously discussed.

It has already been mentioned in this section that the adsorption occurring at low relative pressures, has been attributed

to monolayer formation (92).

In view of this the linear sections at low relative pressures were extrapolated as shown in Fig. 4.6. to give values of X_m, the weight of adsorbate per gram of adsorbent in a monolayer. Surface areas of the carbons were calculated using a value of $17\text{\AA}^2$ for the cross-sectional area of the carbon dioxide molecule in the adsorbed phase. This value is taken from a calculation involving the liquid density of carbon dioxide at $-56°C$ (89) and using Equation 4.3. Recently Anderson et Al (91) claim to have shown that the surface area of the carbon dioxide molecule in the adsorbed phase is between $18\text{\AA}^2$ and $23\text{\AA}^2$, depending on the adsorbent, if the surface area, as measured from adsorption of carbon dioxide at $195°K$, is to correspon to the value obtained from adsorption of nitrogen at $77°K$. Such a comparison would not be possible in the present work, since it has been shown (86) that adsorption of nitrogen on unactivated carbons and slightly activated carbons is restricted by activated diffusion effects. Since no definite conclusion concerning the area of the carbon dioxide molecule in the adsorbed phase has been made in the literature, and since most workers have used a value of $17\text{\AA}^2$ (70, 88,92.) this value is used in the present work. The corresponding surface areas and micro-pore volumes of cellulose and cellulose triacetate carbons of Series (i) and (ii) are summarised in Tables 4.3. and 4.4. The surface areas of both carbons appear to remain constant throughout the activated series at values of

ca.500 $m.g.^{-1}$ for cellulose carbons and ca.600m.g.$^{-1}$ for cellulose

triacetate carbons, decreasing slightly at high burn-out.   This

result is not in accordance with most of the previous work relating

surface area to degree of activation.

Kawahata and Walker (93) and Lamond and Marsh (88) for example

have found that the surface area of a carbon varies on activation.

In view of this, the alternative explanation by Dubinin (85) seems

more likely.   This is that one kind of micro-pore filling is

occurring, followed at higher relative pressures by the filling of

larger micro-pores.   It is still remarkable, however, that the pore

volume of this smaller type of micro-pore should remain constant on

activation and this remains unexplained.   However, evidence

consistent with this theory comes from values of D_{ϱ} (Tables 4.3.

and 4.4.) obtained from the slopes of the linear sections of the

Dubinin plots at lower relative pressures. D_{ϱ} remains constant

throughout the activated series of each carbon, i.e. the size

distribution of this type of pore remains constant on activation.

The values of r in Tables 4.3. and 4.4. are the mean micro-

pore radii of the activated carbons and were calculated from

Equation 4.7. using the values of surface area and micro-pore

volume in Tables 4.1. to 4.4.

The mean micro-pore radii of both cellulose and cellulose

triacetate carbons increase with activation.   This is in accord

with the evidence of the values of Du, which also increase with

increasing activation. The values of r range from ca.7Å for unactivated carbons to ca.50Å for highly activated cellulose carbons and ca.30Å for highly activated cellulose triacetate carbons. These values would appear to be high by a factor of two according to Dubinin's specifications of micro-pore size, which range from 4Å to 25Å for unactivated to highly activated carbons respectively.

This is probably due to the limitations of Equation 4.7. The assumption of a cylindrical pore model in which the pores are not interconnected is an oversimplification of the pore structure of carbon. In addition this is further evidence that the values of surface area used in Equation 4.7. are of doubtful significance.

One further interesting feature from the Dubinin plots is shown in Figs. 4.13. and 4.14. where values of $\log^2 {}^{Po}/P$ corresponding to the point of intersection of the two linear sections of each Dubinin plot, are plotted against the degree of burn-out of the activated carbon. The resulting plots for both cellulose and cellulose triacetate carbons are smooth curves resembling the shape of the curves obtained for the variation of values of Du with degree of burn-out. (Cf. Figs. 4.11. and 4.12.)

Hence it appears that the movement of the point of intersection of the linear sections of the Dubinin plots through an activated series is an effect due to variation in the pore size of carbons.

The lack of detectable adsorption of carbon dioxide on polyacenaphthylene carbons is in marked contrast to cellulose and

cellulose triacetate carbons. This is a reflection of its more graphitic nature, (Chapters 1 and 2. Sections 1.3. and 2.3.3.) and consequently polyacenaphthylene carbon has few spaces between the micro-crystals for adsorption to occur. The evidence of the adsorption experiments is in accordance with the evidence from rates of reaction and mercury density determinations. Since the mercury density does not change on activation, weight loss on activation of polyacenaphthylene carbon is postulated to take place entirely from the external surface (Section 4.3.3.), this results in slow rates of activation and an undetectable development of porosity. These points are further discussed in Chapter 5.

4.3.3. Mercury Densities

The variation of mercury density of cellulose carbons of Series (i) and (ii) with degree of burn-out (Fig.4.15.) is a smooth curve slightly convex to the axis of burn-cut, in contrast to the smooth curve for cellulose triacetate carbons of Series (i) which is slightly concave to the axis of burn-out.

During the process of activation of a carbon, weight loss can occur from both the external and internal surface. The mercury density of a carbon defines its external surface, (Section 4.1.2.b.) providing mercury cannot enter pores of less than 10^5 $\overset{o}{A}$ in diameter, but can penetrate all the spaces between the granules in the sample. If this is the case an analysis of the mercury densities of an activated series of carbons may be undertaken (63) which leads to an estimate of the ratio of internal to external weight loss throughout

the activated series. The external weight loss Xg. of 1g. carbon at a burn-out of $a\%$ is given by:-

$$X = \left(\frac{1}{\rho_{Hg_o}} - \frac{(100 - a)}{100. \rho_{Hg_a}} \right). \rho_{Hg_o}$$ - Equation 4.20.

where ρ_{Hg_o} is the mercury density of unactivated carbon, and ρ_{Hg_a} is the mercury density of the carbon at a burn-out of $a\%$. The quantity (100 - a% burn-out) has been termed the activation yield of carbon (63).

W.J. Thomas has shown (94) that the inequality

$$\frac{\sqrt{2.kr.Deff}}{Lk^1} > 1$$, represents the condition that burn-out

will occur to a greater extent in the interior of the carbon compared with the exterior; k and k' are first order chemical rate constants for the internal and external reactions respectively, Deff is the effective diffusion coefficient of the reacting gas, and r and L are values of the mean pore radius and length respectively calculated from a cyclindrical pore model. In the present work the inequality has not been applied due to lack of information for values of Deff, k and k'.

The external weight loss of cellulose triacetate carbons (Fig.4.16.) is a linear function of the degree of burn-out. The ratio of internal to external burn-out, $^{int}/ext$, is calculated

from $^{int}/ext$ $= \dfrac{1 - I}{I}$ - Equation 4.21.

where I is the value of the external weight loss at a burn-out of 100%. For cellulose triacetate carbons of Series (i), $^{int}/ext = 0.72$ and is constant. The linearity of the variation of external weight loss with degree of burn-out for cellulose triacetate carbons agrees with the linearity of a similar plot for activated coconutshell carbons found by Kipling and McEnaney (63).

Thus during the process of activation of cellulose triacetate carbons, a slightly greater weight loss of carbon takes place from the external surface compared with the internal surface and the ratio of internal to external attack remains constant.

The variation of the external weight loss of cellulose carbons of Series (i) and (ii) with degree of burn-out is in the form of a curve, (Fig. 4.16.). Up to a burn-out of ca. 30% the external weight loss is very small, but it increases markedly thereafter hence $^{int}/ext$ decreases on activation. An attempt is made in Chapter 5 to explain the differences of the internal to external burn-out ratios found for cellulose and cellulose triacetate carbons in terms of the evidence of rates of reaction and optical micrography

The Development of Total Porosity on Activation using assumed "true" Densities

It was pointed out in Section 4.1.2.b. of this Chapter that the total pore volume of a carbon could be obtained from a knowledge of

the apparent density in mercury, and the "true" density of the carbon. It was also pointed out that methods of establishing the density of the solid material alone, i.e. the so called "true" density had several practical and theoretical limitations when applied to porous carbons. However, a picture of the development of total pore volume (the sum of macro- and micro-pore volumes) of a carbon may be obtained if an estimate of its "true" density can be obtained. In the present work neither helium densities (Section 4.1.2.b.) nor X-ray densities of carbons were obtainable due to practical limitations.

There is reason to believe, however, from the work of Kipling and McEnaney (63) and Dubinin (95) that the "true" density of a carbon does not vary significantly with activation at temperatures below 1000°C. Kipling and McEnaney showed that the helium densities determined at 300°C, for an activated series of coconutshell carbons remained constant almost at 1.93 g.cm.$^{-3}$. Dubinin found that the densities of activated sucrose carbons determined from X-ray measurements remained nearly constant throughout the series at 1.96 g.cm.$^{-3}$. In the present work values for the helium densities of unactivated cellulose and cellulose triacetate carbons at 935°C have been obtained by interpolation between the values at 700°C and 1500°C quoted by Kipling et Al (96) for carbons prepared from the same polymers. Assuming that these values remain approximately constant on activation, the total pore volumes of cellulose carbons

series (i) and (ii) and cellulose triacetate carbons Series (i)
have been obtained. (Tables 4.7. and 4.8.) In view of the assump-
tions made, it should be emphasised that the following discussion
is of qualitative value only, however, a reasonable picture of the
development of total and macro-pore volumes of the carbons may be
obtained.

The total porosities of both cellulose and cellulose triacetate
carbons (Figs. 4.18. and 4.19.) are increased on activation, the
relation between the degree of burn-out and total pore volume being
a smooth curve in each case. A difference in the development of
total pore volume for cellulose and cellulose triacetate carbons is
revealed by Figs. 4.20 and 4.21. which show the total pore volumes
expressed as cm.^{3}g.$^{-1}$ of unactivated carbon. These figures show
that for cellulose carbons the total pore volume increases to a
maximum at a burn-out of ca. 40% and then decreases. This result
is in qualitative agreement with the result obtained by Kawahata and
Walker (93) for the total porosity development of an activated series
prepared from anthracite. They found that the total pore volume
of anthracite reached a maximum at ca. 40% burn-out. For cellulose
triacetate carbons, the total pore volume expressed as cm.^{3}g.$^{-1}$ of
unactivated carbon remains virtually constant over the entire range
of burn-out investigated (to 75%). This result is in qualitative
agreement with the result obtained for coconutshell carbon by Kipling
and McEnaney (63). They found that the total pore volume of

coconutshell carbon remained constant over the range of burn-out 0 to ca. 70%.

The macro-pore volumes of cellulose and cellulose triacetate carbons were calculated as the difference between the total pore volumes and micro-pore volumes of the carbons obtained from the Dubinin plots. The variation of macro-pore volume with degree of burn-out for cellulose carbons Fig. 4.18. is approximately linear. This is in contrast to cellulose triacetate carbons for which the macro-pore volume decreases in the initial stages of activation (Fig. 4.19.) and then increases on further activation. In Chapter 5 an attempt is made to correlate the differences between the total pore developments of cellulose and cellulose triacetate carbons with the evidence obtained from rates of activation and optical micrography.
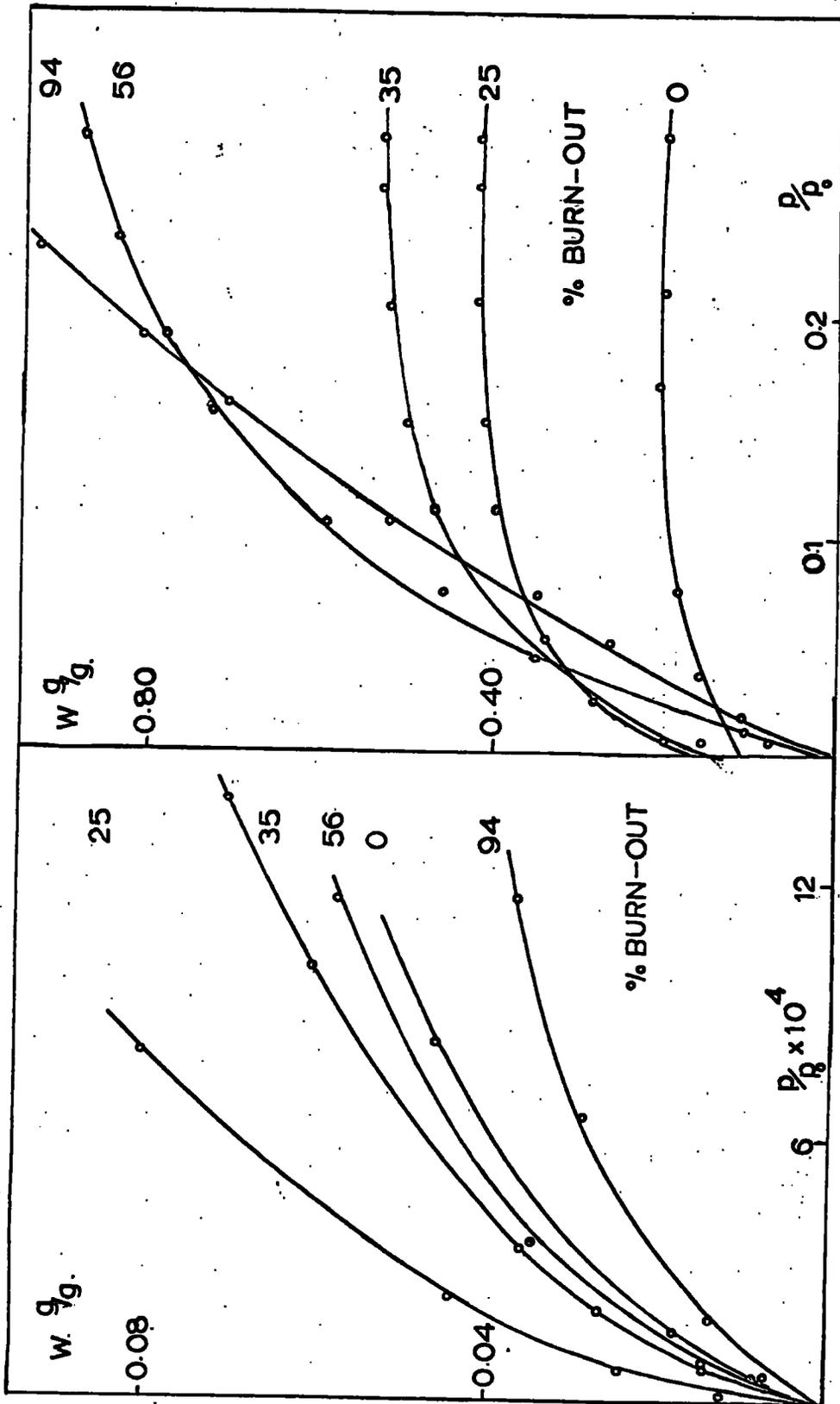
FIG. 4.1 ADSORPTION OF CO_2 ON CELLULOSE CARBONS AT $195°K$. SERIES (i)
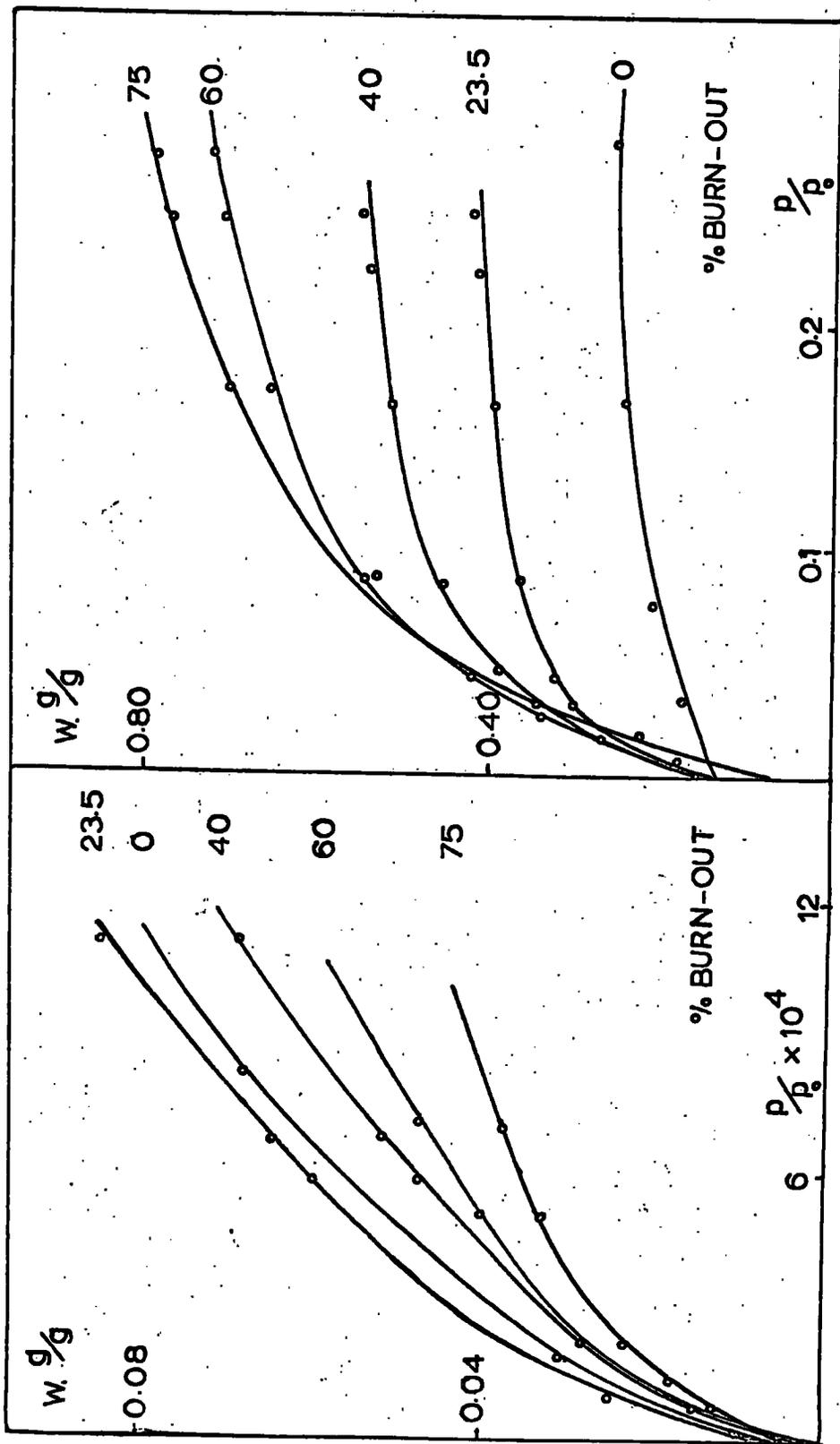
FIG. 4.2. ADSORPTION OF CO_2 ON CELLULOSE TRIACETATE CARBONS AT 195°K

SERIES (i)

FIG. 4. 3. DUBININ PLOT (EQN. 4.17.) FOR CELLULOSE CARBONS OF SERIES (i)

FIG. 4.4 DUBININ PLOT (EQN. 4.17.) FOR CELLULOSE TRIACETATE CARBONS OF SERIES (i)
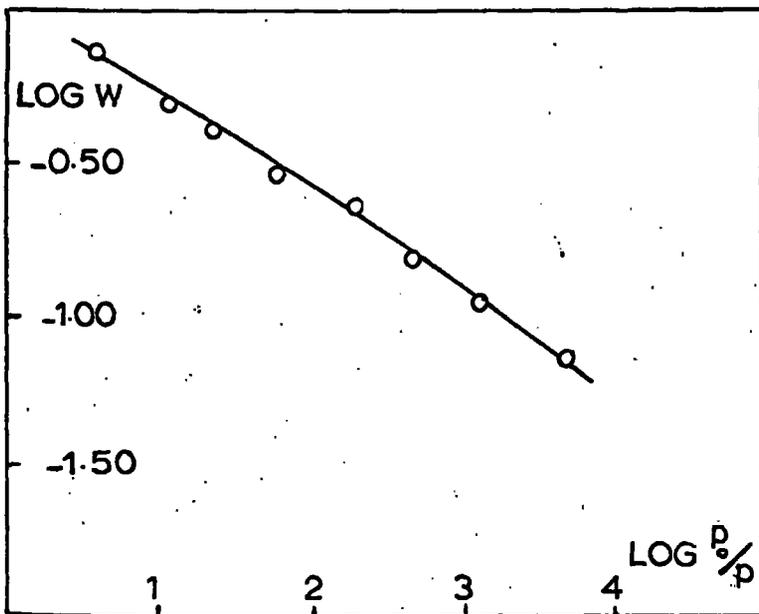
FIG. 4. 5. ISOTHERM PLOTTED ACCORDING
TO EQUATION 4.18. FOR A HIGHLY ACTIVATED
CELLULOSE CARBON.
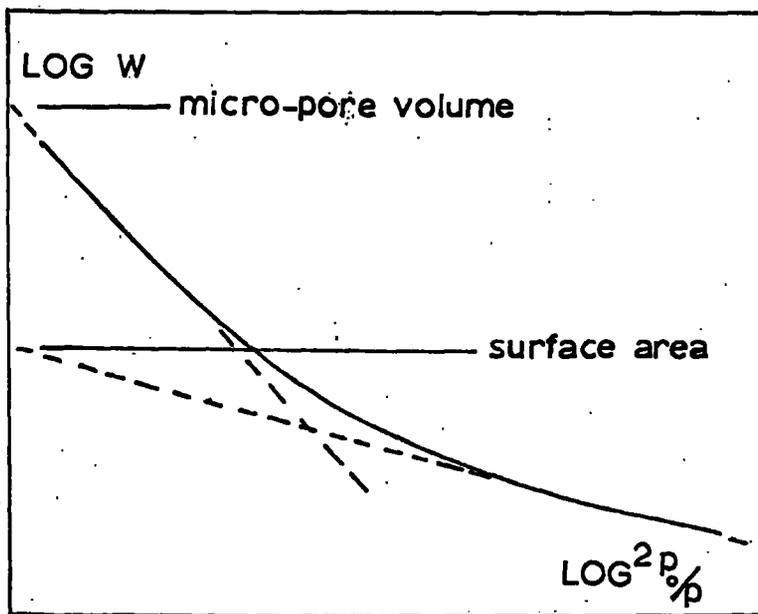
FIG. 4. 6. THE TWO POSSIBILITIES FOR
THE EXTRAPOLATION OF A DUBININ PLOT
(EQN 4.17.)
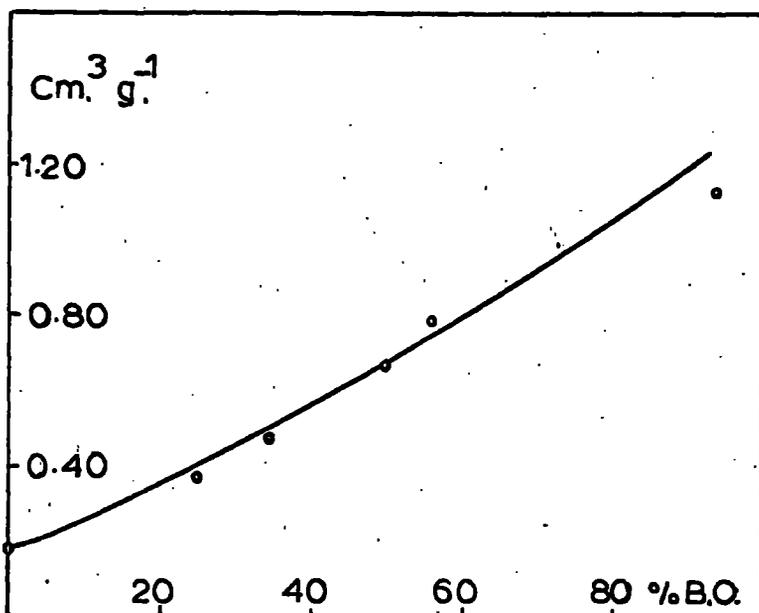
FIG. 4.7. MICRO-PORE VOLUMES OF
CELLULOSE CARBONS SERIES(i).
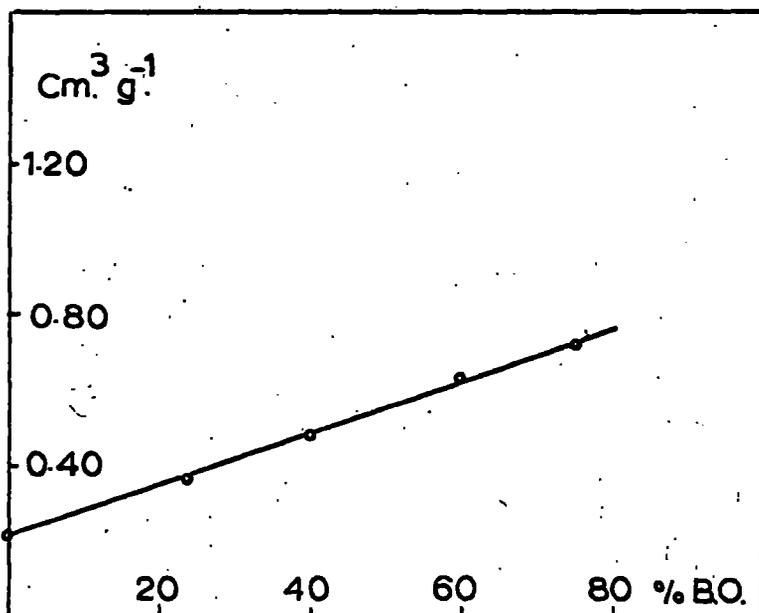
FIG. 4.8. MICRO-PORE VOLUMES OF
CELLULOSE TRIACETATE CARBONS
SERIES (i)
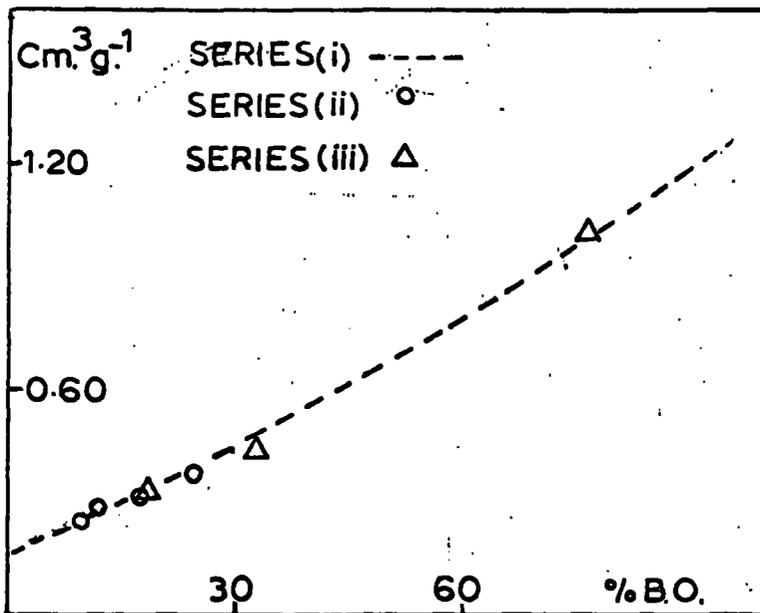
FIG. 4.9. MICRO-PORE VOLUMES OF
CELLULOSE CARBONS. SERIES (ii)&(iii)
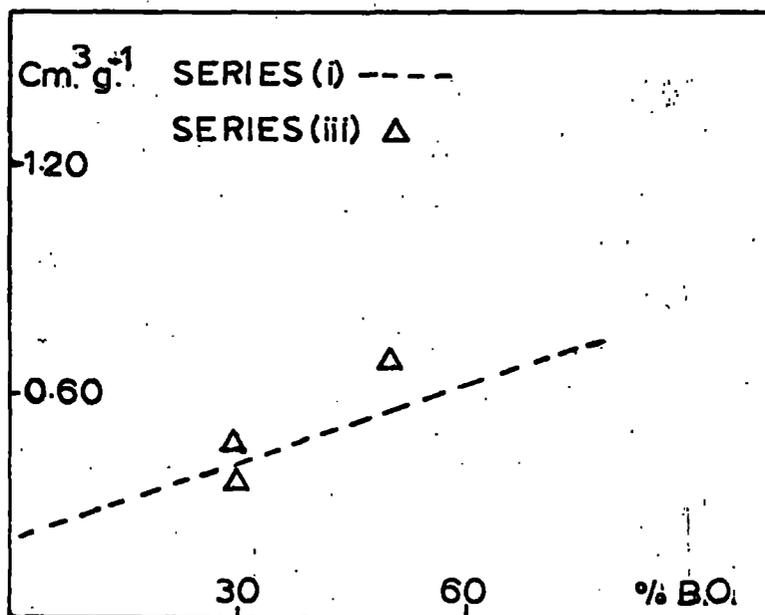
FIG. 4.10. MICRO-PORE VOLUMES OF
CELLULOSE TRIACETATE CARBONS
SERIES (iii)
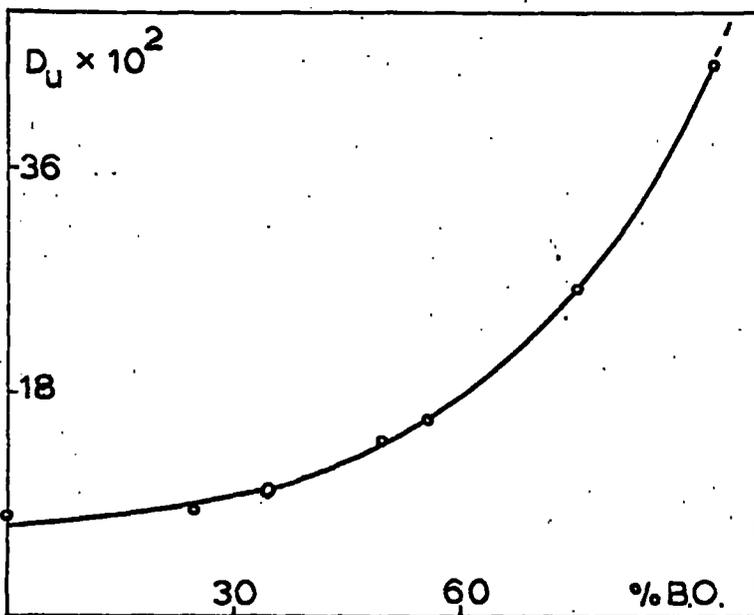
FIG. 4.11. D_u VALUES FOR   CELLULOSE
          CARBONS   SERIES(i)
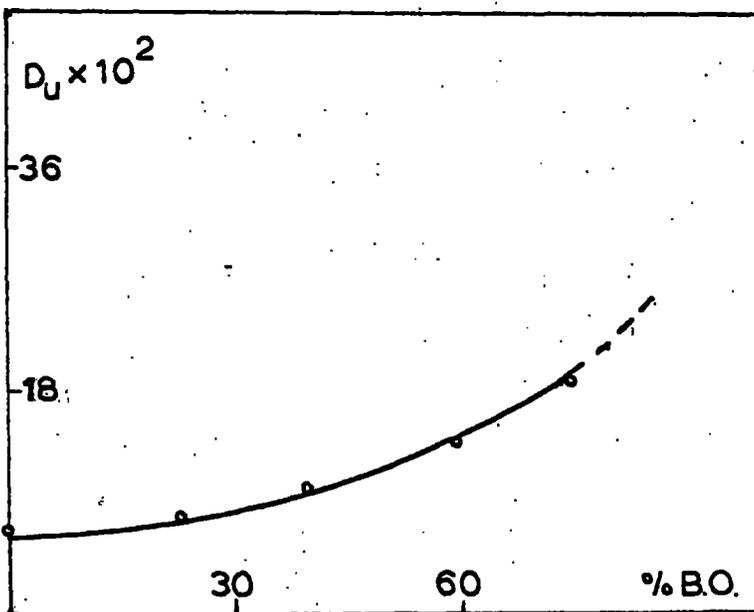
FIG. 4.12. D_u VALUES FOR CELLULOSE
TRIACETATE   CARBONS   SERIES(i)
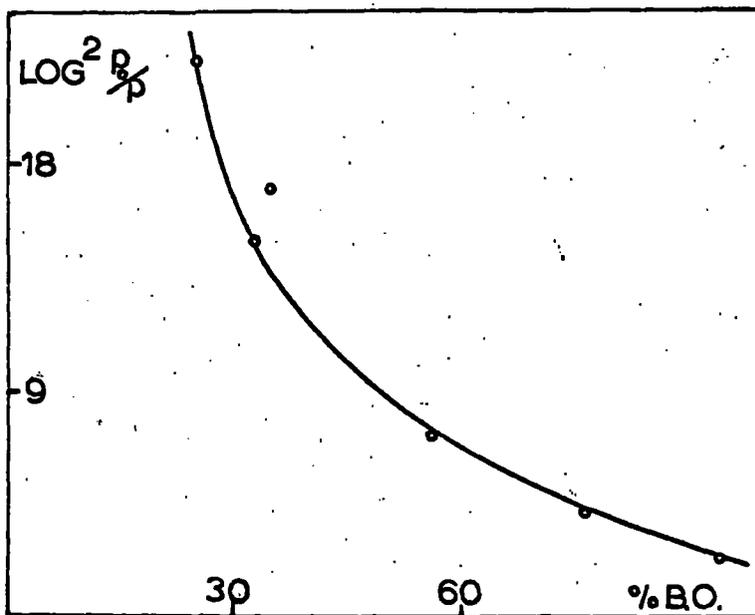
FIG. 4.13. $\text{LOG}^2 \frac{p_0}{p}$ (int) Vs. % B.O.
CELLULOSE CARBONS OF SERIES (i)
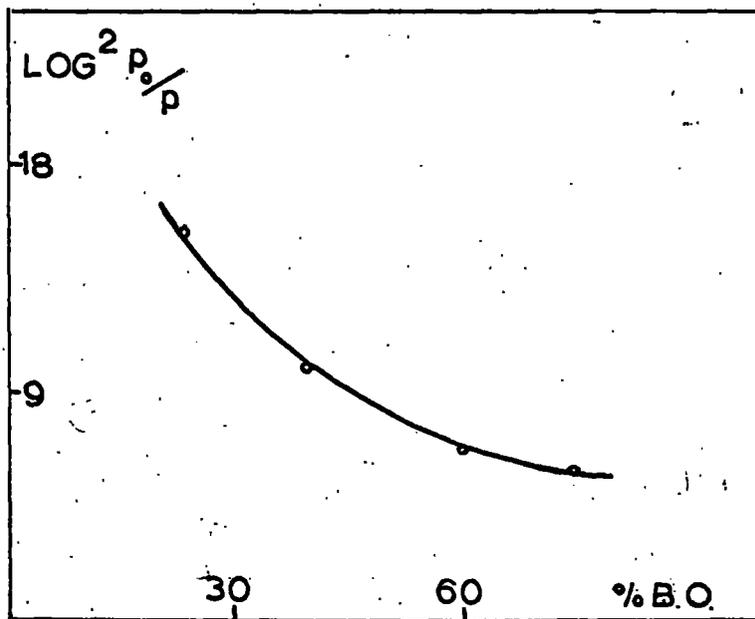
FIG. 4.14. $\text{LOG}^2 \frac{p_0}{p}$ (int) Vs. % B.O.
CELLULOSE TRIACETATE CARBONS
OF SERIES (i)
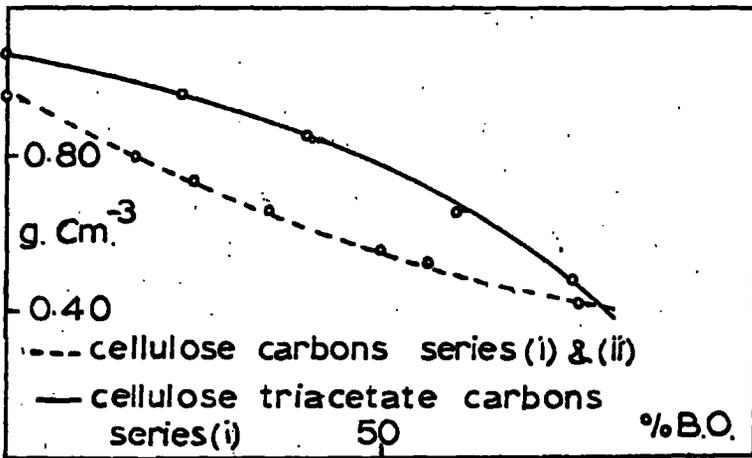
FIG. 4.15. MERCURY DENSITIES
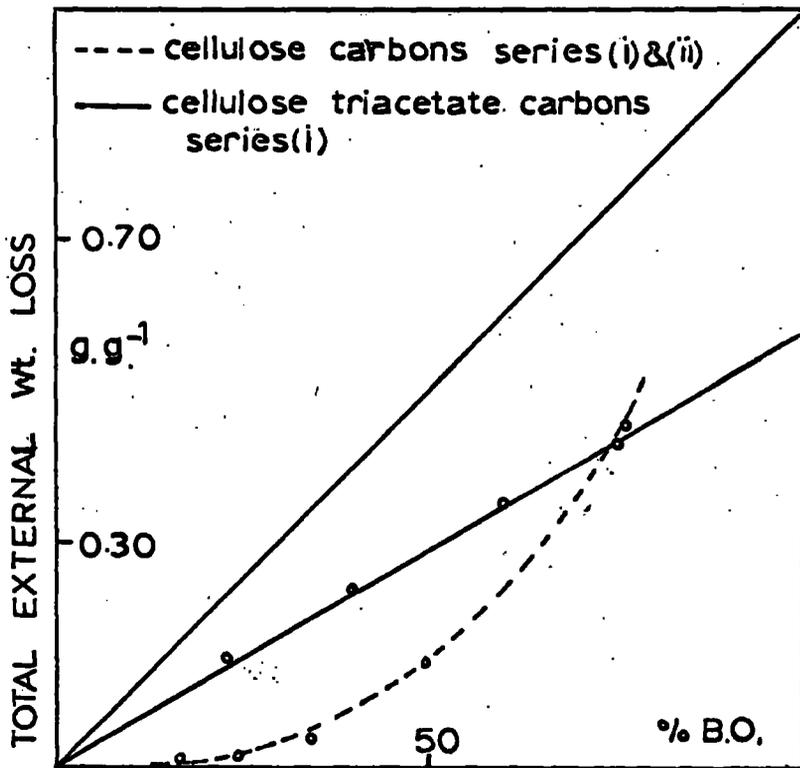
FIG. 4.16. EXTERNAL/INTERNAL Wt. LOSS
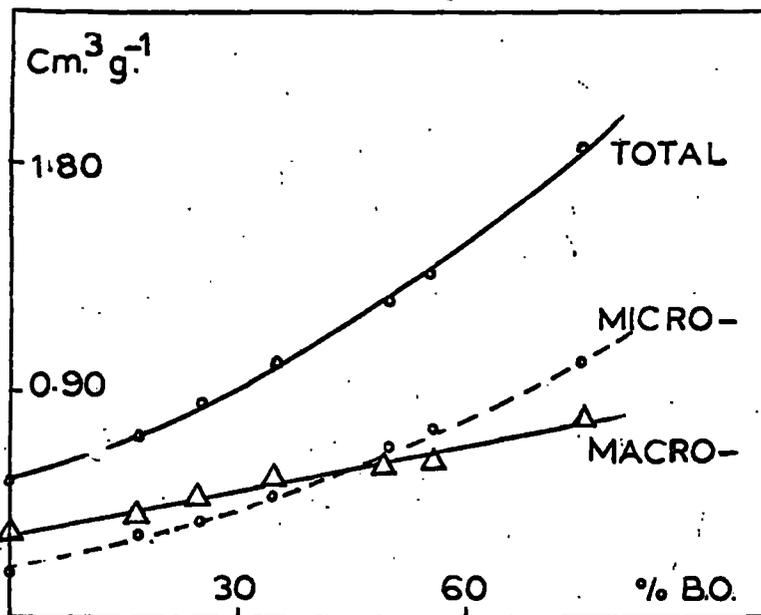
FIG. 4.17 PORE VOLUMES CELLULOSE
CARBONS OF SERIES (i) &(ii)
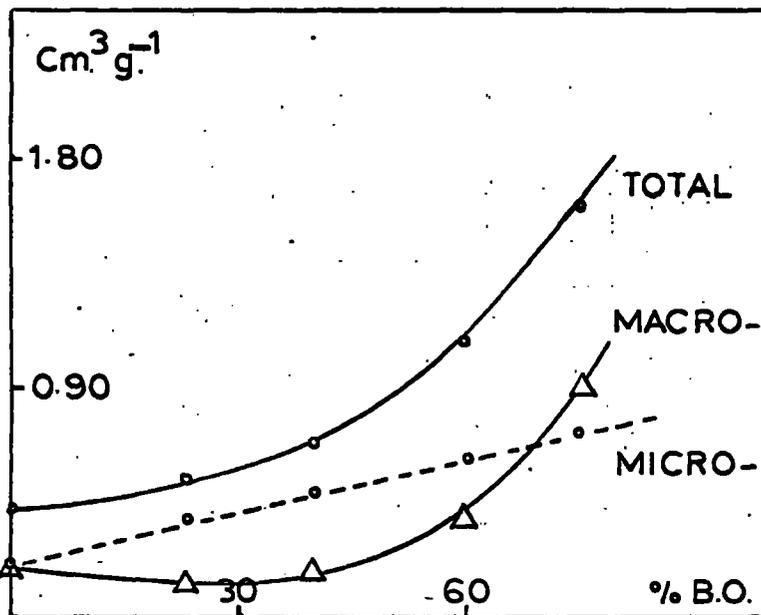
FIG. 4. 18. PORE VOLUMES CELLULOSE
TRIACETATE CARBONS OF SERIES (i)
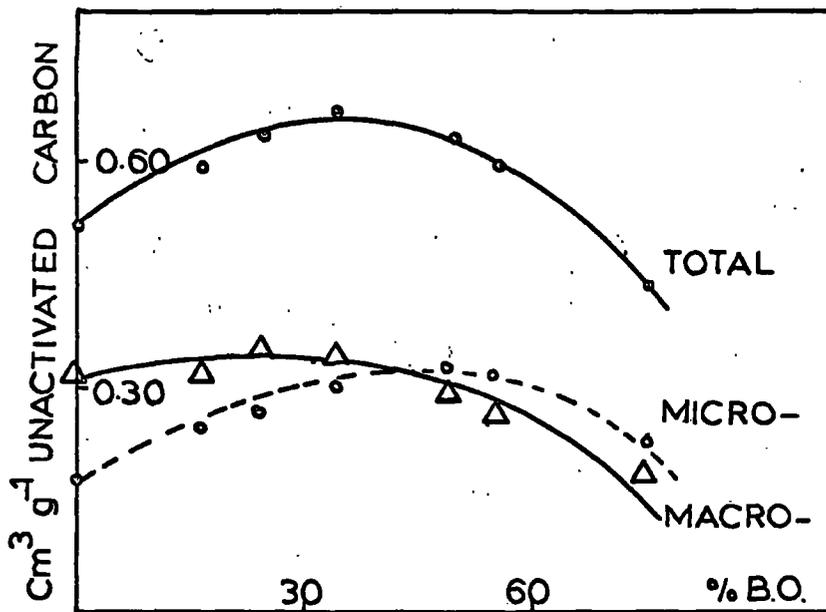
FIG. 4.19. PORE VOLUMES OF CELLULOSE
CARBONS OF SERIES (i) & (ii)
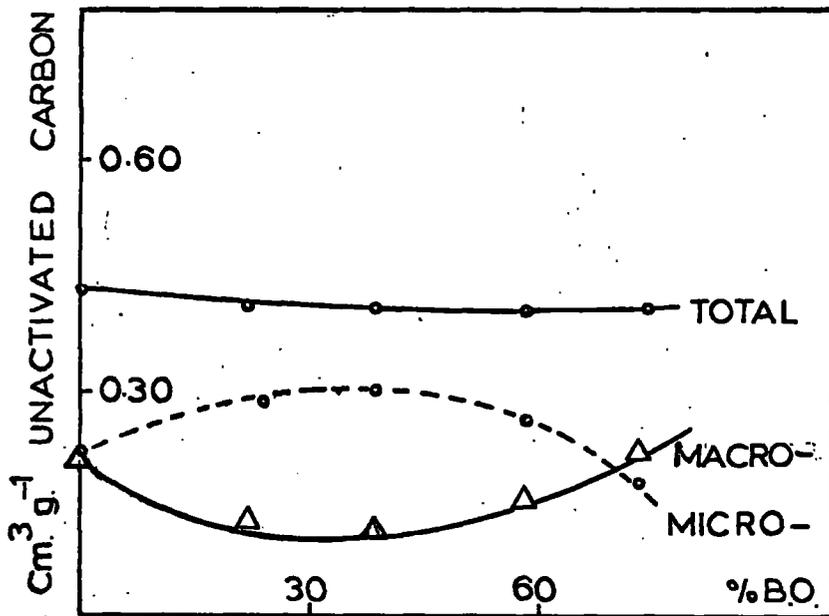
FIG 4.20. PORE VOLUMES OF CELLULOSE
TRIACETATE CARBONS OF SERIES (i)

Table 4.1.

Micro-Pore Volumes for Activated Cellulose Carbons

Series	Degree of Activation (%B.O.)	Temperature of Activation ($^{\circ}$C)	D_u x 10^2	Micro-Pore Volumes (cm.^{3} g.$^{-1}$)
(i)	0	935	7.6	0.18
(i)	25	935	8.9	0.37
(i)	35	935	9.7	0.47
(i)	50	935	14.4	0.66
(i)	56	935	15.6	0.78
(i)	94	935	44.0	1.12
(ii)	17.5	935	8.1	0.32
(ii)	32.5	935	8.6	0.44
(ii)	76	935	25.0	1.02
(iii)	9.5	890	7.2	0.26
(iii)	12.5	955	7.1	0.29
(iii)	18.0	903	7.0	0.32
(iii)	25.0	917	8.0	0.38

D_u refers to slope of Dubinin Plot at high relative pressures.

D_ℓ refers to slope of Dubinin Plot at low relative pressures.

Table 4.2.

Micro-Pore Volumes for Activated Cellulose Triacetate Carbons

Series	Degree of Activation (% B.O.)	Temperature of Activation (^{o}C)	$D_u \times 10^2$	Micro-Pore Volumes (cm.^{3} g.$^{-1}$)
(i)	0	935	6.4	0.21
(i)	23.5	935	8.2	0.36
(i)	40	935	10.6	0.48
(i)	60	935	14.3	0.63
(i)	75	935	18.8	0.72
(iii)	30	960	8.3	0.38
(iii)	30	903	9.4	0.45
(iii)	50	919	15.8	0.68

Table 4.3.

Surface Areas and Mean Micro-Pore Radii for Cellulose Carbons

Series	Degree of Activation (% B.O.)	Surface Area (M.^{2} g.$^{-1}$)	D_{β} x 10 $\text{\AA}$	Mean Micro-Pore Radius (Å)
(i)	0	512	7.6	7.2
(i)	25	512	7.5	14.8
(i)	35	512	7.6	18.8
(i)	50	560	7.4	26.4
(i)	56	512	7.5	31.6
(i)	94	400	8.0	56.0
(ii)	17.5	512	6.0	12.8
(ii)	32.5	512	6.1	16.5
(ii)	76	535	7.5	40.8

Table 4.4.

Surface Areas and Mean Micro-Pore Radii for Cellulose Triacetate Carbons

Series	Degree of Activation (% B.O.)	Surface Area (M.^{2} g.$^{-1}$)	D_{β} x 10 $\text{\AA}$	Mean Micro-Pore Radius (Å)
(i)	0	600	6.4	7.0
(i)	23.5	580	6.6	12.5
(i)	40	580	7.0	16.5
(i)	60	580	7.0	22.0
(i)	75	490	7.0	29.5

Table 4.5.

Mercury Densities of Activated Cellulose Carbons

Series	Degree of Activation (% B.O.)	Mercury Density (g.cm.$^{-3}$)
(i)	0	0.96
(i)	25	0.73
(i)	35	0.65
(i)	50	0.56
(i)	56	0.53
(i)	94	-
(ii)	17.5	0.81
(ii)	32.5	0.67
(ii)	76	0.42

Table 4.6.

Mercury Densities of Activated Cellulose Triacetate Carbons

Series	Degree of Activation (% B.O.)	Mercury Density (g.cm.$^{-3}$)
(i)	0	1.08
(i)	23.5	0.96
(i)	40	0.85
(i)	60	0.66
(i)	75	0.47

Table 4.7.

Distribution of Pore Volumes for Cellulose Carbons.Using a "True" Density of 1.90 g.cm.$^{-3}$

Series	Degree of Activation (% B.O.)	Total Open -Pore Volume (cm.^{3}g.$^{-1}$)	Micro-Pore Volume (cm.^{3}g.$^{-1}$)	Macro-Pore Volume (cm.^{3}g.$^{-1}$)
(i)	0	0.51	0.18	0.33
(i)	25	0.84	0.37	0.47
(i)	35	1.01	0.47	0.54
(i)	50	1.26	0.66	0.60
(i)	56	1.36	0.74	0.63
(i)	94	-	-	-
(ii)	17.5	0.70	0.32	0.38
(ii)	32.5	0.97	0.44	0.53
(ii)	76	1.85	1.02	0.83

Table 4.8.

Distribution of Pore Volumes for Cellulose Triacetate Carbons. Using a "True" Density of 2.00 g.cm.$^{-3}$

Series	Degree of Activation (% B.O.)	Total Open -Pore Volume (cm.^{3}g.$^{-1}$)	Micro-Pore Volume (cm.^{3}g.$^{-1}$)	Macro-Pore Volume (cm.^{3}g.$^{-1}$)
(i)	0	0.43	0.21	0.22
(i)	23.5	0.54	0.37	0.17
(i)	40	0.68	0.49	0.19
(i)	60	1.02	0.62	0.40
(i)	75	1.63	0.72	0.91

Chapter 5.

Correlations between the Rates of Activation and the Development

of Porosity of the Carbons

5.1. Introduction

There have been few studies which attempt to relate the reactivity of carbons to the development of porosity, and therefore a separate review of such studies is not reported. Instead reference to other workers' findings is made at appropriate points in the Chapter.

In Chapter 1 (Section 1.4.) it was anticipated that two factors likely to be of particular importance in determining the rate of activation and the development of pore structure of a carbon are the nature of the carbonisation process and the graphitic character of the carbon. In addition, other factors to be considered in studies of the activation of carbons include the starting weight of carbon, the amounts of internal and external weight loss and the temperature of activation.

In this Chapter therefore, in order to discuss the results in the light of the aims of the thesis outlined in Chapter 1 (Section 1) the rates of activation and the development of pore volume of the carbons are compared under the following headings:-

(i) The influence of graphitic character,

(ii) the influence of the nature of the carbonisation process,

(iii) the influence of the starting weight of carbon for activation,

(iv) the amounts of internal and external weight loss,

(v) the influence of temperature of activation.

5.2. The Influence of Graphitic Character on the Rates of Activation and Development of Pore Volume of the Carbons

It is clear from the results so far presented in this thesis that there is a considerable difference between the behaviour of the graphitic polyacenaphthylene carbon and the non-graphitic cellulose and cellulose triacetate carbons.

From Tables 3.1. to 3.3., it can be seen that the ratios of the linear rates of activation of cellulose triacetate, cellulose and polyacenaphthylene carbons at $935^{\circ}C$ are 8.5 : 5 : 1, when ca.0.4g starting weight of carbon are used. The corresponding ratios when small starting weights of carbons are used, are difficult to estimate

This is due to the anomalous rates of reaction obtained for polyacenaphthylene carbons and the initial, non-linear rates of reaction of cellulose triacetate carbons (Chapter 3. Section 3.5.2.) when small starting weights of carbon were used.

However, the times taken to reach a burn-out of 50%, may be compared for small starting weights of the carbons activated at $935^{\circ}C$. These times are shown in Table 5.1.

It is clear that generally polyacenaphthylene carbon is inherently less reactive than cellulose and cellulose triacetate carbons by a factor of about ten. The low reactivity of

polyacenaphthylene carbon compared with cellulose and cellulose triacetate carbons can be ascribed to its more graphitic character. This conclusion is in agreement with the findings of Smith and Polley (57) discussed in Chapter 3 (Section 3.3.2.) who found that the rate of oxidation of a fully graphitised carbon black was about two hundred times slower than an ungraphitised carbon black at the same temperature. In a graphitised carbon the majority of the crystallites have their basal planes parallel to the surface, and it is known (56), that the reactivity parallel to the basal planes of a carbon is less than that perpendicular to them. Hence it appears that in polyacenaphthylene carbon a greater proportion of the crystallites have their basal planes parallel to the surface compared with the other two carbons, thus reducing the overall rate of attack by an oxidising gas. However, it is clear that polyacenaphthylene carbon, prepared at $950^{\circ}C$ is not as graphitic in character as a fully graphitised carbon black prepared by heating to $3000^{\circ}C$, since the ratio of its reactivity to those of the non-graphitic cellulose cellulose triacetate carbons is a factor of twenty less than the ratio for the fully graphitised carbon black and ungraphitised carbon black, found by Smith and Polley. However, since unactivated polyacenaphthylene carbon has a small open pore volume (96), whilst a fully graphitised carbon black is non-porous, the discrepancy in the two ratios may be partly due to the influence of the porosity of the polyacenaphthylene carbon on its reactivity. Unactivated cellulose

and cellulose triacetate carbons have considerably greater open pore volumes than unactivated polyacenaphthylene carbons (Chapter 1. Section 1.4.). On activation the non-graphitic cellulose and cellulose triacetate carbons therefore react faster and their micro-pore structures are developed considerably compared with the graphitic polyacenaphthylene carbon. For example the increases of micro-pore volume which occur when the three carbons are activated at $935^{\circ}C$ to 50% burn-out are shown in Table 5.2. Activation of polyacenaphthylene carbon does not increase the micro-pore volume and would appear to involve removal of the external surface only, (Chapter 3. Section 3.6.1.).

The rates of activation and the development of porosity of the three carbons therefore show a clear distinction between the graphitic polyacenaphthylene carbon and non-graphitic cellulose and cellulose triacetate carbons.

In general it is difficult to compare the rates of reaction and development of porosity reported in these investigations with those found by other workers for other carbons. This is principally due to the fact that few workers have attempted such a correlation, much of the work that has been reported has been concerned only with the initial stages of burn-out. However, work reported by Dubinin(97) using sucrose carbon, (a non-graphitic carbon) provides a relevant comparison with the results obtained in the present work for cellulose and cellulose triacetate carbons.

Dubinin has reported that the rate of activation of sucrose carbon, in the presence of excess carbon dioxide or steam is given by:-

$$-\,dm/dt \;=\; km \qquad\qquad - \qquad \text{Equation 5.1.}$$

where m is the mass of sucrose carbon reacting at time t, and k is the rate constant expressed by Dubinin in units of Hr^{-1}. This equation suggests that Dubinin found that the rate of activation of the carbon decreased exponentially with time. This is, therefore, in marked contrast to the present results and those of numerous other workers, (39, 48, 61.) who find linear rates of activation over a considerable range of burn-out. It is therefore of interest to note that the values of the initial rates reported by Dubinin for the activation of sucrose carbon compare quite well with those found in the present work. For example, Dubinin found that the initial rate of activation of sucrose carbon at $935^{o}C$ was 2.58×10^{-5} $g.sec^{-1}.g^{-1}$ which compares with a value of 2.67×10^{-5} $g.sec^{-1}.g^{-1}$ found in the present investigations for the activation of cellulose carbon at the same temperature. In the absence of further experimental details of Dubinin's work, it is impossible to decide whether Dubinin's results may have been consistent with zero order as well as first order kinetics. Since in the present work the reactions have been observed to be linear over an extensive range of burn-out in nearly every case, they are consistent only with zero order kinetics. In addition

the activation energy reported by Dubinin for the activation of sucrose carbon (using 0.5g. samples) over the temperature range $850^\circ C - 1000^\circ C$ is 52 k.cal.mole.$^{-1}$ compared with a value of 67 k.cal.mole.$^{-1}$ over the temperature range $890^\circ C - 930^\circ C$ found for cellulose carbon in the present work.

It is also interesting to note that Dubinin (95) has reported that the micro-pore volume of sucrose carbon is increased from 0.08 cm.^{3}g.$^{-1}$ to 0.46 cm.^{3}g.$^{-1}$ on activation to a burn-out of ca.35% at $850^\circ C$. For cellulose carbon activated at $935^\circ C$, the corresponding increase in micro-pore volume is from 0.18 cm.^{3}g.$^{-1}$ to 0.47 cm.^{3}g.$^{-1}$. The discrepancy in the micro-pore volumes of unactivated cellulose and sucrose carbons may be due to a molecular sieve effect. Dubinin used benzene as the adsorbate on sucrose carbon, and benzene has a larger molecular diameter than carbon dioxide, the adsorbate in the present work for cellulose carbon.

5.3. The Influence of the Nature of the Carbonisation Process on the Rates of Activation and the Development of Pore Volume of the Carbons

Polyacenaphthylene and cellulose triacetate polymers both fuse during carbonisation (Chapter 1. Section 1.4.) and form cokes, whilst cellulose does not and forms a char. However, it is clear from the work of Kipling and Shooter (18), Brookes and Taylor (38) and from the micrographical evidence of the present work (Chapter 2. Section 2.3.3.) that the resemblance of polyacenaphthylene carbon to

cellulose triacetate carbon is superficial only. The rate of
activation and development of porosity of cellulose triacetate
carbons resembles that of cellulose carbons rather than polyacenaph-
thylene carbons.   Hence the nature of the carbonisation process
appears to influence the rate of activation and development of
porosity of carbons only in so far as it influences the graphitic
character of the carbons (Chapter 2. Section 2.1.2.). It is the
graphitic character of the carbons which directly influences the
rate of activation and development of porosity.

5.4. The Influence of Starting Weight of Carbon on the Rates of
Activation and the Development of Pore Volume of the Carbons

It has been shown in Chapter 3 (Section 3.6.3.) that as the
starting of carbon is increased above 0.1g., the rates of activation
at 935°C of cellulose and cellulose triacetate carbons become almost
independent of starting weight. It has also been found in Chapter 4
(Section 4.3.2.) that over the range of starting weight, 0.4g. to
1g. of carbon the development of micro-pore volume is independent of
starting weight. Thus variations in starting weight over the range
0.4 - 1g. influence neither the rate of activation nor the
development of pore structure. to any significant degree.

However, it was found in Chapter 3 (Section 3.5.2.) that the
rates of activation of cellulose and cellulose triacetate carbons
varied significantly when different starting weights of less than
0.1g. carbon were used. It would, therefore, be desirable to

determine whether there was a corresponding variation of micro-pore volume in order to examine further the influence of the starting weight of carbon on the development of porosity. However, it has already been pointed out (Chapter 3.Section 3.5.1.) that this is not feasible using the present techniques for the determination of porosity.

5.5. The Relation between the Rates of Activation, Development of Pore Volume and the amount of Internal and External Weight Loss from the Carbons

The lack of development of micro-pore volume during the activation of polyacenaphthylene carbon, revealed by adsorption measurements (Chapter 4. Section 4.2.1.) can be related to the lack of internal burn-out revealed by mercury density measurements. Both these effects are clearly due to its graphitic character compared with cellulose and cellulose triacetate carbons. Although activation of polyacenaphthylene carbon involves surface attack only, comparison of the optical micrographs for an unactivated and an activated sample of the carbon (Figs.2.9. and 5.3.) however shows that the nature of the external surface of the carbon does not change significantly on activation.

It is interesting to note that for cellulose triacetate carbons, the ratio of internal to external burn-out (Fig.4.16)and the rate of activation (Fig.3.5.) are both linear functions of degree of burn-out. For cellulose carbons, however, although the rates of activation remain linear to a burn-out of over 60% (Fig.3.4.), the ratio of

internal to external burn-out (Fig. 4.16.) decreases as activation proceeds.

.In the initial stages of activation, weight loss from the internal surface of cellulose carbons exceeds that from cellulose triacetate carbons (Fig.4.16.). The development of micro-pore volume, expressed in $cm^3g.^{-1}$ of unactivated carbon, (Figs.4.19 and 4.20.) for both carbons is similar, particularly in the initial stages of activation, hence the large internal burn-out from cellulose carbons in the initial stages of activation can be attributed to a development of macro-pore volume as well as micro-pore volume. This conclusion is consistent with the results shown in Fig.4.19. which show that both micro-pore volume and macro-pore volume increase in the initial stages of activation. Further, in the later stages of activation Fig.4.19. shows that the macro-pore volume of cellulose carbons decreases more rapidly than the micro-pore volume, which is consistent with an increase in the amount of external weight loss as activation proceeds.

For cellulose triacetate carbons Fig.4.20. shows that in the initial stages of activation the macro-pore volume decreases, hence the internal burn-out from cellulose triacetate carbons in the initial stages of activation is apparently exclusively concerned with the development of micro-pore volume. Comparison of the optical micrographs of unactivated cellulose and cellulose triacetate carbons (Figs.2.7. and 2.8.) suggests a possible explanation for the initial

macro-pore development of cellulose carbons on activation, and the lack of such development of cellulose triacetate carbons.

The surface of unactivated cellulose carbon is covered with small pits, which presumably are large macro-pores; in contrast the surface of unactivated cellulose triacetate carbon is devoid of such pits. Hence it may be that the presence of existing large macro-pores in unactivated cellulose carbon favours the development of macro-pore volume during the initial stages of activation, whilst the absence of such pores in cellulose triacetate carbon inhibits a similar development. If this explanation is correct, then it might be expected that the large macro-pores of unactivated cellulose carbon would increase in size during activation. However, the optical micrographs of activated samples of both cellulose and cellulose triacetate carbons (Figs.5.1. and 5.2.) closely resemble those obtained for the unactivated samples of both carbons. Therefore, the large macro-pores present in unactivated cellulose carbon do not appear to change in size during activation, and the evidence for the explanation remains inconclusive.

5.6. <u>The Influence of temperature of Activation on the Rates of Activation and the Development of Pore Volume of the Carbons</u>

Cellulose carbons react more slowly with carbon dioxide than cellulose triacetate carbons at the same temperature. However, the former develop a greater micro-pore volume than the latter in the course of activation. For example Table 5.3. shows the corresponding

rates of activation at 935°C (using 0.5g. samples of carbon) and micro-pore volumes of the carbons at a burn-out of 50%.

Since the activation energies for these carbons in this region (Table 3.5.) are almost the same, the difference of a factor of two in the rates of activation must reflect differences in the nature of the carbons. Thus both the rate of activation at a given temperature and the development of micro-pore volume depend on the nature of the carbon. It is tempting to relate the lower rate of activation of cellulose carbon to the greater pore volume developed compared with cellulose triacetate carbon, since it might be expected that a lower rate of activation would produce a greater degree of internal burn-out. This is corroborated by the analysis of mercury densities (Fig.4.16.) since these show that the amount of internal burn-out of cellulose carbons is more than that of cellulose triacetate carbons below 75% burn-out.

Thus it appears that there is some correlation between the rate of activation at a given temperature and development of pore structure of a carbon, when two different carbons are compared, and a slower rate of activation favours the development of pore structure.

Variation of the temperature of activation over the range studied, although markedly affecting the rates of activation, does not appear to influence significantly the development of micro-pore structure of cellulose and cellulose triacetate carbons (Chapter 4. Section 4.3.2.).

It thus appears that the principal factor that determines both the rate of activation at a given temperature and the development of pore structure, is the nature of the carbon. These conclusions will be considered further in Chapter 6 and proposals for further work to test and elaborate them will be outlined.
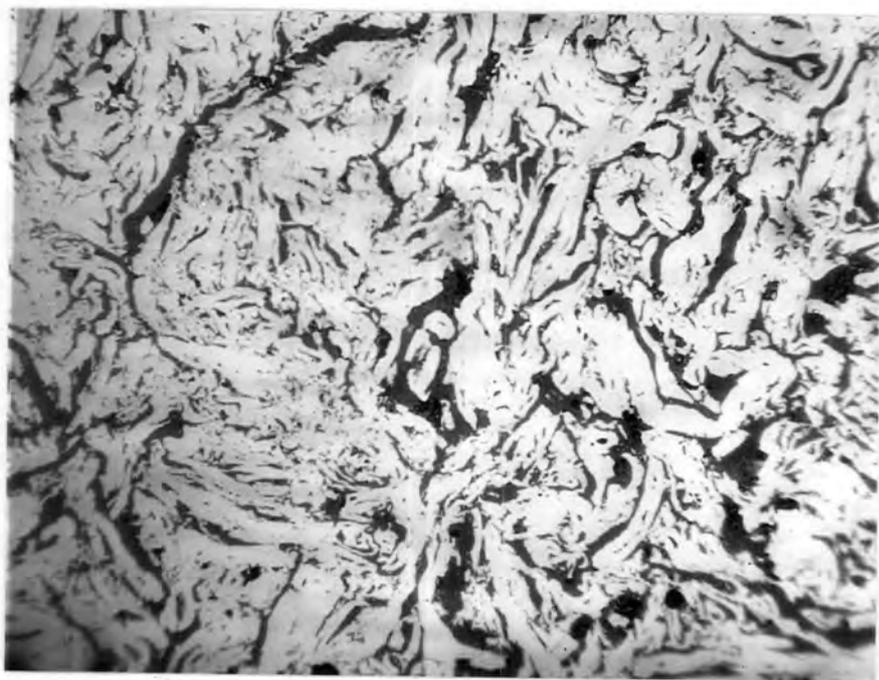
FIG. 5.1.   ACTIVATED   CELLULOSE   CARBON.
(X300)

FIG. 5.2. ACTIVATED   CELLULOSE   TRIACETATE
CARBON. (x100)
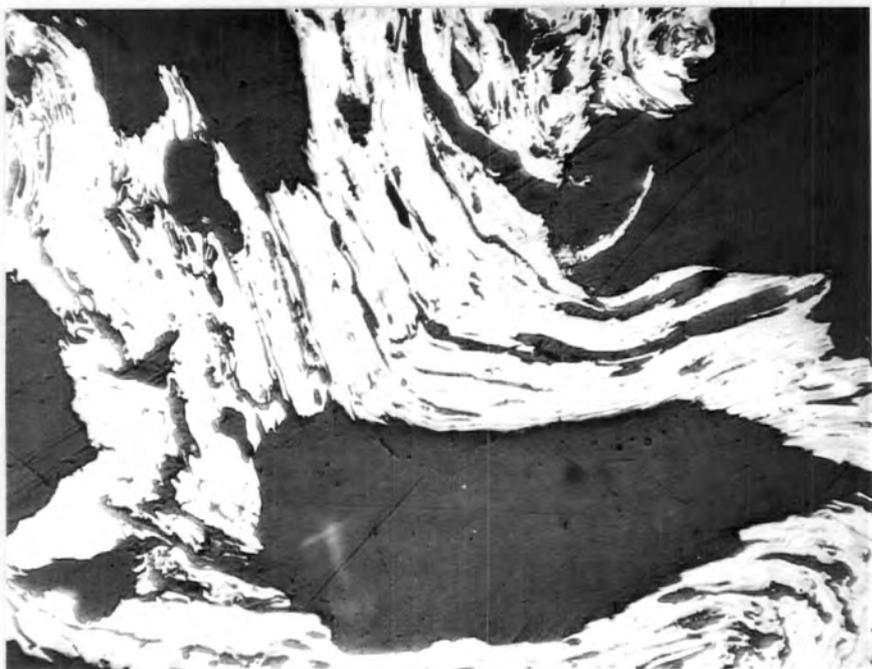
FIG. 5.3. ACTIVATED POLYACENAPHTHALENE CARBON. (X150)

Table 5.1.

The Times taken to reach a Burn-out of 50% for small starting Weights

of Carbon activated at 935°C

Polymer Carbon	Starting Weight (g.)	Time to reach 50% Burn-out (min.)
Cellulose	0.02	31
Cellulose triacetate	0.01	33
Polyacenaphthylene	0.01	300 - 600

Table 5.2.

The Increases in Micro-Pore Volumes of the three Carbons on activation

at 935°C to a burn-out of 50%

(Volumes in $cm.^3 g.^{-1}$)

Polymer Carbon	graphitic character	micro-pore volume of unactivated carbon	Micro-pore volume at 50% Burn-out	increase in micro-pore volume
Cellulose	non-graphitic	0.18	0.66	0.48
Cellulose triacetate	non-graphitic	0.21	0.55	0.34
Polyacenaph-thylene	graphitic	less than 10^{-3} $cm.^3 g.^{-1}$	less than 10^{-3} $cm.^3 g.^{-1}$	-

Table   5.3.

A comparison of the Rates of Activation at 935°C and Development of
Micro-Pore Volume of Cellulose and Cellulose Triacetate Carbons

Polymer Carbon	Rate of Activation $(g.sec.^{-1}g.^{-1})$	Increase in Micro-Pore Volume at 50% Burn-out. $(cm.^3g.^{-1})$
Cellulose	2.08×10^{-5}	0.48
Cellulose Triacetate	4.08×10^{-5}	0.34

Chapter 6.

Summary and Conclusions

6.1. Introduction

In this Chapter the findings of the present work, and conclusions drawn from these findings are presented and linked with the aims of the thesis set out in Chapter 1. (Section 1.4.) The Chapter is concluded with proposals for further development of the work.

6.2. Summary of Findings

6.2.1. Summary of Findings in Chapter 2

Measurements of carbon yields and electron spin resonance both indicate that the procedure adopted for the carbonisation of the polymers is suitable for obtaining reproducible carbons. An increase in the starting weight of polymer produces an increase in the carbon yield; this is presumably due to the trapping of volatiles which then undergo secondary carbonisation in the increased bulk of the decomposing polymer. This effect is, therefore, the reverse of that observed when carbonisation is carried out in a vacuum.

Quantitative information including activation energies which characterise the carbonisation of the polymers may be obtained by application of non-isothermal kinetic analysis to the carbonisation

thermograms. For cellulose and cellulose triacetate polymers the values of the activation energies obtained are less than 60 k.cal. mole.$^{-1}$ and compare favourably with values obtained by other workers using conventional isothermal methods. In contrast the value of 225 k.cal.mole.$^{-1}$ obtained for the carbonisation of polyacenaphthylene is unrealistically high. An unrealistically high value for the activation energy of the pyrolysis of a polymer can be obtained if the pyrolysis is influenced by mass transport of reaction products. If this is the case then it is probable that a slower rate of heating of the polymer would minimise this influence and hence a more realistic value for the activation energy of the pyrolysis of polyacenaphthylene might be obtained.

The three polymer carbons are characteristically different and these differences are clearly emphasised by the optical micrographs. Cellulose carbon is a non-graphitic char, and its external surface largely consists of small pits; cellulose triacetate carbon is also non-graphitic but is a coke, and its external surface is almost featureless. Polyacenaphthylene carbon is graphitic and therefore a coke, its surface is characterised by flow patterns and striations typical of an optically anisotropic material.

6.2.2. Summary of Findings in Chapter 3

In general the rates of activation of the three polymer carbons by reaction with carbon dioxide are linear at a given temperature. Hence it would appear that in the flow-system used in

the present work there is no build up in concentration of carbon monoxide which could retard the reaction. The rate of activation can be expressed therefore by a form of Equation 3.1. in which the rate is constant and hence $k_3 P_{CO_2}$ is very much greater than $k_2 P_{CO}$ and unity, i.e. rate = k_1/k_3.

The rate of activation of a polymer carbon can vary with the starting weight of carbon. For cellulose and cellulose triacetate carbons, the rates, expressed in units of grams of carbon lost per second, per gram of starting weight of carbon, decrease with increasing starting weight of carbon until they become independent of the starting weight when the starting weight exceeds a value of ca. 0.3g. This value is probably a function of the geometry of the furnace and crucible.

The linear rates of activation of the carbons at different temperatures can be plotted according to the Arrhenius Equation, and activation energies can be obtained in order to identify the reaction according to Wicke's classification. For small starting weights of cellulose and cellulose triacetate carbons and for large starting weights of polyacenaphthylene carbon log k is a linear function of $(T^o K)^{-1}$ throughout the temperature range investigated. The activation energies and pre-exponential factors in these cases are high indicating the reactions to be in Zone I of the Wicke Classification. For large starting weights of cellulose and cellulose triacetate carbons log k varies with $(T^o K)^{-1}$ in the form

of a smooth curve over the temperature range investigated. . At lower temperatures in this range the activation energies correspond to Zone I, and at higher temperatures they correspond to Zone II of the Wicke Classification. This indicates that diffusion becomes the rate determining step at higher temperatures in the range.

The activation energies found for the gasification of the three carbons in Zone I are different; and ranged from 50 to 70 k. cal. mole.$^{-1}$. The value of the activation energy obtained for the gasification of cellulose carbon in Zone I closely corresponds to the value reported by Greenhalgh and co-workers (48) for poorly outgassed samples of polyvinyl chloride and polyvinylidene chloride carbons. Gregg and Tyson (61) have also found that the activation energy for the gasification of carbons with oxygen varies with heat treatment temperature of the carbons. Thus in addition to the starting weight of carbon, other factors which influence the. activation energy, include the nature, the amount of outgassing, and the heat treatment temperature of the carbon.

For a number of reasons it appears that the concept proposed by Rossberg (62) of a 'Universal Activation Energy' applying to all carbons undergoing gasification in Zone I of the Wicke Classification is of doubtful significance. Firstly 'Universal' values reported by Wicke (49) and Ergun (43) are not in agreement; secondly Walker (39) has argued that the rate determining step operating in Zone I, and hence the activation energy, may vary, depending on the

reaction conditions.   Finally the present results indicate that
the activation energy in Zone I also depends upon the nature of the
carbon.

6.2.3. Summary of Findings in Chapter 4

The adsorption isotherms, obtained for the activated series
of cellulose and cellulose triacetate carbons, using carbon dioxide
at $195^{\circ}K$ as the adsorbate, show that the bulk of adsorption occurs
at relative pressures of less than 0.05, and therefore takes place
principally in micro-pores.   The adsorption isotherms indicate
that the micro-pore size increases with increasing activation.

The adsorption isotherms for cellulose and cellulose triacetate
plotted according to the Dubinin Equation (Equation 4.17.) vary
from being linear for the unactivated carbons, to shallow curves
for slightly activated carbons, and to pronounced curves for highly
activated carbons.   Extrapolation of the Dubinin plots at high
relative pressures yields reasonable values for the micro-pore
volumes of cellulose and cellulose triacetate carbons.   These
values increase with increasing activation as do the values of Du,
the slope of a Dubinin plot at higher relative pressures;   this is
further evidence that the micro-pore size increases on activation.
Extrapolation of the Dubinin plot from lower relative pressures can
be used to calculate the surface areas of the carbons, as previously
described by Marsh and Lamond (92).   The values of surface area
so obtained remain almost constant throughout activated series of
both cellulose and cellulose triacetate carbons.   This is in

contrast to many other workers' findings, who find that the surface areas of carbons increase on activation. A more likely explanation suggested by Dubinin (85) is that the adsorption at low relative pressures, represents the filling of a smaller type of micro-pore. It is not unexpected, therefore, that mean micro-pore radii calculated from the volume to surface area ratios appear to be rather high. However, they too show qualitatively that the micro-pore size increases on activation.

Variations in the starting weight of carbon over the range 0.4g. to 1g., and variations in temperature of activation over the range 890° to $960^{\circ}C$ appear to have little or no effect on the development of micro-pore volume of cellulose and cellulose triacetate carbons.

Analyses of the mercury densities for activated series of cellulose and cellulose triacetate carbons indicate that extensive internal burn-out occurs during the process of activation of these carbons. Hence these analyses confirm the conclusions drawn from the adsorption results.

Total pore volumes of cellulose and cellulose triacetate carbons can be calculated from mercury densities and assumed 'true' densities of the carbons. These results are thus semi-quantitative but show that the total pore volumes of both cellulose and cellulose triacetate carbons increase on activation. There is evidence from the optical micrographs, mercury density analyses and the total and micro-pore volumes to show that macro-pore development also occurs

in addition to micro-pore development in the initial stages of
activation of cellulose carbons, but not for cellulose triacetate
carbons.

Results obtained from measurements of adsorption of carbon
dioxide on polyacenaphthylene carbons show that unactivated
polyacenaphthylene carbon has an undetectable micro-pore structure
and that no development of this structure occurs on activation.
Measurements of mercury density indicate that little or no internal
burn-out occurs on activation; this confirms the conclusions
drawn from adsorption results and also suggests that there is no
macro-pore development on activation of polyacenaphthylene carbon.

6.3. Ceneral Conclusions

The main aim of the work reported in this thesis has been to
investigate the influence of reactivity to an activating gas on the
development of porosity of some polymer carbons. The detailed
aims of the thesis have been outlined in Chapter 1. (Section 1.4.)
and the results obtained in this work have been discussed in detail
in the light of these aims in Chapter 5. In this section the
conclusions drawn from these results are summarised.

It is possible to prepare reproducibly activated series of
polymer carbons using the standardised procedure adopted for
carbonisation and activation. Activation of polymer carbons may
or may not develop the pore structure depending on the nature of
the carbon. The non-graphitic carbons, cellulose and cellulose

triacetate are more reactive to carbon dioxide than graphitic polyacenaphthylene carbon. The difference between the carbonisation processes of cellulose and cellulose triacetate has little effect on the reactivity and development of porosity of the carbons produced. Cellulose carbon has a bigger internal burn-out on activation than cellulose triacetate carbon and develops as a result a larger pore structure. Polyacenaphthylene carbon does not develop a pore structure on activation, since there is no internal burn-out.

In general, therefore, a non-graphitic carbon reacts faster, and develops a larger pore structure than a graphitic carbon. Hence graphitic character influences both reactivity and development of pore structure of polymer carbons. The nature of the carbonisation process of a polymer would appear to influence the reactivity and development of porosity only in so far as it influences the degree of graphitic character of the resultant carbon.

The Wicke Classification of reaction Zones provides a suitable means of characterising the general mechanism of activation of a carbon. Variations in the temperature of activation of polymer carbons within Zone II, and on the border line of Zones I and II of the Wicke Classification although influencing the rate of activation of carbons, appear to have little effect on the development of pore volume of carbons. The positions of the Zones

of the Classification vary not only with temperature of activation,
but also with the starting weight of carbon.   There is also some
evidence to suggest that they may also vary depending on the
nature of the carbon.

The rate of activation of a carbon varies in certain cases
with the starting weight of carbon.   This is because the starting
weight of carbon influences the extent of diffusion of the
activating gas through the mass of carbon.   If the starting weight
is small, the influence of diffusion is small;   in contrast for
large starting weights of carbon,   diffusion of the activating gas
becomes an important factor in the rate of activation.

A comparison of the rates of activation at the same temperature
of two different non-graphitic carbons suggests that a slower rate
of activation favours the development of pore structure of a carbon.
Thus it appears that the principal factor which determines both the
rate of activation and the development of pore structure of a
carbon is the nature of the carbon.

6.4.   Proposals for further Development of the Work

Evidence has been produced in this thesis which shows that the
development of porosity of polymer carbons is closely related to
their nature and reactivity.   In order to test and extend some of
the conclusions made from these findings and so develop the present
work, the following programme is suggested:

(i) An investigation of the kinetics of activation of the polymer

carbons over a wider temperature range to compare the influence
of reactivity on porosity development in Zone III with that of
Zone II of the Wicke Classification.   It might be expected that
carbons activated in Zone III would develop a much smaller pore
structure than if they were activated in Zone II.   This is because
penetration of the activating gas into the carbon is less
important when a carbon is activated in Zone III.

(ii) An investigation of other carbonising polymers using the
present practical programme in order to further test the influence
of the nature of a carbon on reactivity and development of porosity.
For example it is known (14) that the carbon produced from the
highly cross-linked polymer phenol-formaldehyde is non-graphitic
and yet in contrast to the carbons produced from cellulose and
cellulose triacetate does not develop a large pore structure on
activation; however little is known about its reactivity.

(iii) An investigation of other activating gases and their influence
on reactivity and development of pore structure of polymer carbons.
Activating gases that could be used include nitrous oxide, nitric
oxide, and hydrogen.   It is known (39) that hydrogen reacts more
slowly with a given carbon at the same temperature than carbon
dioxide, but little is known about the development of porosity
of carbons using hydrogen as the activating gas.

    In final summary, this work has been an initial assessment
of the relation between the rate of activation and development of

porosity in polymer carbons. A number of conclusions have been drawn from this work and the need for further work both to support and elaborate these conclusions, and to extend this type of study to other systems has been clearly demonstrated.

Appendix

Introduction

The first three sections of the Appendix contain details of apparatus and experimental procedure for the preparation of the polymers, carbonisation and activation studies, determination of adsorption isotherms and mercury densities. The Appendix is concluded with tables of primary data and the list of References from the text.

Appendix (I)

Preparation of Cellulose Pellets

Whatman's chromatographic grade cellulose powder was moistened with distilled water, sieved to pass 22 B.S.S. mesh and was then pelleted in a pharmaceutical press to produce samples of approximately 100 mg.

Preparation of Polyacenaphthylene

The method used is described by Brazier (24). Acenaphthylene, supplied by B.D.H., was not improved by further recrystallisation (observed m.p. 91°C, lit.m.p.92°C), and was used without further purification. 50g. of acenaphthylene were sealed into a heavy bore pyrex tube in an atmosphere of nitrogen. The tube was heated in an oven at 130°C for ten days, this resulted in the formation of a clear, brown solid. The solid was ground to a powder and the polyacenaphthylene extracted from it by refluxing with benzene in a Soxhlet apparatus for two days. Pale Yellow crystals of polyacenaphthylene were precipitated from the benzene extract on addition of ethyl alcohol at -20°C. Polyacenaphthylene was characterised from the infra-red spectral data quoted by Brazier (24). The infra-red spectrum was obtained from a sample of the polymer dispersed in a KBr disc, using a Unicam SP 100 infra-red spectrophotometer. The characteristic frequencies of absorption for polyacenaphthylene are listed in Table A2 in Appendix (V). The

absence of a strong band at 730 cm.$^{-1}$, indicates that the double bond

present in acenaphthylene, has been eliminated by polymerisation.

Preparation of Cellulose Triacetate (98)

50g. of Whatman's chromatographic grade Cellulose powder was

placed in a beaker and 225g. of glacial acetic acid added.   The beaker

was covered with a clock glass and immersed in a water-bath at 55 - 60°C

for thirty minutes;   the contents of the beaker were stirred frequently

during this time.   The beaker was removed from the bath and allowed to

cool to 30 - 35°C, before an acetylating mixture of 150 cc. of acetic

anhydride and 3 cc. of concentrated sulphuric acid was added.   In order

to minimise the degradation of the cellulose, the temperature of the

reaction mixture was prevented from rising above 60°C by surrounding the

beaker with an ice-bath.   After a few minutes when the initial reaction

had subsided, the beaker was removed from the ice-bath and immersed in

a water-bath at 55°C for ninety minutes, the contents of the beaker

being frequently stirred.   Cellulose triacetate was precipitated from

the resulting solution by careful addition of water, with stirring, to

the point of precipitation, followed by rapid addition of a large volume

of water.   The product was filtered, washed for several hours with

distilled water to remove acetic acid and dried.   It was soluble in

chlorinated solvents, and insoluble in acetone.   The yield was 90% of

the theoretical amount.   The cellulose triacetate was characterised by

determination of acetyl content (99).   Two samples of cellulose

triacetate were heated overnight at 65°C to drive off moisture and any

free acetic acid remaining from the preparation. The samples were hydrolysed by addition of excess socium hydroxide solution. The excess alkali was determined by back-titration with standardised hydrochloric acid solution. The acetyl determination of the two samples indicated triacetylation.

Polyacenaphthylene and cellulose triacetate samples were pelleted in the same manner as cellulose.

Appendix (II)

Apparatus for Carbonisation and Activation Studies. Basic Requirements

Since the properties of carbons depend sensitively on the conditions during carbonisation, (Chapter 2. Section 2.1.1.), it is essential that these conditions be as carefully controlled and as reproducible as possible. In particular it is necessary for the polymer to be in a compact, reproducible form to facilitate the formation of a coherent carbon. Carbonisation should be carried out using a linear rate of heating and in an inert atmosphere with provision for the removal of volatile reaction products; an accurate measure of the temperature of the sample is also required. Since activation is to be carried out immediately after carbonisation is is necessary to have a method of changing from the inert gas to the activating gas with the minimum delay between the change-over and the onset of reaction. An apparatus incorporating a Stanton Thermobalance, Model TR-01 (sensitivity 10^{-4} g.) was developed to provide these conditions.

The Stanton Thermobalance consists of an analytical balance and an electric furnace (maximum temperature $1000^{o}C$). The sample is placed on a platform on top of a silica support rod which is connected to the rear pan of the balance. The furnace is mounted above the balance and can be moved into position to enclose the sample. Changes in the weight of the sample are followed continously by means of the capacitance of an air

gap between a fixed plate and a plate mounted on the beam of the balance. A Pt/Pt, 13% Rh thermocouple on the inside wall of the furnace is used to measure temperature and, in conjunction with a cam driven by an electric motor, also controls the linear rate of heating of the furnace. Weight and temperature changes are transmitted electronically to a twin-pen recorder. The balance can measure weight changes of up to 100 mg. automatically; this range can be extended by manual counterpoising.

Modification of the Balance. (100)

In the unmodified balance the sample is exposed to the atmosphere. Modifications for work in controlled atmospheres must effectively exclude air from the sample but must not impede the movement of the silica support rod. A number of modifications have been described (101,102,103) for the Stanton Thermobalance TR-1 (sensitivity 10^{-3}g.) but none of these was found suitable for the more sensitive balance used in the present work. Either air was not completely excluded from the sample or there was appreciable "noise" on the weight change record due to buoyancy effects associated with gas flow. The modified apparatus shown in Fig A1. was used. The silica sheath which encloses the sample fits inside the collar of the gland as tightly as expansion allowance permits. Gas is admitted to the furnace through a cylindrical jacket which surrounds the central tube of the gland. Small holes are distributed about the internal circumference of the jacket to permit even diffusion of gas into the furnace. Gas is drawn over the sample by extraction from the top of the sheath. The rate of extraction is less than the rate of input of

gas, the purpose of the excess gas being to prevent the diffusion of
air into the furnace from the balance chamber. The excess gas itself
is prevented from diffusing into the balance chamber by extraction
through another cylindrical jacket situated beneath the inlet jacket on
the central tube of the gland. This is necessary since diffusion of
carbon dioxide into the balance chamber has undesirable effects. With
this design of gland there are no difficulties in positioning the silica
support rod. In some earlier designs the rod passes through a small
hole so that it needs to be accurately positioned. Also "Noise" on the
weight change record is less than 10^{-4}g., which is superior to the
unmodified balance.

Control and Calibration of Gas Flow

The general arrangement for the control and clibration of gas flow
is shown schematically in Fig. A2. Nitrogen or carbon dioxide is fed from
cylinders through a two-stage reducing valve and through a diaphragm valve
(made by Scientific Instruments and Model Co.). The gas is passed
through a drying tower containing silica gel and through a flowmeter
before entering the furnace. Two-way taps are used to isolate either gas
supply from the furnace. Gas extracted from the gland is drawn through
a flowmeter by means of a rotary oil pump, the rate of flow of gas being
controlled by a bleed valve in conjunction with a diaphragm valve of the
type mentioned above. Gas is extracted from the top of the furnace in a
similar way except that a cotton wool trap is included to remove tars
formed during the carbonisation stage. The flowmeters are of the

capillary type with dibutyl phthalate as the indicating fluid; they were calibrated using a soap-bubble flowmeter. Flow-rates ranged from 1000 to 200 ml.min.$^{-1}$ they were measured to an accuracy of $\pm$ 6 ml.min.$^{-1}$ at the fastest rates and $\pm$ 1 ml.min.$^{-1}$ at the slowest. The variation of flow-rates over a complete run was less than $\pm$ 12 ml.min.$^{-1}$ at the fastest rates used and $\pm$ 5 ml.min.$^{-1}$ at the slowest. These variations have no effect on the buoyancy of the sample.

Temperature Measurement

The Thermocouple supplied with the balance is mounted on the furnace wall and is outside the sheath in the modified apparatus. This thermocouple registers a higher temperature than that of the sample due principally to the cooling effect of gas flow inside the sheath. Another Pt/Pt, 13% Rh thermocouple was therefore used to measure the temperature of the sample directly (see Fig. A1.). The tip of the thermocouple fits into the recessed base of the platinum crucible containing the sample; the leads pass through twin-bore tubes inside the silica support rod to terminals on the balance pan. The connection between these terminals and the compensated leads at the back of the balance chamber is by two 0.001" diameter wires; these fine wires do not interfere with the movement and sensitivity of the balance. The cold junction is maintained at 0°C and the e.m.f. indicated on a recording millivoltmeter. With this arrangement the temperature of the sample is measured to $\pm$ 2 deg. in the 900°C region; the variation in temperature as the sample moves in the furnace is $\pm$ 4 deg. in the 900°C region.

Inertness of the Furnace Atmosphere

The oxidation of a sample of graphitised carbon black (Spheron 6, 2,700°C) was used as a test for the inertness of the furnace atmosphere. Weight loss due to oxidation of the carbon black was immediately observed above 600°C if air was present. A slight amount of oxidation (ca. 2×10^{-6} g.sec.$^{-1}$g.$^{-1}$) was observed in the present apparatus for a 1500 dmg. sample of the carbon black heated to 935°C, in an atmosphere of nitrogen. The flow-rates were those adopted as standard for carbonisation and activation: input 1000 ml.min.$^{-1}$, furnace extract 250 ml.min.$^{-1}$, gland extract 650 ml.min.$^{-1}$. It was found that this small amount of oxidation could be eliminated by shutting off the furnace extract when the temperature reached 800°C.

Buoyancy Corrections

The use of a sensitive analytical balance in conjunction with a flow system requires that particular care be taken in making buoyancy corrections. A particular advantage of the present design of gland is that these corrections are minimal. Fig. A3. shows the influence of rising temperature on the weight of a sample of carbon black in nitrogen; this curve is typical. (101) The apparent increase in weight is known to be the result of the interplay of several factors, the most predominant being the decreasing density of the gas with increasing temperature. Variation of the weight of the sample over the range used in the present work (1g. to zero) has negligible effect on buoyancy; this is as expected since the weight of the sample is a small fraction of the

combined weight of the crucible, platform and support rod.

Fig.A4a. shows the effect of the variation of the rate of input of nitrogen on buoyancy at room temperature both with and without extraction of gas from the gland;   Fig.A4b, contains the same results for carbon dioxide.   The increase in buoyancy with increasing flow-rate in both cases is due to the down-thrust of the gas on the rear pan of the balance.   This effect for nitrogen is almost reduced to zero at the standard flow-rate of 1000 ml.min.$^{-1}$.   The very large buoyancy effect obtained with carbon dioxide is due to its greater density compared with air.   Diffusion of carbon dioxide into the balance chamber also produces a random drift in the weight change record presumably due to buoyancy effects on the balance itself.   With extraction from the gland this effect is removed.   The small negative buoyancy effect at low flow rates of carbon dioxide is presumably due to its greater density compared with air.

Experimental Procedure for Carbonisation and Activation

The experimental procedure for a complete run on the small scale is illustrated in Fig. A5, which shows the carbonisation in nitrogen of a cellulose pellet to 950°C and the subsequent activation at 905°C of the carbon product.   Thermal decomposition of the polymer (AB) occurs under a linear rate of heating of 3.85 deg.min.$^{-1}$ (HI) to yield a carbon residue. The carbon is maintained at 950°C for approximately thirty minutes and then the temperature is then lowered to that required for activation (KL). Nitrogen is then replaced by carbon dioxide, which produces a small apparent weight loss (CD) due to the greater density of carbon dioxide,

·this is followed by reaction (DE). When reaction is complete (EF) carbon dioxide is replaced by nitrogen (FG) as a check on the buoyancy effect due to exchange of gases. Finally a mass balance calculation is performed, i.e. the total weight loss recorded by the thermobalance after applying corrections for buoyancy, is compared with the difference between the initial and final weights of the crucible and its contents. The weight losses calculated by the two methods agree to $\pm$ 2 x 10^{-4} g. (0.2%).

For carbonisation and activation of large samples ($>$ 0.1g.) the procedure had to be modified slightly due to limitations imposed by the capacity of the balance. Samples of polymer (ca.5g.) were carbonised in bulk exactly as described, and were then cooled in nitrogen to room temperature. Due to the bulk of the sample no record of weight loss during carbonisation was obtained. In the activation experiments the appropriate amount of carbon was then reheated in exactly the same manner as in the carbonisation, and activated at the required temperature.
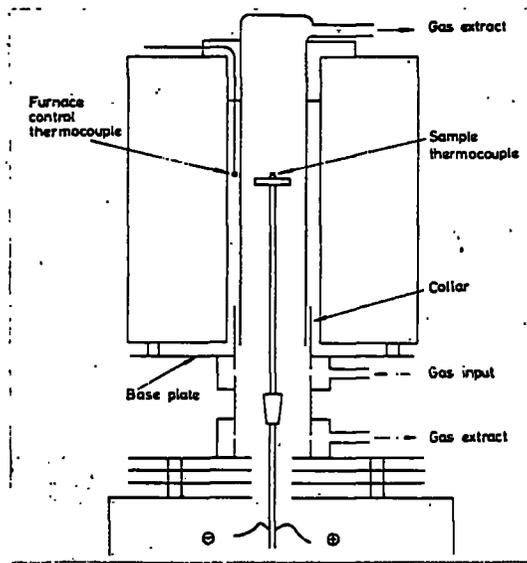
FIG. A.1. MODIFIED THERMOBALANCE.
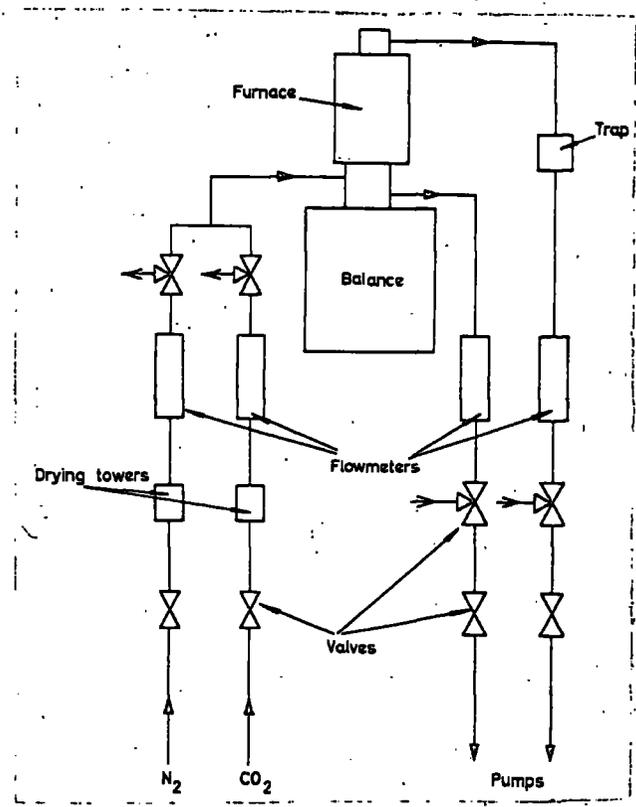
FIG. A.2. ARRANGEMENT FOR THE
CONTROL OF GAS FLOW.
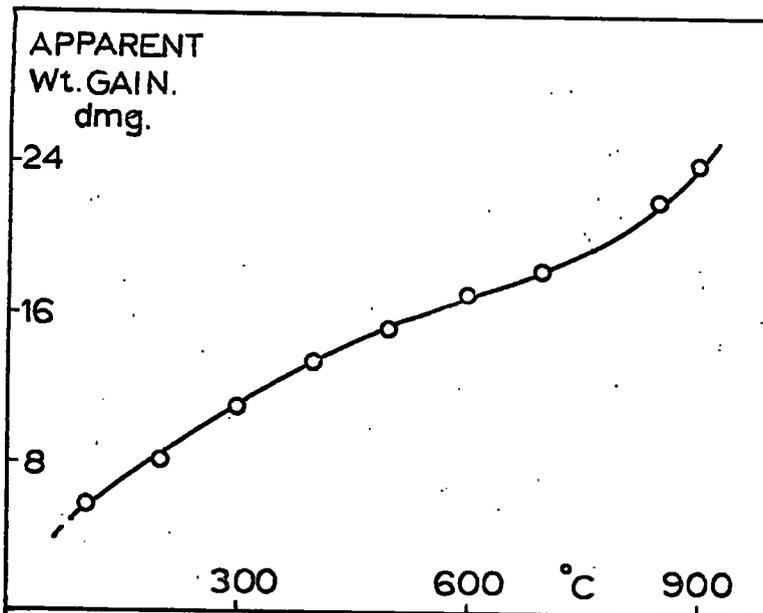
FIG. A.3.   BUOYANCY   Vs. TEMPERATURE
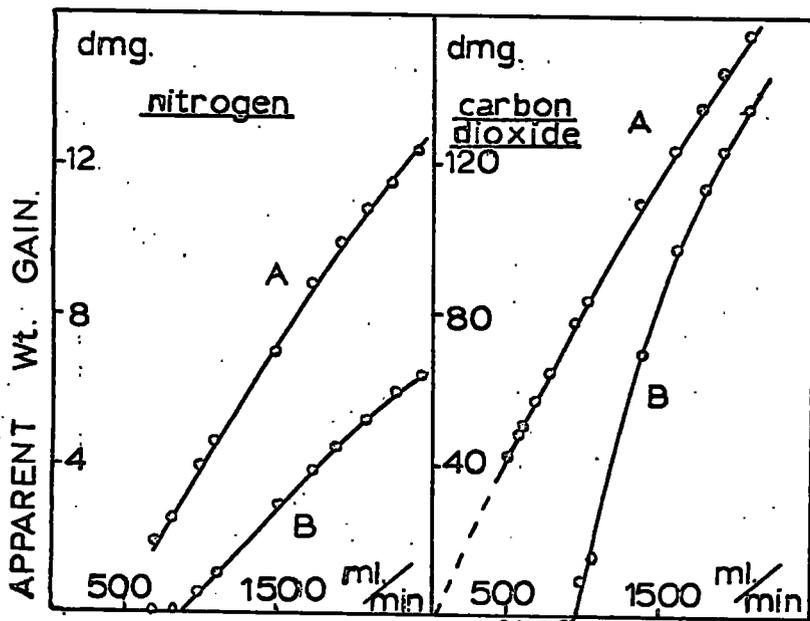
FIG. A.4a.   FIG. A.4b.

(A)   WITHOUT   GLAND   EXTRACT

(B)   WITH   GLAND   EXTRACT   650 ml.min.$^{-1}$
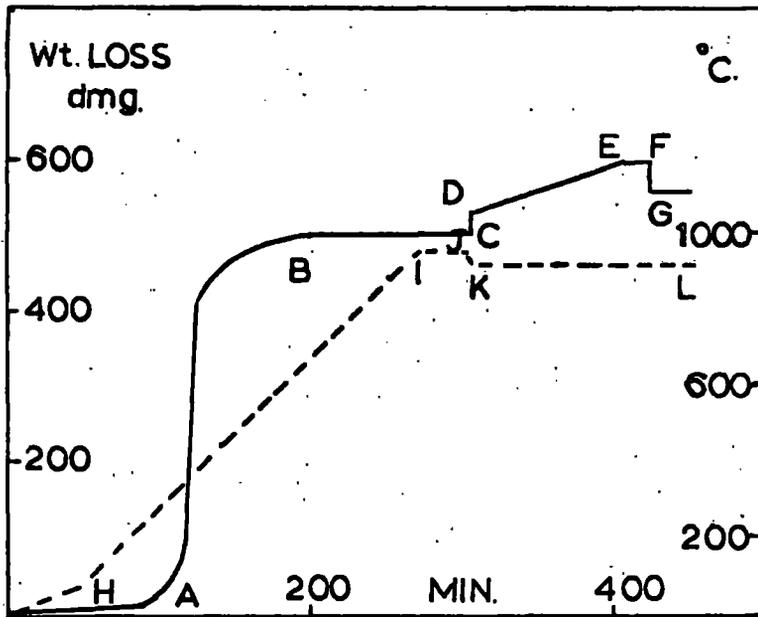
FIG. A.5. TYPICAL THERMOGRAM FOR
THE CONSECUTIVE CARBONISATION AND
ACTIVATION OF A PELLET OF CELLULOSE.

Appendix III

Apparatus for the Determination of the Carbon Dioxide Adsorption

Isotherms

The adsorption isotherms were obtained at 195°K using carbon

dioxide as the adsorbate. The apparatus is designed so that the

adsorption chambers can be evacuated and then supplied with carbon

dioxide at a measured pressure (Fig.A6.).

Adsorption is measured using the principle of the McBain-Bakr

Spring Balance (104). Two tubes A and B are the adsorption chambers

and are mounted vertically. The use of two adsorption tubes permits

two samples of carbon to be examined simultaneously. The tubes are

connected with cone and socket ground glass joints to the gas supply

line at C and D. The samples of carbon are placed in small glass

buckets E and F which are hung from slings attached to helical silica

springs G and H. The springs are suspended by glass hooks from

bridges I and J, situated across the neck of the cones C and D. Two-

way taps 1 and 2 isolate the adsorption tubes from each other and from

the gas supply line. The springs are calibrated by adding standard

weights to the buckets and measuring the extensions produced with a

cathetometer to $\pm$ 0.005 cm. Buoyancy corrections are less than

10^{-3} g. and can therefore be neglected.

The adsorption tubes and the gas supply line may be evacuated to 10^{-7} cm.Hg. by opening taps 1 to 9, to the main vacuum manifold K. The vacuum is obtained using an oil diffusion pump backed by a rotary oil pump. A liquid air trap freezes out volatiles from the gas stream pumped from the adsorption tubes. Solid carbon dioxide is placed in trap P and distilled under vacuum to Q. P is surrounded by a salt-ice bath to retain less volatile impurities. From Q the carbon dioxide is redistilled into the reservoir R.

Carbon dioxide is admitted to the adsorption tubes via the dosing system S, the dose being regulated by careful manipulation of taps 7 to 11 whilst noting the pressure in S by means of the manometer T.

Low pressures in the adsorption tubes are measured by McLeod Gauges U and V, which have ranges of 10^{-7} to 10^{-2} cm.Hg. and 10^{-2} to 1 cm.Hg. respectively; higher pressures are measured by the U-tube manometer W. The McLeod Gauge U is also used to measure the pressure in the main manifold K.

Weight and pressure measurements obtained at low pressures ($< 10^{-1}$ cm.Hg.) using this experimental arrangement, are subject to errors of thermal transpiration due to the temperature gradient in the adsorption tubes. However, the maximum error in weight due to this effect is of the order of micrograms (105) and can therefore be neglected in the present work since weights are only measured to $\pm 10^{-3}$ g.

Corrections to pressure readings due to the effect of thermal transpiration may be applied using Liang's empirical equation as described

by Bennett and Tompkins (106).   The errors in pressure readings at various pressures due to this effect are shown in Table A.1. for the present work.   It can be seen that the error is less than 1% above a pressure of 10^{-3}cm.Hg. and can therefore be neglected above this pressure.

Table   A.1.

Corrections to Pressure Readings due to Thermal Transpiration

Pressure Reading (cm.Hg.)	Error in Pressure Reading (%)
10^{-2}	0.1
10^{-3}	1
10^{-4}	13.6

Experimental Procedure for the Determination of Adsorption Isotherms

The samples of carbon (ca.0.15g.) are mounted in the apparatus as previously described.   Tubes A and B, and the gas supply line are evacuated to 10^{-7} cm.Hg.   Heating coils are placed round the adsorption tubes so that the samples of carbon are surrounded.   The current in the coils is adjusted by means of a rheostat so that the samples of carbon are heated under vacuum to a temperature of 250°C in order to remove adsorbed gases.   After several hours outgassing a pressure of 10^{-7} cm. Hg. is reached.   The adsorption system is isolated from the vacuum pumps and the heaters are replaced by baths of solid carbon dioxide (at 195°K). Carbon dioxide is then admitted to A and B at a pressure just below

10^{-3} cm.Hg., and the system allowed to equilibrate. When equilibrium is attained, the extensions of the springs and the pressure in A and B are measured and tabulated. This procedure is repeated at regular intervals of pressure, until the pressure in A and B is approximately 40 cms. of Hg.

Apparatus for the Determination of Mercury Densities

The apparatus is shown in Fig.A7. It consists of a burette, which can be attached to vacuum and pressure supply lines by a cone and socket joint K. A U-tube manometer adjacent to K is used to register pressure in the apparatus. The main body of the burette AB is made of 0.3 mm. bore, thick-walled capillary tubing, and the sample rests in the bottom of this limb, i.e. in CB. The side arm D is made from 0.1 mm. bore capillary tubing, and is joined to the tip of the burette T with a length of 0.05 mm. bore capillary tubing which has a mark M_1 etched on it. Another mark M_2 is situated just below A. The tip of the burette dips into a weighing bottle containing mercury which is isolated from the burette by a tap E.

Experimental Procedure for the Determination of Mercury Densities

The samples of carbon are gently broken into particles of ca.1mm. diameter on a filter paper.

A weighed amount of sample is then carefully poured from a filter paper into the socket of the burette and allowed to fall into the space between C and B. The burette is then attached to the vacuum line. The burette is evacuated to a pressure of ca.1 mm.Hg. with tap E closed.

E is opened and mercury from the bottle is allowed to rise until M_1 is reached. Tap E is closed and the bottle of mercury weighed. The bottle is replaced, E is reopened and mercury admitted to the burette until level M_2 is passed. The vacuum is then isolated and compressed air is admitted until the pressure is about 30 cm. above 1 atmosphere. The mercury is thus forced around the granules of carbon; the mercury level is then lowered to M_2 by opening E. E is closed and the bottle of mercury reweighed. The volume between M_1 and M_2, without any sample present, is obtained from previous blank experiments. A known weight of carbon displaced a known volume of mercury, and the density of the sample in mercury may be calculated.

Using this method, mercury densities of carbons may be calculated to within $\pm$ 2% for coarse grained samples of carbon. For fine grained samples of carbon, the mercury is not always able to penetrate the small spaces between the grains and error may be introduced, resulting in low densities. For polyacenaphthylene and cellulose triacetate carbons which had undergone fusion, the samples were coarse and presented no difficulty; for cellulose carbons, however, the particles tended to be fine and prone to powdering. Hence some unknown error may have been present in the determination of the mercury densities of cellulose carbons. The determinations of mercury density were in all cases reproducible within $\pm$ 0.02 g.cm.$^{-3}$.

FIG. A.6.   ADSORPTION APPARATUS
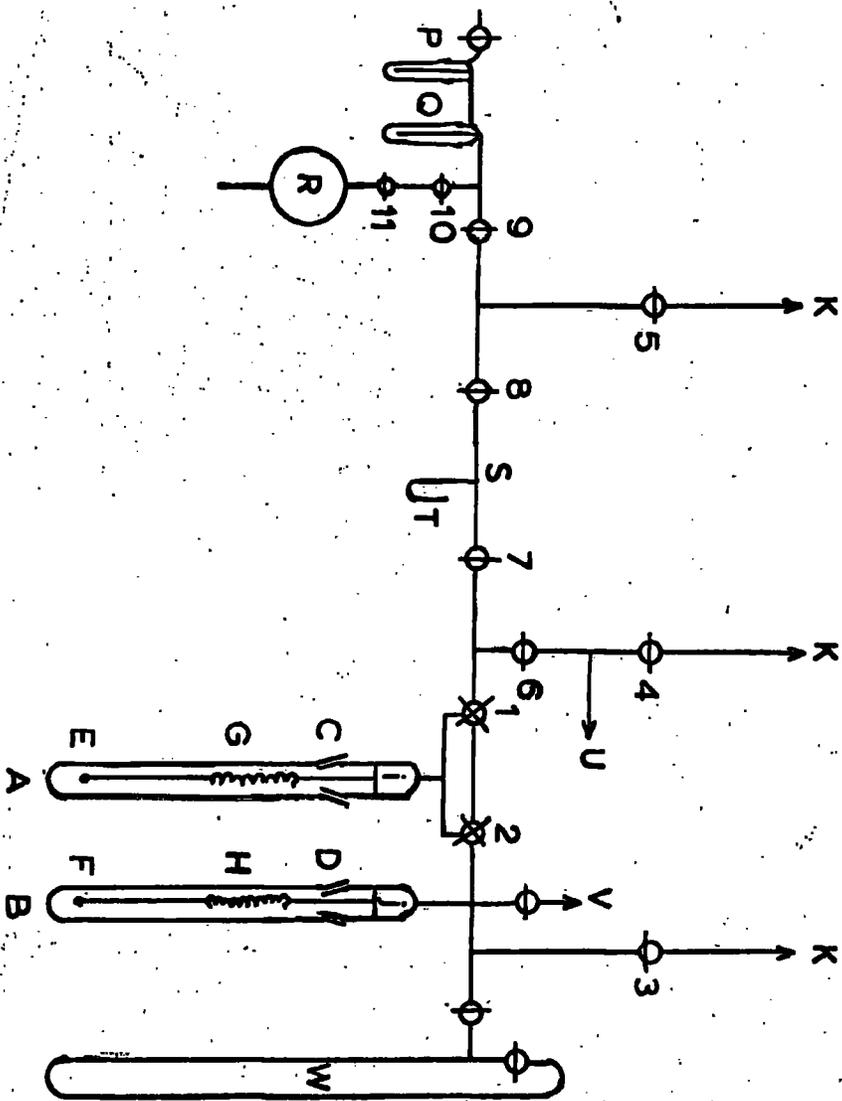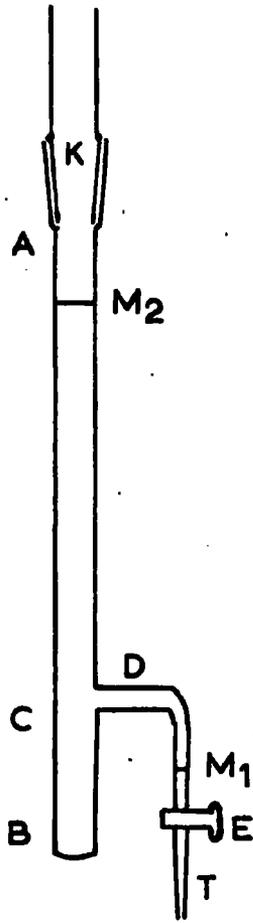
FIG. A.7. MERCURY DENSITY
APPARATUS.

Appendix IV

References

The abbreviations are those recommended by the Chemical Society.

(1) Trezbiatowski, Roczniki. Chem.1937, 17, 73.

(2) Franklin, Acta Cryst., 1951, 4, 253.

(3) Ubbelohde and Lewis, 'Graphite and its Crystal Compounds'.

(4) Dubinin, Quart.Rev., 1955, IX, No. 2.

(5) Juhola and Wiig, J.Amer.Chem.Soc., 1949, 71, 2078.

(6) Milner, Spivey and Cobb, J.Chem.Soc., 1943, 578.

(7) Blayden, Gas World, Coking Section, 1954, 140, 9.

(8) Ingram et Al Nature, 1954, 174, 797.

(9) Uebersfeld, Etienne and Combrisson, ibid., 1954, 174, 614.

(10) Pope and Gregg, Brit.J.Appl.Phys., 1959, 10, 507.

(11) Jackson and Wynne-Jones, Carbon, 1964, 2, No.3, 227.

(12) Uebersfeld and Erb, 'Proceedings of the Third Conference on
       Carbon', Pergamon Press, N.Y., 1959, p.103.

(13) Diamond and Hirsch, 'Industrial Carbon and Graphite' (First
       Conference) Society for Chemical Industry, London, 1958,p.197.

(14) McEnaney, Ph.D. Thesis, Hull University, 1961.

(15) Gilbert and Kipling, Fuel., 1962, 41, 249.

(16) Kipling and McEnaney, Fuel., 1964, 43, 367.

(17) Kipling et Al Carbon, 1964, 1,No.3, 315.

(18) Kipling and Shooter, 'Industrial Carbon and Graphite.', (Second Conference) Society for Chemical Industry, London, 1966.

(19) Blayden and Westcott, 'Proceedings of the Fifth Conference on Carbon'., Pergamon Press, London, 1963, VOL.2. p.97.

(20) Wilson, M.Sc.Thesis, Hull University, 1960.

(21) Urbanski et Al, Bul.Acad.Polon.Sci.,Ser.Sci.Chim.,Geol.,Geog., 1959, 7, 851.

(22) Tang and Bacon, Carbon, 1964, 2, No.3, 211.

(23) Cobb, Fuel in Science and Practice, 23, No. 5, 121.

(24) Brazier, M.Sc.Thesis, Hull University, 1964.

(25) Ingram et Al, Trans.Faraday Soc. 1958, 54, 400.

(26) Jackson, Ph.D.Thesis, Durham University, 1960.

(27) Jackson, Private Communication.

(28) Freeman and Carroll, J.Phys.Chem.,1958,62, 394.

(29) Doyle, J.Appl.Polymer Sci., 1961, 5, 285.

(30) Van Krevelen et Al, Fuel, 1951, 30, 253.

(31) Horowitz and Metzger, Analyt.Chem.,1963,35, 1464.

(32) Coats and Redfern, Analyst, 1963, 88, 906.

(33) Horowitz and Metzger, Fuel, 1963, 42, 418.

(34) Smith, Trans.Inst.Rubber Ind., 1963, 39, No.6, T275.

(35) Madorsky, J.Polymer Sci., 1952, 2, 133; 1953, 11, 491.

(36) Van Krevelen et Al, Fuel, 1956, 35, 462.

(37) Van Krevelen and Schuyer, 'Coal Science'., Elsevier Publishing Co. 1957. p.302.

(38) Brookes and Taylor, Carbon, 1965, 3, No.2, 185.

(39) Walker et Al, ''Advances in Catalysis'., XI, p.133, Academic
    Press, N.Y. and London, 1959.

(40) Langmuir, J.Amer.Chem.Soc., 1915, 37, 1139.

(41) Gadsby et Al, Proc.Roy.Soc., 1948, A.193,357.

(42) Reif,J.Phys.Chem.,1952, 56, 785.

(43) Ergun, J.Phys.Chem.,1956, 60, 480.

(44) Strickland Constable, J.Chim.Phys.,1950, 47, 356.

(45) idem, Proc.Roy.Soc., 1947, A189, 1.

(46) Bonner and Turkevich, J.Amer.Chem.Soc.,1951, 73, 561.

(47) Brown, Trans.Faraday Soc., 1952, 48, 1005.

(48) Greenhalgh et Al, Carbon, 1965, 3, No.1, 73.

(49) Wicke 'Fifth Symposium on Combustion'., Rheinhold, N.Y.,1955,p.245.

(50) Rossberg, and Wicke, Chem.-Ingr.-Tech.,1956, 28, 181.

(51) Hedden and Wicke, 'Proceedings of the Third Conference on Carbon'.,
    Pergamon Press, N.Y., 1959, 249.

(52) Weisz and Prater, 'Advances in Catalysis'., VI, p.143, Academic
    Press, N.Y. and London, 1954.

(53) Wheeler, ibid, III, p.249, 1951.

(54) Walker and Raats, J.Phys.Chem.,1956, 60, 364.

(55) Day, Ph.D.Thesis, Pennsylvania State University, 1949.

(56) Grisdale, J.Appl.Phys.,1953, 24, 1288.

(57) Smith and Polley, J.Phys.Chem.,1956,60, 689.

(58) Walker et Al, 'Proceedings of the Third Conference on Carbon'.,
    Pergamon Press, N.Y.,1959, p.643.

(59) Armington, Ph.D.Thesis, Pennsylvania State University, 1950.

(60) Walker and Nicols, 'Industrial Carbon and Graphite', (First
Conference). Society for Chemical Industry London, 1958.

(61) Gregg and Tyson, Carbon, 1965, 3, No.1, 39.

(62) Rossberg, Z.Elektrochem.,1956, 60, 952.

(63) Kipling and McEnaney, 'Industrial Carbon and Graphite'.,(Second
Conference), Society for Chemical Industry, London 1966.

(64) Brunauer et Al, J.Amer.Chem.Soc.,1940, 62, 1723.

(65) Maggs, Nature, 1960, 186, 956.

(66) Dubinin et Al, Carbon, 1964, 2, No.3, 261.

(67) Franklin, Trans.Faraday Soc., 1949, 45, 274.

(68) Presland, Paper presented at a meeting of The Carbon Group of
the Physical Society, Sheffield 1966.

(69) Hughes and Thomas, Carbon, 1964, 1, No.2, 209.

(70) Emmett and Brunauer, J.Amer.Chem.Soc.,1937, 59,1553.

(71) Livingstone, J.Colloid Sci.,1949, 4,447.

(72) Wynne-Jones, 'Structure and Properties of Porous Materials'.,
Butterworths, London 1958.

(73) Bond and Spencer, 'Industrial Carbon and Graphite' (First
Conference) Society for Chemical Industry, London, 1958, p.231.

(74) Langmuir, J.Amer.Chem.Soc., 1918, 40, 1361.

(75) Fowler, Proc.Cambridge Phil.Soc., 1935, 31, 260.

(76) Hill, J.Chem.Phys.,1949, 17, 520.

(77) Brunauer, Emmett and Teller, J.Amer.Chem.Soc.,1938, 60, 309.

(78) Joyner, Weinberger and Montgomery, J.Amer.Chem.Soc.,1945,67,2182.

(79) Wiggs, Paper presented at a meeting of The Carbon Group of the
Physical Society, Sheffield, 1966.

(80) Polyanyi, Verh.Dtsch.Phys.Ges.,1914,16,1012.

(81) Berenyi, Z.Phys.Chem.,1920,94, 628.

(82) Titoff, Z.Phys.Chem.,1910,74,641.

(83) Dubinin, 'Industrial Carbon and Graphite'.,(First Conference),
Society for Chemical Industry, London, 1958, p.219.

(84) Dubinin, Chem.Rev.,1960,60,235.

(85) Dubinin,Zhur.Fiz.Khim.,1965, 39, 1305.

(86) Marsh and Wynne-Jones, Carbon, 1964, 1, No.3, 269.

(87) Walker and Kini, Fuel, 1965, 44, 453.

(88) Marsh and Lamond, Carbon, 1964, 1, No.3, 293.

(89) Dubinin et Al, 'Surface Phenomena in Chemistry and Biology'.,
Pergamon Press, London, 1958, p.172.

(90) Bridgeman, J.Amer.Chem.Soc.,1927,49,1174.

(91) Anderson et Al, Fuel, 1965, 443.

(92) Marsh and Lamond, Carbon,1964,1, No.3, 281.

(93) Walker and Kawahata, 'Proceedings of the Fifth Conference on
Carbon'.,Pergamon Press N.Y.,1963, p.251.

(94) Thomas, Carbon, 1966, 3,No.4,435.

(95) Dubinin, Carbon, 1964, 2, No.3,261.

(96) Kipling et Al Carbon, 1964, 1, No.3,321.

(97) Dubinin, '4th International Syposium on the Reactivity of Solids'.,
Elsevier, Amsterdam 1961, p.643.

(98) Redfarn and Bedford, 'Experimental Plastics', Interscience, London, 2nd ED.,1960,p.15.

(99) Pinner, 'A Practical Course in Polymer Chemistry', Pergamon Press, London, 1961, p.111.

(100) McEnaney and Rowan, Chem. and Ind.,1965, 2032.

(101) Stonhill, J.Inorg.Nucl.Chem.,1959,10,153.

(102) Smith, Anal.Chem.1963,35, 1306.

(103) Kipling et Al, Polymer, 1962, 3, 1.

(104) McBain and Bakr, J.Amer.Chem.Soc.,1926, 48, 690.

(105) Thomas and Williams, Quart.Rev.,1965,19, No.3,231.

(106) Bennett and Tompkins,Trans.Faraday Soc.,1957,53,185.

Appendix   V

Table   A2.

Infra-red Absorption Frequencies of Polyacenaphthylene

Frequency (cm^{-1})	Band Assignment
3050 (m)	= C - H stretching
2910 (m)	- C - H stretching
1625 (m)	}
1600 (s)	} conjugated C = C stretching (aromatic)
1510 (s)	}
1440 (m)	} 6 membered ring deformation
1380 (s)	} (characteristic of polyacenaphthylene)
1175 (m)	}
1020 (m)	}
975 (m)	} 1, 2, 3, aromatic substitution
780 (s)	}
680 (m)	}
820 (s)	not assigned (characteristic of polyacenaphthylene)

(s) = strong   (m) = moderate

Primary Data from the Determination of the Isotherms

Series (i)

Cellulose Carbon 0% B.O.		Cellulose Carbon 25% B.O.		Cellulose Carbon 35% B.O.	
Pressure P.cm.Hg x 10^{-1}	Amount Adsorbed W.g/g x 10^{-1}	Pressure P.cm.Hg x 10^{-1}	Amount Adsorbed W.g/g x 10^{-1}	Pressure P.cm.Hg x 10^{-1}	Amount Adsorbed W.g/g x 10^{-1}
0.014	0.012	0.013	0.028	0.003	0.027
0.033	0.027	0.116	0.119	0.013	0.031
0.144	0.146	0.237	0.237	0.116	0.145
0.286	0.167	0.343	0.308	0.237	0.200
1.15	0.477	0.514	0.442	0.343	0.234
5.00	0.987	1.85	0.859	0.514	0.340
1.45	1.19	1.89	1.11	1.85	0.704
52	1.69	3.38	1.33	2.89	0.926
105	1.91	6.23	1.73	3.38	1.18
200	2.02	10.2	2.08	6.23	1.58
320	2.08	31	2.51	10.2	1.95
400	2.11	59	3.33	31	2.82
		213	4.00	59	3.50
		401	4.19	213	4.92
				401	5.17

Series (i)

Cellulose Carbon 50% B.O.		Cellulose Carbon 56% B.O.		Cellulose Carbon 94% B.O.	
Pressure P.cm.Hg x 10^{-1}	Amount Adsorbed W.g/g x 10^{-1}	Pressure P.cm.Hg x 10^{-1}	Amount Adsorbed W.g/g x 10^{-1}	Pressure P.cm.Hg x 10^{-1}	Amount Adsorbed W.g/g x 10^{-1}
0.026	0.055	0.038	0.066	0.080	0.065
0.075	0.107	0.125	0.150	0.271	0.131
0.200	0.198	0.260	0.216	0.411	0.243
0.560	0.347	0.590	0.359	1.64	0.364
1.35	0.604	0.900	0.421	3.25	0.469
1.80	0.701	1.40	0.520	4.80	0.521
3.30	0.965	3.75	0.918	13	0.785
4.80	1.20	5.00	1.06	22	1.03
6.60	1.44	7.20	1.38	32	1.55
8.50	1.63	8.40	1.59	43	2.13
22	2.76	22	2.74	53	2.28
45	3.82	42	3.90	74	2.60
76	4.82	62	4.79	100	3.45
157	6.15	129	6.52	151	5.16
396	7.22	235	8.05	228	7.03
		400	8.74	335	9.34
				400	10.5

Series (ii)

Cellulose Carbon 17.5% B.O.		Cellulose Carbon 32.5% B.O.		Cellulose Carbon 76% B.O.	
Pressure P.cm.Hg x 10^{-1}	Amount Adsorbed W.g/g x 10^{-1}	Pressure P.cm.Hg x 10^{-1}	Amount Adsorbed W.g/g x 10^{-1}	Pressure P.cm.Hg x 10^{-1}	Amount Adsorbed W.g/g x 10^{-1}
0.009	0.053	0.009	0.062	0.038	0.056
0.029	0.114	0.029	0.096	0.125	0.155
0.069	0.166	0.069	0.159	0.260	0.207
0.210	0.323	0.210	0.283	0.590	0.310
0.340	0.432	0.340	0.391	0.900	0.376
0.610	0.600	0.610	0.503	1.40	0.422
0.800	0.694	0.800	0.595	3.75	0.750
1.00	0.764	1.00	0.694	5.00	0.836
2.00	1.04	2.00	0.937	7.20	1.12
3.50	1.35	3.50	1.27	8.40	1.27
6.40	1.73	6.40	1.68	22	2.27
7.80	1.85	7.80	1.86	42	3.46
11.5	2.16	11.5	2.26	62	4.33
29	2.75	29	3.15	129	6.38
230	3.56	230	4.77	235	8.77
345	3.67	345	4.92	400	10.7
420	3.75	420	4.97		

Series (iii)

Cellulose Carbon 9.6% B.O.890°C.		Cellulose Carbon 12.3% B.O.955°C.		Cellulose Carbon 25.4% B.O.917°C.	
Pressure P.cm.Hg x 10^{-1}	Amount Adsorbed W.g/g x 10^{-1}	Pressure P.cm.Hg x 10^{-1}	Amount Adsorbed W.g/g x 10^{-1}	Pressure P.cm.Hg x 10^{-1}	Amount Adsorbed W.g/g x 10^{-1}
0.015	0.058	0.015	0.068	0.006	0.040
0.027	0.094	0.027	0.117	0.040	0.130
0.052	0.170	0.052	0.184	0.135	0.245
0.105	0.244	0.105	0.275	0.500	0.481
0.210	0.379	0.210	0.410	1.10	0.726
0.385	0.499	0.385	0.538	1.75	0.906
0.560	0.633	0.560	0.683	3.50	1.30
2.60	1.20	2.60	1.32	6.30	1.53
6.00	1.63	6.00	1.77	9.00	1.96
7.30	1.75	7.30	1.93	13	2.34
14	2.12	14	2.35	34	3.11
39	2.52	39	2.84	63	3.61
88	2.78	88	3.14	130	4.03
174	2.89	174	3.30	233	4.30
382	3.06	382	3.48	380	4.45

Series (iii)		Series (i)			
Cellulose Carbon 18% B.O. 903°C.		Cellulose Triacetate Carbon 0% B.O.		Cellulose Triacetate Carbon 23.5% B.O.	
Pressure P.cm.Hg x 10^{-1}	Amount Adsorbed W.g/g x 10^{-1}	Pressure P.cm.Hg x 10^{-1}	Amount Adsorbed W.g/g x 10^{-1}	Pressure P.cm.Hg x 10^{-1}	Amount Adsorbed W.g/g x 10^{-1}
0.006	0.063	0.014	0.018	0.008	0.022
0.040	0.139	0.033	0.029	0.041	0.097
0.135	0.297	0.144	0.257	0.150	0.241
0.500	0.587	0.288	0.302	0.840	0.584
1.10	0.805	0.570	0.338	0.960	0.638
1.75	0.995	1.16	0.674	1.60	0.831
3.50	1.37	1.91	0.633	2.40	1.02
6.30	1.69	5.01	1.00	3.50	1.24
9.00	1.97	14.5	1.33	5.10	1.45
13	2.25	52	1.74	6.60	1.59
34	2.82	105	2.10	10.7	2.00
63	3.13	238	2.27	22.5	2.56
130	3.38	329	2.43	45	2.99
233	3.53	401	2.53	59.5	3.18
380	3.66			121	3.54
				235	3.86
				319	4.05
				356	4.12

Series (i)

Cellulose Triacetate Carbon 40% B.O.		Cellulose Triacetate Carbon 60% B.O.		Cellulose Triacetate Carbon 75% B.O.	
Pressure P.cm.Hg x 10^{-1}	Amount Adsorbed W.g/g x 10^{-1}	Pressure P.cm.Hg x 10^{-1}	Amount Adsorbed W.g/g x 10^{-1}	Pressure P.cm.Hg x 10^{-1}	Amount Adsorbed W.g/g x 10^{-1}
0.008	0.053	0.027	0.078	0.027	0.063
0.041	0.101	0.055	0.127	0.055	0.096
0.150	0.180	0.110	0.163	0.110	0.126
0.840	0.470	0.300	0.294	0.300	0.242
0.960	0.514	0.720	0.357	0.720	0.263
1.60	0.677	1.00	0.478	1.00	0.372
2.40	0.875	2.45	0.751	2.45	0.623
3.50	1.08	4.00	1.00	4.00	0.818
5.10	1.30	6.00	1.26	6.00	1.03
6.60	1.44	7.40	1.41	7.40	1.18
10.7	1.92	11.0	1.83	11.0	1.53
22.5	2.67	23.5	2.64	23.5	2.33
45	3.45	39.0	3.41	39.00	3.09
59.5	3.78	64.0	4.18	64.0	3.88
121	4.48	124	5.35	124	5.31
235	5.05	242	6.49	242	6.97
319	5.33	347	7.01	347	7.61
356	5.40	390	7.17	390	7.79

Series (iii)

Cellulose Triacetate Carbon 30% B.O.960°C.		Cellulose Triacetate Carbon 50% B.O.919°C.		Cellulose Triacetate Carbon 30% B.O.903°C.	
Pressure P.cm.Hg x 10^{-1}	Amount Adsorbed W.g/g x 10^{-1}	Pressure P.cm.Hg x 10^{-1}	Amount Adsorbed W.g/g x 10^{-1}	Pressure P.cm.Hg x 10^{-1}	Amount Adsorbed W.g/g x 10^{-1}
0.030	0.074	0.25	0.200	0.25	0.257
0.080	0.163	0.54	0.321	0.54	0.442
0.185	0.264	1.00	0.419	1.00	0.636
0.390	0.403	2.35	0.763	2.35	0.971
0.690	0.541	4.20	0.988	4.20	1.30
1.15	0.662	6.80	1.38	6.80	1.66
2.05	0.899	13	1.95	13	2.22
5.40	1.41	30	3.06	30	3.03
7.50	1.60	61	4.19	61	3.70
10.5	1.97	131	5.56	131	4.34
24	2.59	291	6.70	291	4.90
50	3.13	420	7.55	420	5.18
118	3.69				
265	4.18				
387	4.44				